

**Analysis of Geophysical Evidence of Cretaceous-Paleocene
Forearc Strata in the Santa Catalina Basin,
California Inner Continental Borderland**

A Dissertation

Presented to

the Faculty of the Department of Earth & Atmospheric Sciences,

University of Houston

In Partial Fulfillment

of the Requirements for the Degree

Doctor of Philosophy

By

Christopher Gantela

May 2015

**Analysis of Geophysical Evidence of Cretaceous-Paleocene
Forearc Strata in the Santa Catalina Basin,
California Inner Continental Borderland**

Christopher Gantela

APPROVED:

Dr. Hua-wei Zhou, Chairman

Dr. Stuart Hall

Dr. Tom Bjorklund

Dr. Aibing Li

Dr. Michael P. Thornton

Dean, College of Natural Sciences and Mathematics

Acknowledgments

My gratitude and sincere thanks to Dr. Hua-wei Zhou for his constant support, encouragement, infinite patience and guidance over the course of this research endeavor. Thanks to Dr. Stuart Hall, a member of the committee, who was also my advisor during the absence of Dr. Hua-wei Zhou from the Department of Earth and Atmospheric Sciences. Thanks to the other members of the committee: Dr. Tom Bjorklund, Dr. Aibing Li, and Dr Michael Thornton for their help and suggestions. Thanks to Dr. Aifei Bian for reverse time migration code and processing. Special thanks to Dr. Tom Bjorklund for many valuable discussions on the geology of the California continental borderland. Thanks to him for spending much of his time in making my manuscript “in pretty good shape” due to his revisions, edits, modifications, and reviews. Paradigm’s processing packages FOCUS and Echos were used for all basic processing. I would like to express my sincere appreciation to everyone who helped me completing this dissertation.

Multichannel seismic reflection data LARSE.1 MCS: Data Set 02-006 USGS Open-File Report 95-228 was available for the present study. Thanks to the US Geological Survey, Menlo Park, California for providing 1990 California Borderland Survey data. Very special thanks to my wife Sarojini and sons, for their constant encouragement, patience, and support. I gratefully dedicate this work to my mother and my wife’s mother.

**Analysis of Geophysical Evidence of Cretaceous-Paleocene
Forearc Strata in the Santa Catalina Basin,
California Inner Continental Borderland**

An Abstract of a Dissertation

Presented to

the Faculty of the Department of Earth & Atmospheric Sciences,

University of Houston

In Partial Fulfillment

of the Requirements for the Degree

Doctor of Philosophy

By

Christopher Gantela

May 2015

ABSTRACT

The California continental borderland has a complex tectonic history but limited quality of geophysical data. By the use of multichannel seismic reflection data, geophysical studies were conducted to define the upper crustal structure and delineate the main lithotectonic belts of the region. Due to a highly reflective sea bottom, however, strong multiples were generated masking all primary reflections beyond the arrival of the first-order multiple waves. In this study, using a new prestack two-way reverse time migration (RTM) which treats multiples as signal rather than noise, the multiple artifact was significantly attenuated in the Los Angeles Region Seismic Experiment (LARSE) data. The RTM maps both the primaries and multiples to their points of origination: seabed multiples to the sea bottom and primaries to the reflecting interfaces. Based on these results, five stratigraphic units were recognized to a depth of 6 km. The upper two units are Pliocene plus younger strata and Miocene syntectonic fill. The two deeper stratigraphic units are interpreted to be forearc sedimentary strata, though previous studies had interpreted the top unit as the Catalina Schist. The seismic characteristics of these units are similar to those of the Cretaceous-Paleogene forearc section of the Outer Continental Belt. Miocene volcanic layers form the fifth unit. Shallow plutons are inferred to be present under several bathymetric high areas.

Two additional seismic profiles in the inner continental borderland (ICB), northwest of LARSE lines, revealed evidence of forearc Cretaceous-Paleogene strata. This evidence was tied to the OCS-CAL P289 well drilled in the ICB, which has 1250 m of forearc strata. In previous studies, this forearc section of Cretaceous to early Miocene sedimentary rocks was not thought to be preserved in the ICB. This newly found forearc tectonic section in ICB, bounded by the San Clemente Fault to the southwest and Santa Catalina Fault to the northeast, is mapped from the south of Catalina Island to a well near Santa Barbara Island. The existence of the forearc sedimentary belt in the Catalina Basin has important geologic significance to suggest significant revisions of the current structural and stratigraphic interpretations of the California borderland.

CONTENTS

1. Introduction	1
1.1 Tectonic overview	1
1.2 Geologic setting and data	4
1.2.1 OCB-ICB boundary	4
1.2.2 Stratigraphic drill holes	5
1.2.3 Catalina Schist	6
1.2.4 Remnants of forearc strata in the inner borderland	7
1.3 Processing of LARSE and USGS 1990 data	7
1.3.1 Reverse time migration	8
2. Marine reflection data processing	10
2.1 Seismic surveys	10
2.2 Seismic data quality and sea bottom multiple attenuation	12
2.3 LARSE data processing	16
2.4 SRME	19
2.5 USGS 1990 data processing	20
2.5.1 USGS Line 128	23
2.5.2 USGS Line129	25
2.6 Imaging with multiples	28
2.6.1 An example of RTM using synthetic data	28

3. Depth imaging of LARSE data by reverse time migration	34
3.1 Reverse time migration	35
3.2 Velocity models for reverse time migration	35
3.3 Reverse time migration technique	39
3.4 Results and discussion	42
4. Processing and interpretation of USGS 1990 data	51
4.1 Well data	52
4.2 Seismic data processing of USGS 1990 data	55
4.2.1 Line 128	56
4.2.2 Line 109	58
4.2.3 Line 129	60
5. Forearc sedimentary in Santa Catalina Basin strata of the ICB	66
6. Summary	74
7. References	77

LIST OF FIGURES

Figure 1.1	Map of southern California Borderland and western Transverse Ranges showing lithostratigraphic belts and simplified major faults. East Santa Cruz fault (9) marked by a dashed line is the inferred boundary between inner and outer borderland. Study area is enclosed by a rectangle	2
Figure 1.2	Fault and tectonic map of California borderland with location of Santa Barbara Island (*) within the inner borderland	5
Figure 2.1	Map of the California continental borderland with track lines of MCRS profiles. “*” marks the well locations and red rectangle encloses study area	11
Figure 2.2	Map of California inner borderland with LARSE MCRS Lines 1 and 2	12
Figure 2.3	USGS California borderland Line 129 shot gathers with auxiliary and non-recording channels	14
Figure 2.4	Raw shot gathers LARSE Line 1 over an area of complex seabed relief	14
Figure 2.5	Constant velocity using water velocity of LARSE Line 1	15
Figure 2.6	Constant water velocity stack of LARSE line 1	17
Figure 2.7	Normal moveout stack using velocity derived from computed grid	17
Figure 2.8	LARSE Line 1 spiking deconvolution stack	18
Figure 2.9	Surface related multiple elimination stack of LARSE Line 1	19
Figure 2.10	Shot point location map of LARSE and USGS 1990 surveys	20
Figure 2.11	Constant water velocity stack of USGS Line 116 without interpretation	21
Figure 2.12	Constant water velocity stack of USGS Line 116 with interpretation.	22
Figure 2.13	Line drawing of USGS Line 116 showing Miocene and forearc strata in OBS	23
Figure 2.14	Constant water velocity stack of USGS line 128	23
Figure 2.15	USGS line 128 Normal moveout stack, missing shot at SP 2646	24
Figure 2.16	USGS line 128 Predictive deconvolution stack, missing shots at SP 2646	24

Figure 2.17	USGS Line 129 constant water velocity stack	25
Figure 2.18	USGS Line 129 NMO stack showing attenuation of sea bottom multiples	26
Figure 2.19	USGS Line 129 prestack predictive deconvolution attenuated sea bottom multiple revealing a primary reflector at time 4 s in the Catalina Basin	26
Figure 2.20	USGS Line 129 prestack predictive deconvolution attenuated sea bottom multiple revealing a primary reflector at time 4 s in the Catalina Basin	27
Figure 2.21	A simple multiple generating model showing velocity-depth and shooting geometry	29
Figure 2.22	Shot gather of shot 10 showing water bottom multiples down to 9th order	29
Figure 2.23	RTM with multiples stack section using correct velocities	30
Figure 2.24	LARSE Line 1 constant water velocity stack. Input shot gathers that produced this stack were input to RTM program that produced the display below	31
Figure 2.25	Reverse time migration of LARSE Line 1 in depth	31
Figure 2.26	LARSE Line 2 constant water velocity stack. Input shot gathers that produced this stack were input to RTM program that produced the display below	32
Figure 2.27	Reverse time migration of LARSE Line 2 in depth	32
Figure 3.1	LARSE Line 1 top: OBS first arrival plot. Bottom: Five layers with variable velocity values cover the entire LARSE line 1	36
Figure 3.2	Migration velocity model for Line 1 with velocity values in km/s	37
Figure 3.3	LARSE line 2 A: Travel time plots of first arrivals from OBS. B: Smoothed depths of velocity interfaces. C: Velocity depth structure from DLT program	38
Figure 3.4	Migration velocity model for Line 2 with velocity values in km/s	39
Figure 3.5	Down going and up going wavefields at 800 ms and 2000 ms of a flat layer velocity model	41

Figure 3.6	Comparison of Line 1 conventional processing with RTM depth profile	45
Figure 3.7	Comparison of Line 2 conventional processing with RTM depth profile	47
Figure 3.8	(a) and (c) LARSE Lines 1 and 2 reflection depth profiles with color overlays of velocity model [plate 1 a and b, ten Brink et al.,2000]. (b) and (d) LARSE Lines 1 and 2 RTM depth sections	49
Figure 4.1	Shot point map of LARSE 1994 and California borderland marine survey 1990	51
Figure 4.2	Lithology-velocity plot of well 1 located in the outer Continental borderland with two-way time correlated to USGS Line 120. All related values are given in the table below	53
Figure 4.3	Shows interpretation of Miocene and top of forearc sedimentary section in the Santa Cruz Basin	56
Figure 4.4	Line drawing of west end of Line 128 with interpretation of Cretaceous-Paleogene and Neogene sedimentary strata	57
Figure 4.5	Predictive deconvolution section of Line 128 with labels of tops of Miocene and forearc stratigraphic section	58
Figure 4.6	Constant water velocity stack section of line 109. Cross lines: 129, 116, 124, 120 & 114	59
Figure 4.7	Spiking deconvolution stack section of Line 109. The blue marker is the top of forearc strata, Paleogene and Cretaceous, undifferentiated. The red marker is the top of acoustic basement, mafic igneous rocks	59
Figure 4.8	Water velocity stack of the entire Line 129 showing complex sea bottom relief and alternating basins and ridges	60
Figure 4.9	Fence diagram of Lines 109 and 129 gives 3D picture of the San Nicolas Basin	61
Figure 4.10	Merge line 109-129 showing continuation of interpretation of Cretaceous marker	62
Figure 4.11	Line 129 constant water velocity stack showing enhanced sea bottom multiples	63
Figure 4.12	Line 129 with interpretation of top of Base of Miocene (P) and pink marker (K) is correlated to pink marker in RTM sections	63

Figure 4.13	Line 129 constant water velocity stack (left) and predictive deconvolution stack (right) with interpretation of forearc section. Yellow marker (P) is an unconformity at the base of Miocene and (K) is the pink marker correlated to the one in RTM section	64
Figure 5.1	Shaded bathymetric relief map of the California Borderland. LARSE Lines 1 and 2 (red), USGS 1990 seismic Lines 109, 129 and 128 (blue)	66
Figure 5.2	RTM section LARSE Line 1 with interpretation of forearc section underlying Miocene formation	69
Figure 5.3	RTM section LARSE Line 2 with interpretation of forearc section underlying Miocene formation Need units for the vertical and horizontal axes and indication of section orientation with respect to N, S, E and W	69
Figure 5.4	Predictive deconvolution stack of line 129 with interpreted tops Paleogene P and Marker K	70
Figure 5.5	Predictive deconvolution stack section of Line 128 showing formation tops from the well	70
Figure 5.6	Composite display of 4 seismic sections showing forearc sedimentary sections in the Santa Catalina Basin, California inner borderland	72
Figure 5.7	Location of seismic lines, well P289 and the inferred distribution of forearc strata in the Santa Catalina Basin. From well and seismic data, forearc strata are inferred to be present between the San Clemente fault and Santa Catalina fault and interpreted to extend from LARSE Line 1 to USGS Line 128. The strata may extend further to the south and north	73

LIST OF TABLES

Table 4.1	Cortes Bank OCS-CAL 75-70 No. 1 well	54
Table 4.2	Santa Barbara Island OCS P289 well	54
Table 4.3	Mobil San Clemente core hole No. 1 well	55
Table 5.1	Width of forearc strata in the Santa Catalina Basin from NW to SE	71

LIST OF ABBREVIATIONS

CCB	California continental borderland
USGS	U.S. Geological Survey
CMG	Coastal and Marine Geology
LARSE	Los Angeles Region Seismic Experiment
ICB	Inner continental borderland
OCB	Outer continental borderland
LAB-IB	Los Angeles Basin – inner borderland
ESCBF	East Santa Cruz Basin Fault
RTM	Reverse time migration
MCRS	Multichannel reflection survey
NMO	Normal moveout
SRME	Surface Related Multiple Elimination
DLT	Deformable Layer Tomography
SP	Shot point

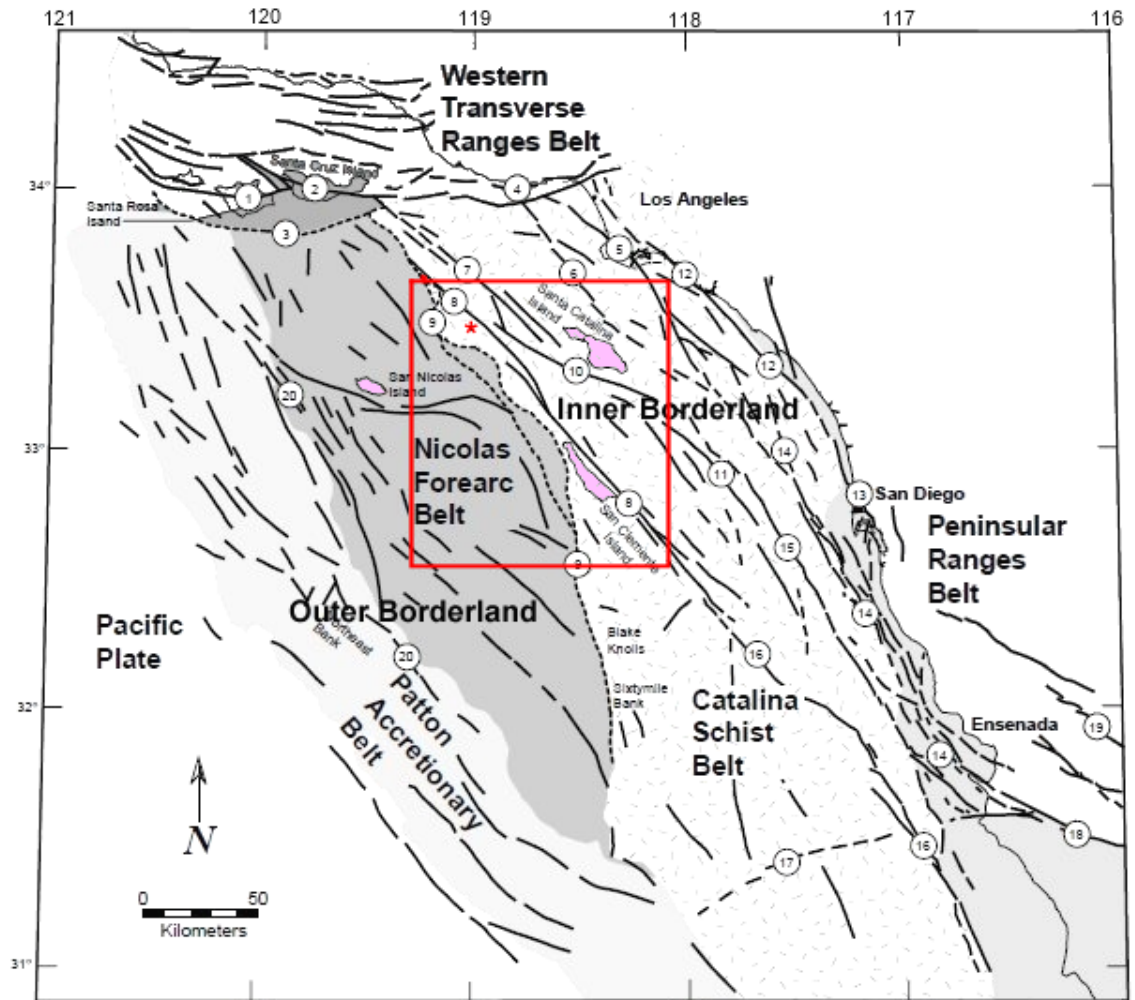
1. Introduction

The California continental borderland (CCB) is covered by water with a few islands that allow direct access to rock exposures. Regional marine seismic reflection surveys, California Borderland 1990 (USGS 1990) and Los Angeles Region Seismic Experiment 1994 (LARSE), were conducted for the purpose of understanding the tectonic framework and geologic history of the area. Numerous studies have detailed the character of rocks assigned to the key lithotectonic belts. Studies that used seismic reflection data were subject to possible misinterpretations due to the limit of interpretation depth imposed by severe sea bottom noise that masks most of the deep part of seismic sections. We have applied advanced seismic processing to attenuate or de-mask the multiple artifact and better constrain interpretations of the tectonic framework and geologic history of the area. The Santa Catalina Basin occupies the central portion of inner borderland between Santa Catalina Island and San Clemente Island.

1.1 Tectonic overview

The southern California continental borderland has a very complex tectonic history. During the Cretaceous and Paleogene, the borderland was the forearc region of the Pacific-North American plate subduction zone and in the Late Paleogene-Early Miocene, collision of the Pacific plate spreading center with North American plate began the formation of the San Andreas transform fault system. In this transition period, southern California experienced plate capture, translation, rotation of crustal blocks, extension and volcanic eruptions. In the Late Miocene, the present transpressional phase of

deformation began with the breakaway of Baja California from the North American Plate and the formation of the present San Andreas Fault system. Structures formed during this period include folds, faults, and inverted grabens (Atwater, 1998; Nicholson et al. 1994).



* MOBIL OCS P-0289 NO. 1

From Bohannon et al. 1998

Figure 1.1 Map of southern California Borderland showing lithostratigraphic belts and simplified major faults. East Santa Cruz fault (9) marked by a dotted line is the inferred boundary between inner and outer borderland. Study area is enclosed by a red rectangle.

The principal lithotectonic belts that comprise California continental borderland are shown in Figure 1.1: 1) the northwest-trending Patton accretionary wedge with rocks similar to the Mesozoic Franciscan Complex, 2) Nicolas Forearc belt with thick section of Cretaceous to Oligocene forearc strata, 3) Inner continental borderland (ICB), Catalina Schist Belt with basement rocks of highly tectonized blueschist to amphibolite-grade rocks overlain by Neogene sedimentary and volcanic rocks and also fragments of Great Valley and forearc basement rocks, and 4) Peninsular Ranges belt with batholithic and volcanic rocks overlain by forearc sedimentary section similar to Great Valley sequence. The Western Transverse ranges, a major clockwise-rotated structural block, adjoin the borderland area on the north (Crouch and Suppe, 1993; Bohannon and Geist, 1998; ten Brink et al., 2000). More on detailed information on tectonic and geologic history of the region is found in Luyendyk, B. P., 1991; Crouch and Suppe, 1993; Nicholson et al., 1994; Atwater, 1998; Bohannon and Geist, 1998; ten Brink et al., 2000; and Sorlien, et al., 2013.

In previous studies, the boundary between the Catalina Schist belt and the Nicolas Forearc belt on the west is inferred to be the west-dipping East Santa Cruz Basin Fault. The boundary between the Catalina Schist belt and the Peninsular Ranges belt on the east is irregular and not well-known. Near the area of this study, many workers have proposed that the Catalina Schist extends only to the Newport-Inglewood fault. Crouch and Suppe (1993) inferred that the boundary is a low-angle, regional detachment fault that dips into the Los Angeles Basin. Most of the inner borderland was uplifted in the early Miocene and further deformed into a series of basins and ridges during a stage of oblique

extension, similar to the extensional Basin and Range province of the Western U.S.

Crouch and Suppe (1993) proposed that the Mesozoic Catalina Schist underlies Neogene strata across the entire inner borderland.

The extent and depth of the Catalina Schist in the inner borderland are not well-established. In most places, Miocene or younger rocks are present on the sea bottom.

Outboard from the inner borderland and onshore in the Los Angeles Basin, Cretaceous to Oligocene forearc strata underlie Miocene and younger rocks. The presence of Miocene plutons in the upper crust can be inferred from gravity and magnetic data and outcrops on Santa Catalina Island (Forman, 1970, Rowland, 1984, Ridgway and Zumberge, 2007).

Volcanic rocks are interbedded with Miocene strata throughout the ICB. The only reported incontrovertible outcrops of Catalina Schist in the inner borderland are on Santa Catalina Island (Boundy-Sanders, et al., 1987).

1.2 Geologic setting and data:

1.2.1 OCB-ICB boundary: Crouch and Suppe, 1993 state that, “The San Clemente fault is undoubtedly a major structural feature, with clear indications of recent right-lateral activity (Legg et al., 1989); however, it does not form the boundary between the LAB-IB rift and outer borderland belts. Instead, the western LAB-IB rift boundary approximately coincides with the East Santa Cruz Basin fault (ESCBF), a boundary fault similar to that depicted in Howell and Vedder (1981) and approximately coincident with the westernmost strand of the ‘East Santa Cruz Basin fault systems’ proposed by Howell and others (1974)”. They have also stated that the boundaries between the LAB-IB rift and

the three surrounding lithotectonic belts are deeply buried both onshore and offshore, so none are well defined, and their precise locations remain controversial.

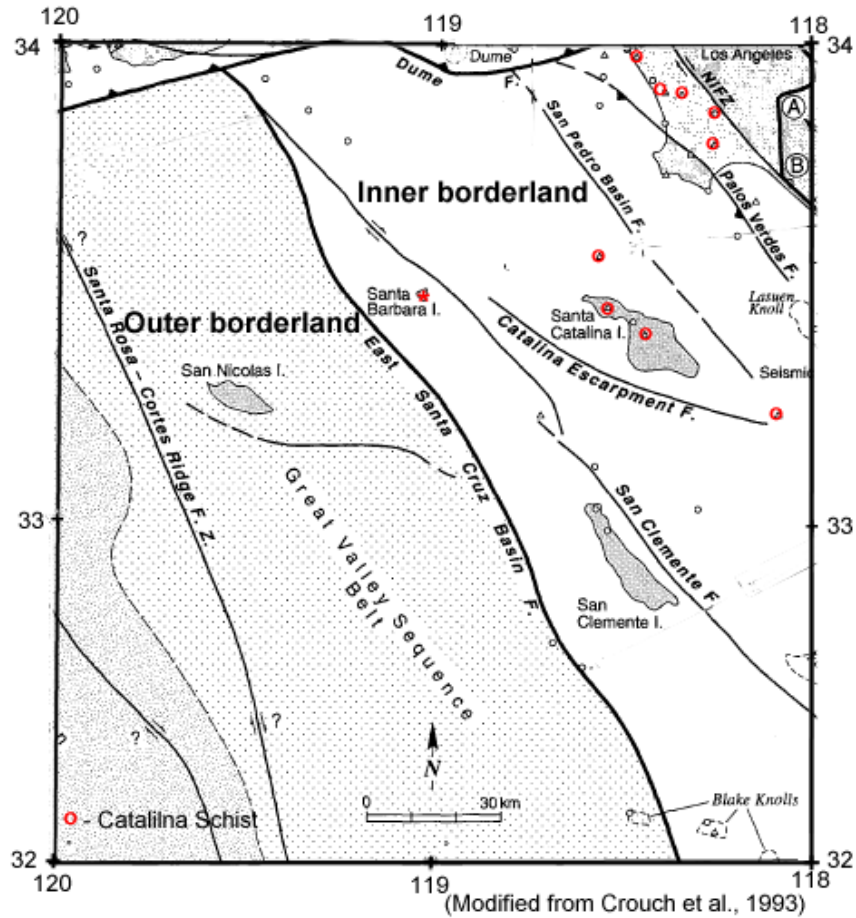


Figure 1.2 Fault and tectonic map of California borderland with location of Santa Barbara Island (*) within the inner borderland.

1.2.2 Stratigraphic drill holes: There are three important deep stratigraphic drill holes: OCS-CAL 75-70, MOBIL OCS P289, and MSCH-1. The first well is located in the outer borderland and the other two are located in the inner borderland drilled close to Santa Barbara Island. Drill hole 75-70, which is located on Cortes Ridge, penetrated 2460 meters of Cretaceous-Paleocene forearc strata overlain by Miocene and volcanic rocks.

Drill hole 75-70 and several other drill holes on Cortes Ridge and seismic data in the San Nicholas Basin establish the presence of the forearc section throughout the outer borderland. Near San Clemente, core hole MSCH 1 penetrated Pliocene and Miocene strata, including the Miocene San Onofre breccia at total depth 1840 m, which directly overlies forearc strata. MSCH 1, onshore well data and outcrops establish the widespread presence of forearc strata in the Peninsular Ranges east of the Newport Inglewood fault zone. Drill hole P 289, located near Santa Barbara Island and within the inner borderland penetrated 120 meters of Cretaceous and 1155 meters of Paleogene forearc strata overlain by Miocene and volcanic rocks similar to the section in drill hole 75-70. Previous studies have not cited the data from 75-70 as a constraint on the areal extent of the Catalina Schist in continental borderland (Crouch and Suppe, 1993; Bohannon and Geist, 1998).

1.2.3 Catalina Schist: Based on mappings of a number of locations of Catalina Schist onshore and 4 locations on and off Santa Catalina Island (red open circles in Figure 1.2), it has been stated that rocks correlated to Catalina Schist form the entire basement of ICB. Except for relatively small areas of Palos Verdes Hills and Santa Catalina Island where Catalina Schist basement is exposed, the basement cannot be seen because Miocene and younger rocks blanket the entire ICB. On the basis of interpretation of seismic profiles in that area, Catalina Schist is inferred to underlie most of the western margin of the Los Angeles basin and the adjacent offshore Santa Monica-San Pedro shelf. The only occurrences of incontrovertible in-place Catalina Schist in ICB are the outcrops on Catalina Island (Boundy-Sanders, et al., 1987).

1.2.4. Remnants of forearc strata in the inner borderland: Crouch and Suppe 1993, recognized small remnants of forearc in the schist belt in their report and interpreted them to be fragments carried along forearc-schist thrust contact in several localities. Vedder et al., 1993, reported a tiny remnant of the forearc section exposed in the easternmost part of the Catalina Island and suggests that those rocks may have once covered parts of the Catalina terrane as well. They consider this evidence of forearc strata in the inner borderland to be uncertain and infer that the Catalina Island fragment and similar fragments elsewhere in the inner borderland are simply isolated remnants of forearc strata stranded on a regional detachment fault that juxtaposes Catalina schist and forearc rocks.

1.3 Processing of LARSE and USGS 1990 data

The previous processing of marine seismic data from two regional surveys, Los Angeles Region Seismic Experiment LARSE (Brocher et al., 1995) and California borderland MCRS 1990 (Bohannon, et al., 1998), was performed using basic methods. These data have severe sea bottom multiples that coincide with primaries and mask the rest of the seismic section after the arrival of the first-order multiple. Bohannon et al., 1998 described that “strong first-order multiples coincided with primaries and even by the use of a multiple attenuating method of inverse velocity stacking, significant levels of energy of multiples remained in the processed results”. The maximum two-way travel time of the primary section from sea bottom time available for interpretation is about 2.5 s depending on depth of sea bottom. Comprehensive papers dealing with development of models for tectonic framework and understanding of geological history have been written in the past

25 years or more (Crouch and Suppe, 1993; Bohannon and Geist, 1998; ten Brink et al., 2000) mainly due to interpretation of primary section free of sea bottom multiple artifact.

1.3.1 Reverse time migration: Prestack reverse time migration (RTM) method (Youn and Zhou, 2001) uses multiples as signal rather than noise to process real seismic and model data. It produces images of primaries and multiples showing overall significant improvement when compared to conventional processing. A two-way RTM was applied in the present study to de-mask the multiple artifact in offshore segments of LARSE lines 1 and 2 in the Santa Catalina Basin (Gantela et al., 2014). The results indicate that much of the artifact due to sea bottom multiples can be de-masked producing high quality depth images that show stratigraphic and structural features not evident in published seismic sections.

Based on the RTM results, five stratigraphic units were recognized from the sea bottom to depths of 6 km. The upper 2 units are Pliocene plus younger strata and Miocene syntectonic fill above an unconformity. Two deeper stratigraphic units, below Miocene formation are interpreted to be sedimentary strata; previous studies identified the unit to be Catalina Schist. Miocene volcanic layers form the fifth unit and a few inferred igneous intrusions form the sixth unit.

Previous studies did not use information from MOBIL OCS P289 well drilled in ICB which has 120 m of Cretaceous and 1155 m of Paleocene forearc strata. Results from RTM and two track profiles of USGS 1990 data revealed the evidence of this Cretaceous-

Paleogene column in the ICB. This new found forearc tectonic block in the ICB, bounded by San Clemente Fault to southwest and Santa Catalina Fault to northeast, is mapped from south of Santa Catalina Island to the well near Santa Barbara Island. These results suggest that the Santa Catalina Basin may be much deeper than previously thought and may have potential for commercial hydrocarbons.

2. Marine reflection data and processing

2.1 Seismic surveys

Marine reflection data from two public domain regional marine reflection surveys were reprocessed in this study. Multichannel seismic-reflection data were acquired by U.S. Geological Survey in southern California borderland (USGS 1990, Figure 1.1) onboard the R/V *S. P. Lee* in 1990 <http://walrus.wr.usgs.gov/infobank/l/1490sc/html/l-4-90-sc.fmeta.outline.html> . (Geophysical data of field activity L-4-90-SC in Southern California from 05/09/1990 to 05/25/1990. Publisher: U.S. Geological Survey (USGS) <<http://www.usgs.gov>>, Coastal and Marine Geology (CMG) <http://walrus.wr.usgs.gov> Publication Place: Menlo Park, CA, Bohannon, et al., 1990).

Twenty-nine seismic profiles, totaling 3100 km, were shot using a 48-channel 2600 m streamer with 4 non-recording channels. A group interval of 50 m, a tuned array of 10 air guns with a total volume of 3.97 m³ (2424 in³) firing every 50 m, resulting in 22 fold data with a common midpoint interval of 25 m. The distance between the source and the nearest receiver was 250 m. The data were recorded to 12 s with a 2 ms sampling rate.

The Los Angeles Region Seismic Experiment (LARSE) was conducted in October 1994 (Figure 2.2). Deep-crustal multichannel seismic-reflection data were acquired in the Inner California Borderland aboard the R/V Maurice Ewing. The survey is a cooperative study of the crustal structure of southern California involving earth scientists from the U.S Geological Survey, Caltech, the University of Southern California, the University of California Los Angeles and the Southern California Earthquake Center (SCEC).

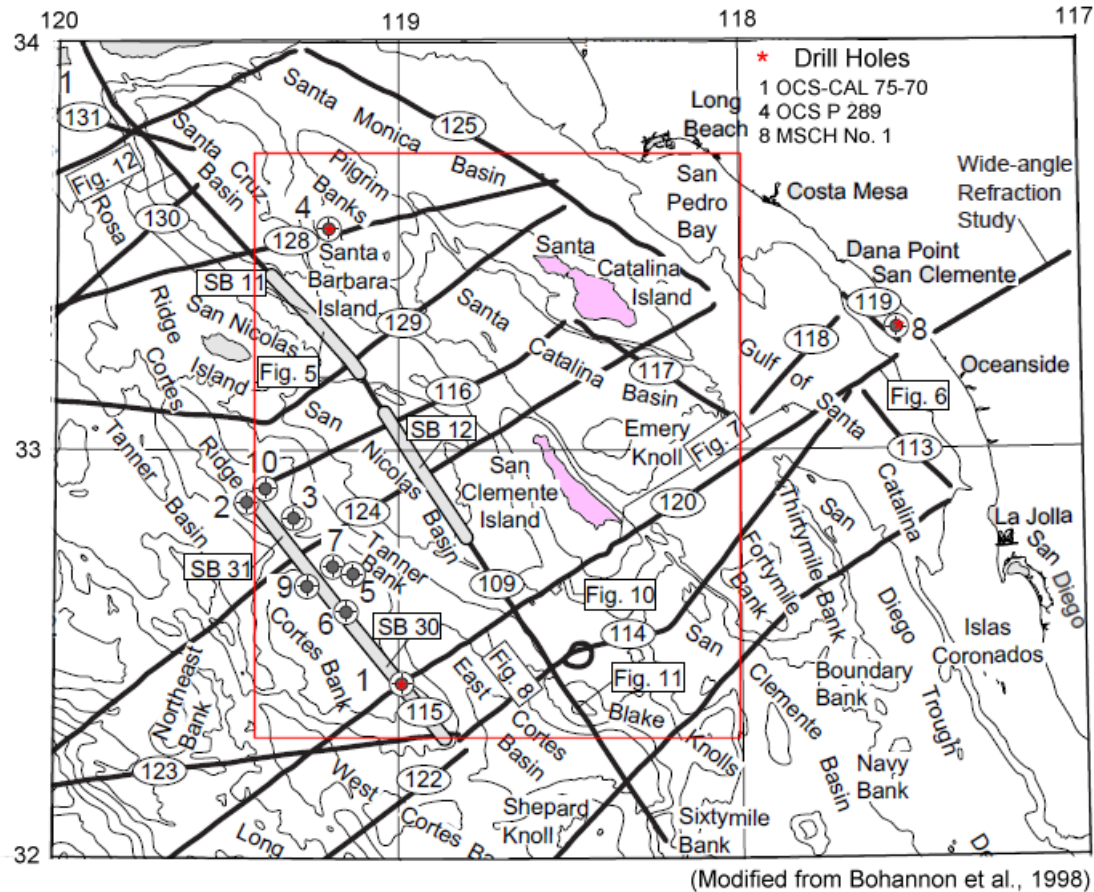


Figure 2.1 Map of the California continental borderland with track lines of MCRS profiles. “*” marks the well locations and red rectangle encloses study area.

The purpose was to study the deep seismic structure of the California continental borderland (Brocher et al., 1995). Data were gathered along three long main profiles by using a digital seismic streamer of length 4.2 km, with 160 channels, generally towed at depths between 10 to 12 meters. Recording was done to 16 seconds with a 2 ms sampling rate. The air gun array was triggered at every 50 m (shot interval), the streamer's group interval was 25 m, and digitizers were located every 100 m (4 groups) along the streamer. The subsurface coverage for this setup is 40 fold and with a mid point interval of 12.5m. The distance between the source and the near receiver was 200m.

Simultaneously, OBS receivers along lines 1 and 2 and four land receivers on Santa Catalina and San Clemente Islands recorded wide angle data.

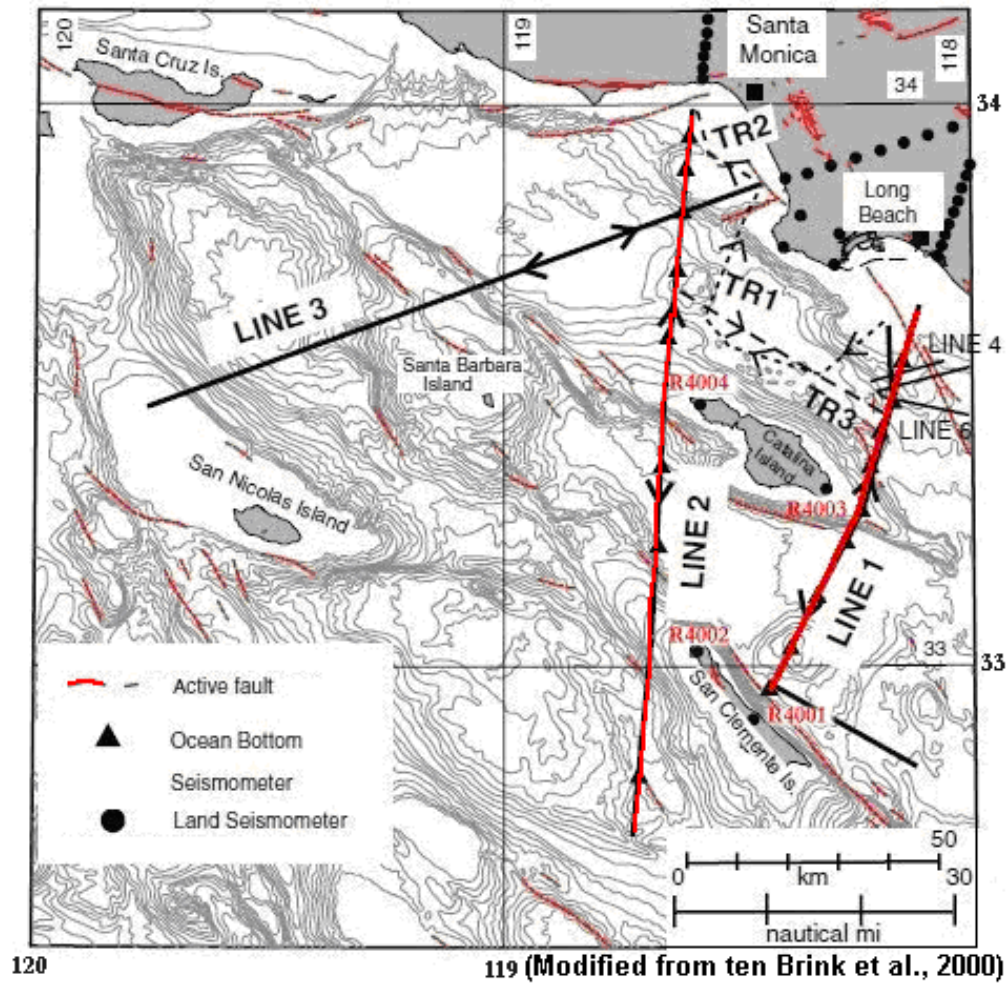


Figure 2.2 Map of California inner borderland with LARSE MCRS Lines 1 and 2.

2.2 Seismic data quality and sea bottom multiples attenuation

A highly reflective sea bottom resulted in strong sea bottom multiples that masked most of the seismic section of the profiles. The length of streamer in the LARSE survey was 4.2 km, compared to 2.6 km in the USGS 1990 survey, and the longer length of the LARSE survey resulted in strong refractions and their multiples on the LARSE long

offset traces. The air gun array volume of the LARSE survey was 8470 cu³, 3.49 times the 2424 cu³ volume of USGS 1990 survey, produced strong and long duration multiples. The problem of multiple-artifact in reflection data from USGS 1990 was less severe. The complex wavefield in these data sets was due to rapid variations of sea bottom with depths ranging from 100 m to 1.2 km, alternating ridges and basins, complex substructure with steep faults, and tilted blocks with steeply-dipping beds.

Figure 2.3 shows shot gathers of USGS Line 129 recorded with a shorter streamer and smaller source volume. Compared to LARSE data, USGS 1990 data shows less severe sea bottom multiples and less noise.

Shot gathers of LARSE Line 1 (Figure 2.4) show a very complex recorded wavefield. Direct arrivals, reflections with arrows pointing to first-order reflection multiples, and refracted arrivals along with their multiples are evident in these shot gather displays. No primary reflections are observed beyond the arrival of the first-order sea bottom multiple.

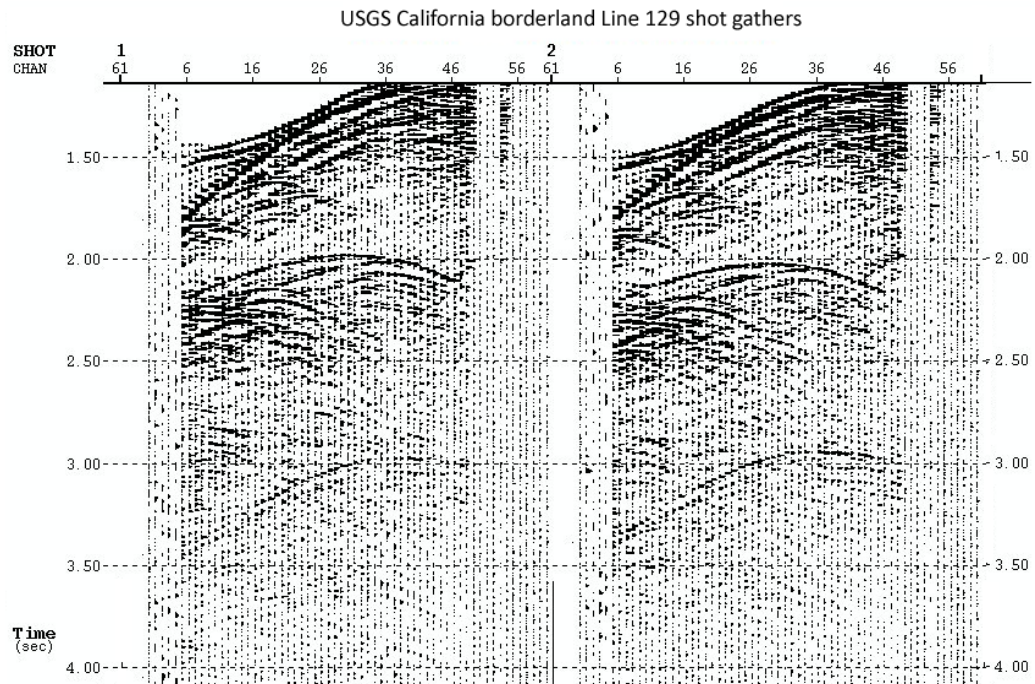


Figure 2.3 USGS California borderland Line 129 shot gathers with auxiliary and non-recording channels.

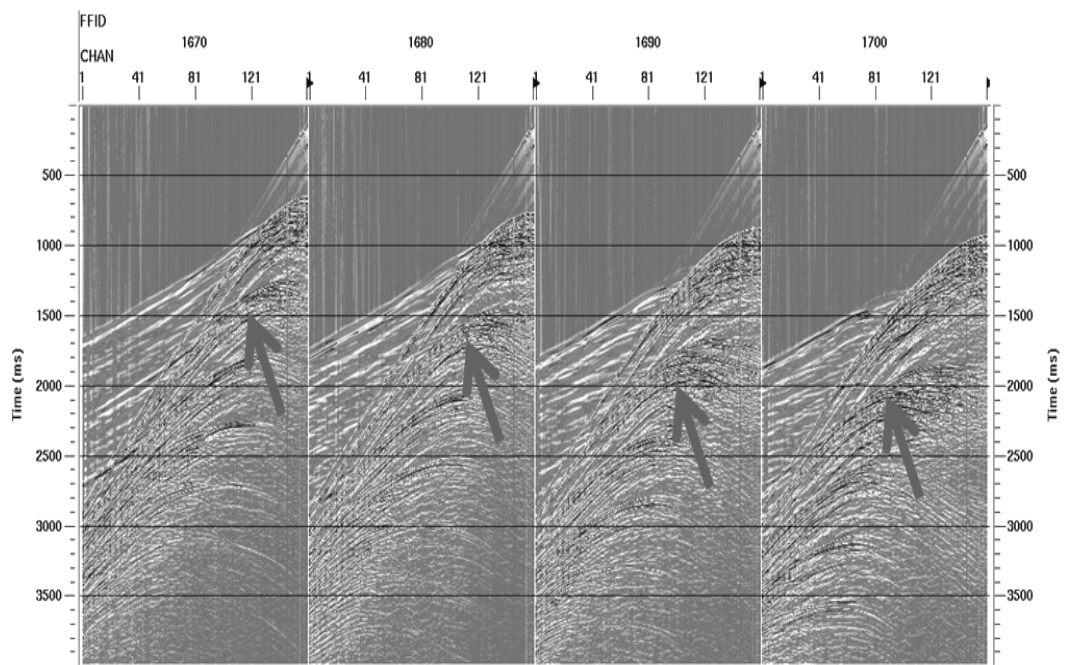


Figure 2.4 Raw shot gathers from LARSE Line 1 over an area of complex seabed relief.

A constant water velocity stack (Figure 2.5) shows several orders of sea bottom multiples. The strong sea bottom multiples mask all of the section after their arrival. Multiples below Emery Knoll, Catalina Basin, and Catalina Ridge range from two under the Catalina Basin to numerous orders of multiples below Catalina Ridge. Under the basin, 1.5 s of sea bottom multiple free section is available for interpretation.

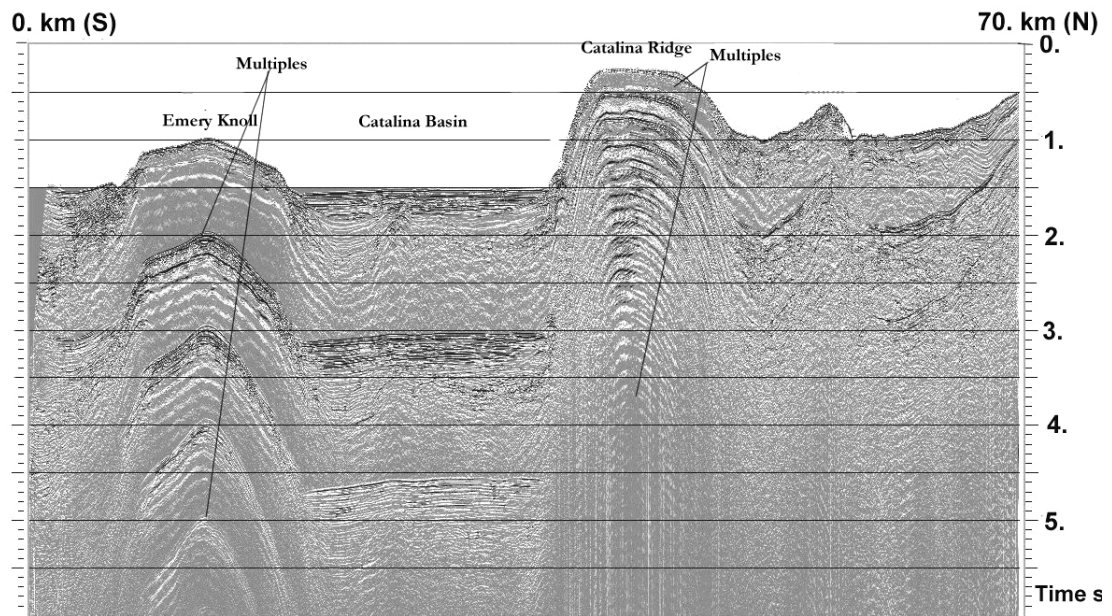


Figure 2.5 Constant velocity stack using water velocity of LARSE Line 1

Where sea bottom is deeper, a window of primary reflections to 2.5 s is present without sea bottom multiples. An inability to significantly attenuate the multiple artifact in previous attempts to process the LARSE data limited the interpretable depths of seismic sections (ten Brink et al., 2001 Plate 1).

2.3 LARSE data processing

The Paradigm Geophysical processing software FOCUS was used for all basic processing. The processing sequence included midpoint sort of shot gathers after edits and mutes, pre-stack spiking deconvolution, predictive deconvolution, normal moveout correction, stack, and filter. Velocity analysis was performed using the semblance option. Where the sea bottom was deep, reflections were very close, resulting in semblance contours without tight closures. Prestack spiking with an operator length of 151 samples and predictive deconvolution with an operator length of 151 samples and gap based on zero crossing were applied with varying results the LARSE and USGS 1990 surveys. Better attenuation of multiples was obtained from the USGS 1990 data compared to LARSE data. Migration with FOCUS module MIGTX was performed on most of the lines. MIGTX performs migration by approximating the Kirchhoff integral by a numerical integration. The constant water velocity stacks like the one in Figure 2.6, were very useful for processing and interpretation because multiples were enhanced and more easily recognizable. The NMO stack (Figure 2.7) shows about 1.5 s of primary reflections followed by a high amplitude first-order multiple and a smeared multiple noise-artifact after the first lobe. The NMO process was not very successful in suppressing multiples particularly in the ridge sections. Noise scattered by faults on the edges of ridges adds to problem and it cannot be easily removed by basic processing.

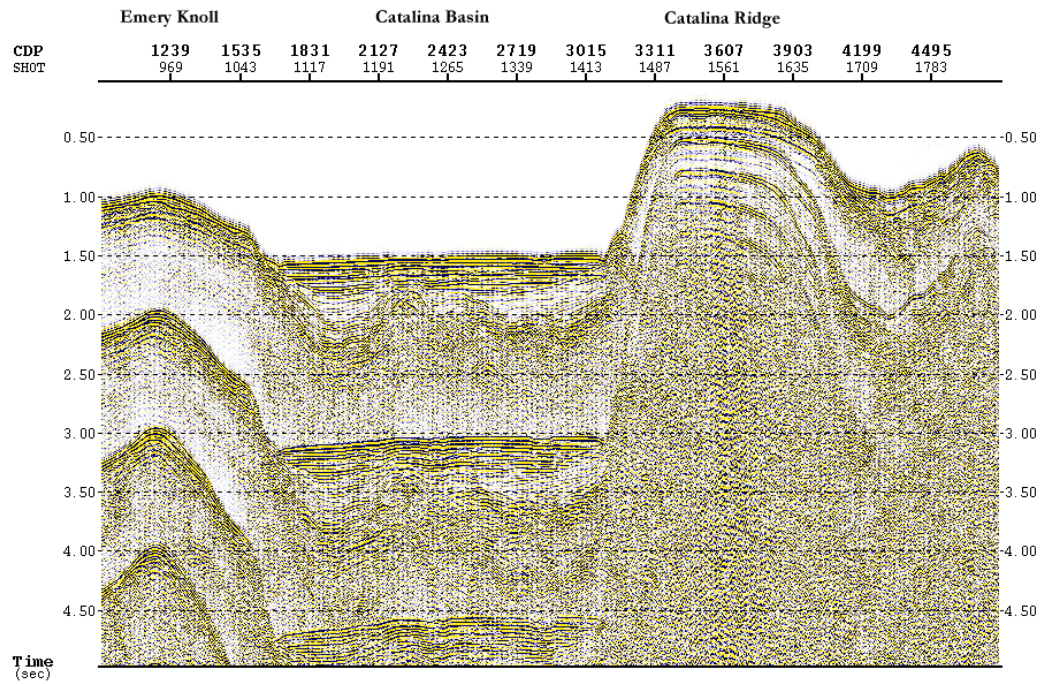


Figure 2.6 Constant water velocity stack of LARSE line 1.

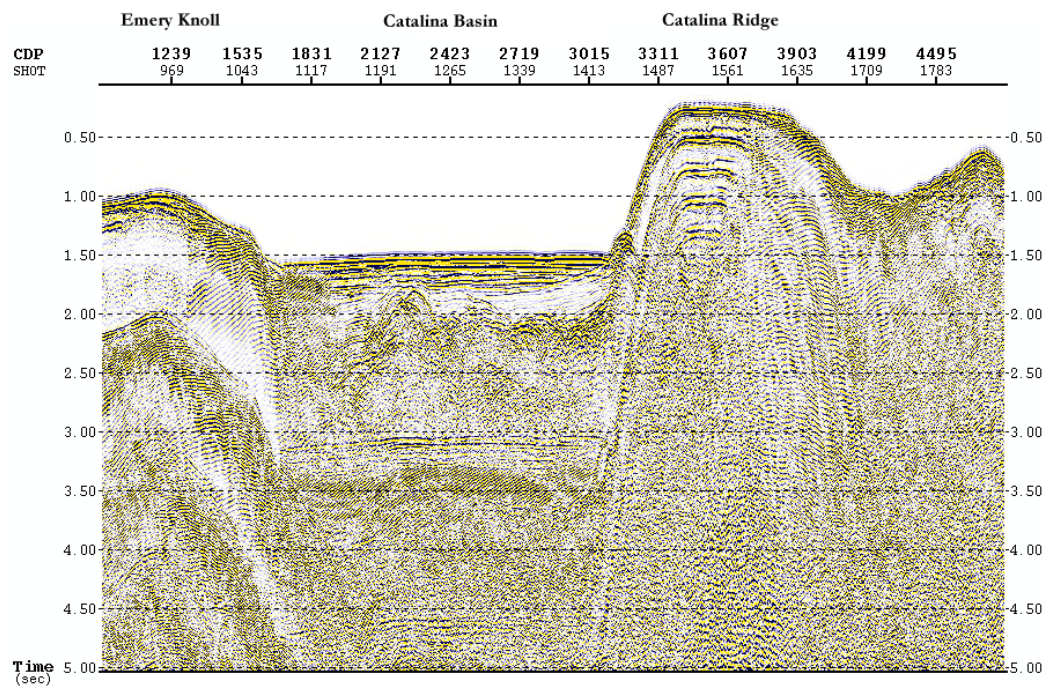


Figure 2.7 Normal moveout stack using velocity derived from computed grid.

Deconvolution explores the periodicity of multiples in order to suppress them. Predictive deconvolution attenuates the predictive part, like multiples, of seismic trace. Spiking deconvolution is a special case where the gap is set to one sample. The prestack spiking deconvolution section (Figure 2.8) shows better resolution of primaries compared to NMO stack (Figure 2.7). Prestack spiking, predictive and spiking plus predictive deconvolution were performed on all lines in LARSE and USGS 1990 surveys. Basic processing of LARSE data was not successful in attenuating multiples and primaries masked by multiples were not evident in processed sections.

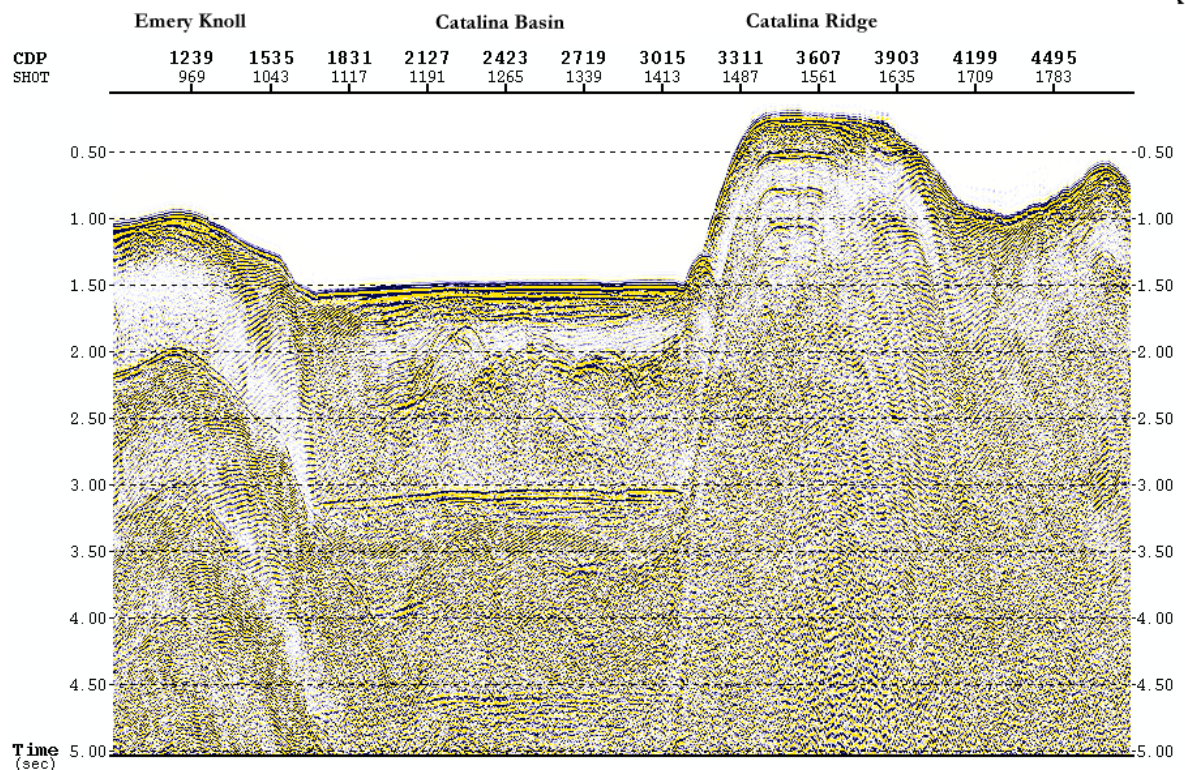


Figure 2.8 LARSE Line 1 spiking deconvolution stack.

2.4 SRME: The Surface related multiple elimination method (SRME) aims to remove all surface related-multiples. Most of the traditional multiple suppression methods rely on velocity discrimination. SRME assumes that each surface multiple is a superposition of several primary reflections from interfaces and uses this assumption to predict multiples, which can then be removed. Paradigm's SRME program, SMACTRM, predicts a multiple model and subtracts it from the shot gathers. SRME attenuated first-order multiples in the basin region (Figure 2.9) but primary reflections that were masked by multiples are not seen the section. In the ridge sections, partially suppressed (eliminated) multiples still remain in the section.

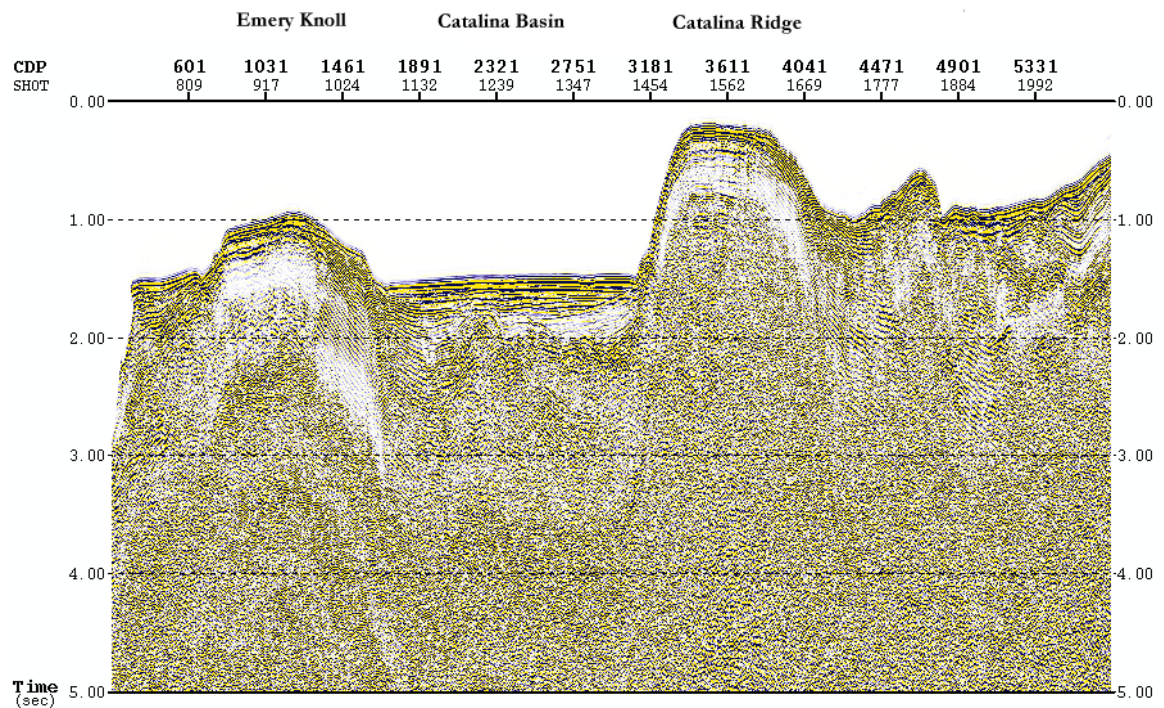


Figure 2.9 Surface related multiple elimination stack of LARSE Line 1

2.5 USGS 1990 data processing: The California borderland 1990 marine seismic data cover the entire borderland (Figure 2.10). In the previous processing of these data (Bohannon et al., 1998), a basic processing sequence was used to produce initial stack sections for interpretation. A second phase of processing sequence included improved velocity analysis, dip-moveout, multiple attenuation and post stack finite difference migration. A multiple attenuation process was applied to these data, but significant levels of multiple energy remained in the processed results.

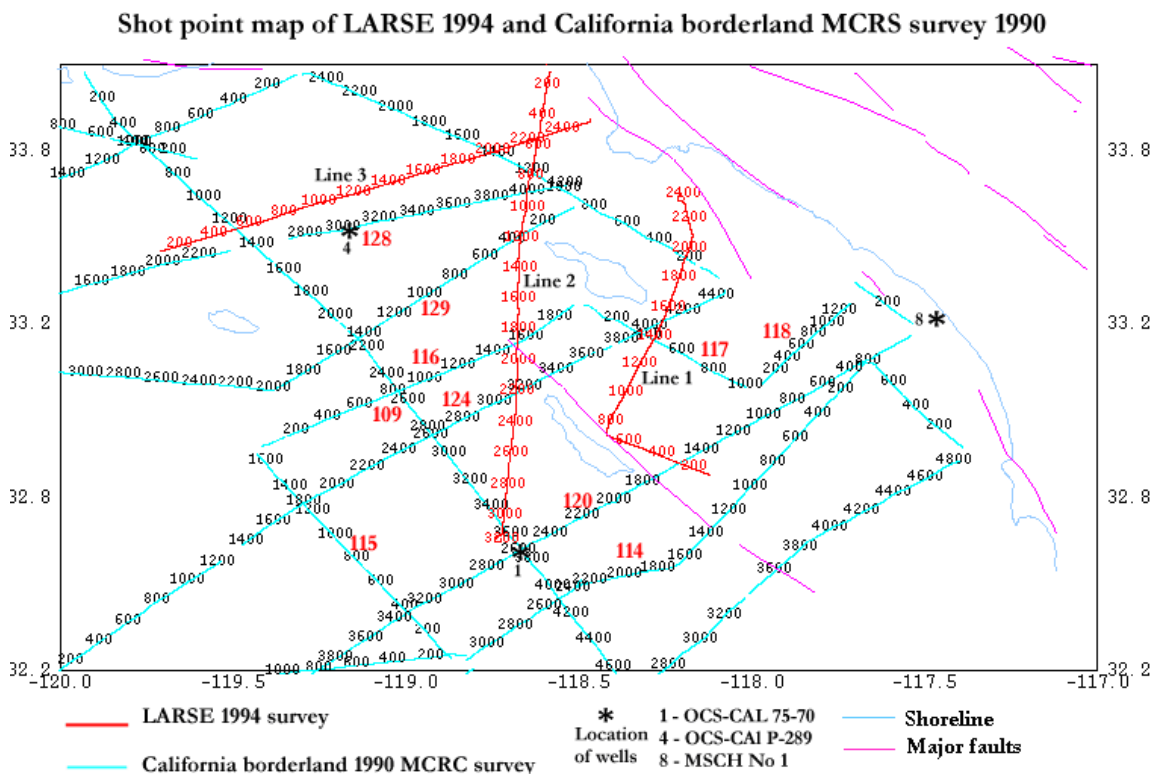


Figure 2.10 Shot point location map of LARSE and USGS 1990 surveys

Use of long operator prestack predictive deconvolution on USGS data gave better results compared to processing of LARSE data. Figure 2.11 shows constant water velocity stack of USGS line 116 with enhancement of sea bottom multiples. Because of the deep sea bottom, the entire stratigraphic column of the San Nicolas Basin is available for interpretation above the sea bottoms multiple waves. That column includes Miocene and younger formations, the Cretaceous-Paleogene section and top basement.

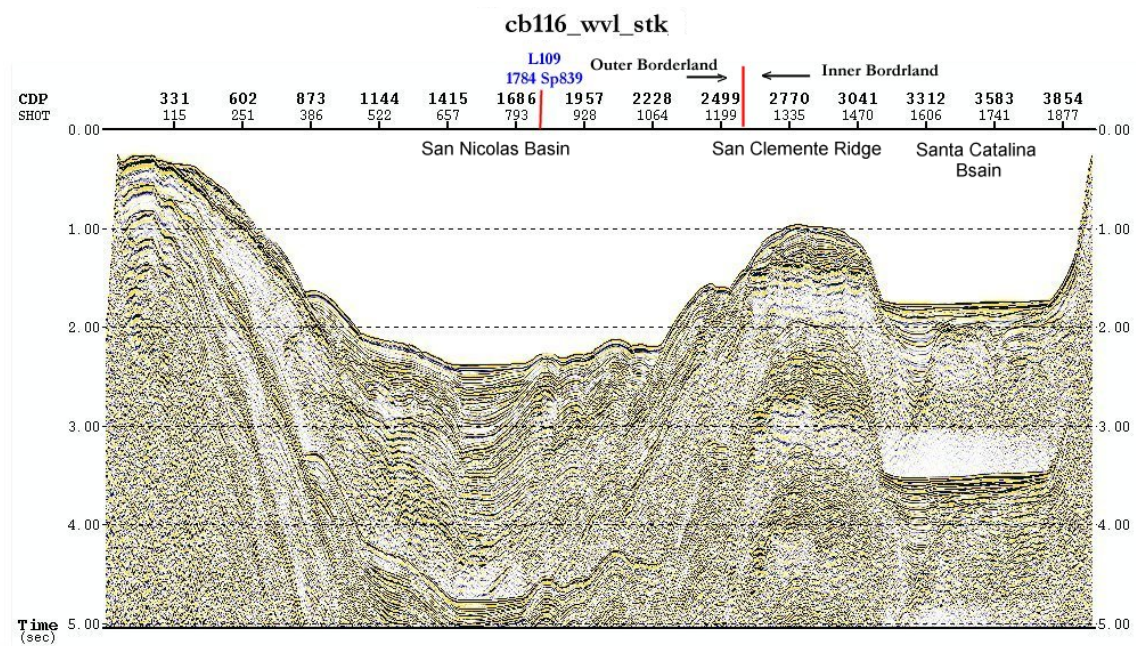


Figure 2.11 Constant water velocity stack of USGS Line 116 without interpretation.

USGS line 116 (Figure 2.11) shows the usefulness of the constant water velocity stack section to show the location of multiples in time and space and to assess the extent of their attenuation in processed sections. The velocities of the shallow strata are close to water velocity. The multiples ray paths are nearly vertical in the water column and result in better subsurface images than the reflections from the target strata, which include scattered noise from the side. Although reprocessing improved the resolution of the

Miocene and forearc strata in the OCB, the problem of continuing correlation of events across the East Santa Cruz Fault from OCB to ICB still exists. Primary seismic reflections from ICB section on the northeast side of San Clemente Ridge in the Santa Catalina Basin are masked by: the section is incomplete on the ridge because of erosion and non-deposition and the basins are separated by faults. A line drawing and interpretation of Bohannon and Geist (1998) of the southwest portion of line 116 is a good illustration of the correlation difficulties that exist throughout the area of this study (Figure 2.12). The stratigraphic correlations established by Bohannon and Geist (1998) in the OCB and additional well data in the ICB provide a basis for our identification of forearc strata in the Santa Catalina Basin.

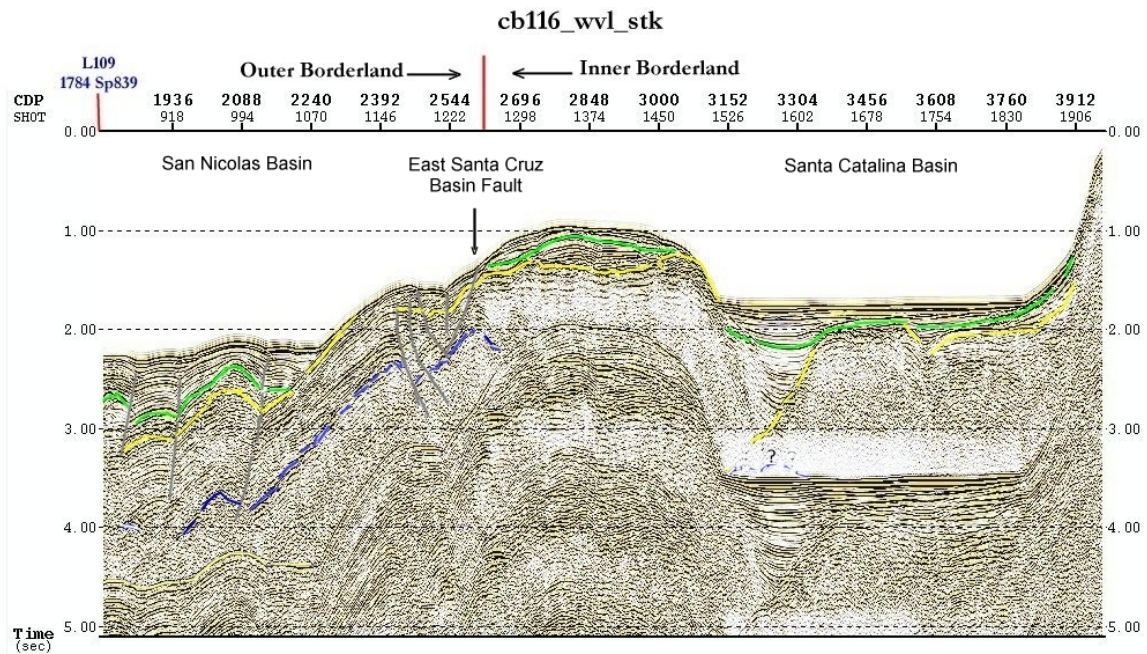


Figure 2.12 Constant water velocity stack of USGS Line 116 with interpretation.

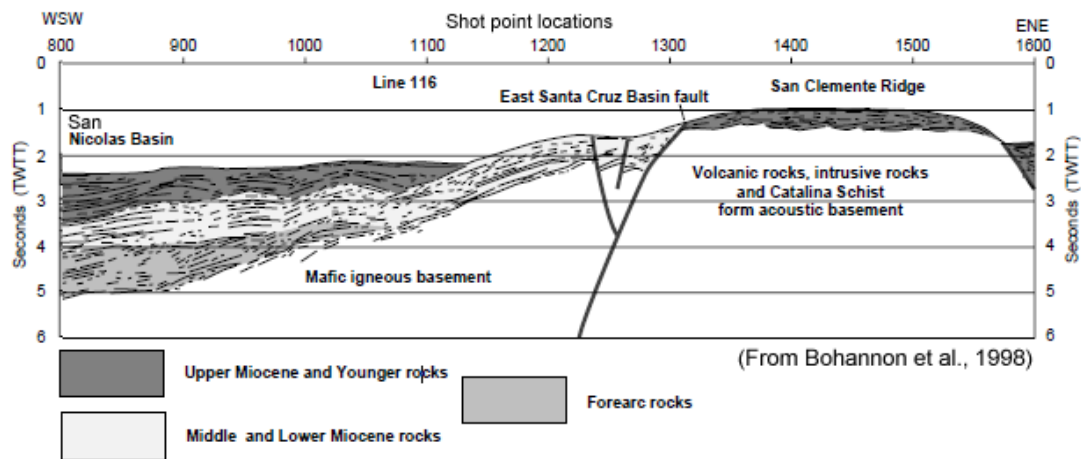


Figure 2.13 Line drawing of USGS Line 116 showing Miocene and forearc strata in OBS.

2.5.1 USGS Line 128: Figures 2.14 to 2.16 show results of that basic processing. Normal moveout stack shows attenuation of multiples (Figure 2.15) in the San Nicolas basin. At the ridge and a narrow basin to right, the sea bottom is shallow and prestack predictive deconvolution has shown some attenuation of multiples (Figure 2.16). Figure 2.18 shows interpretable results of shallow sediments going down to about 2.5 s.

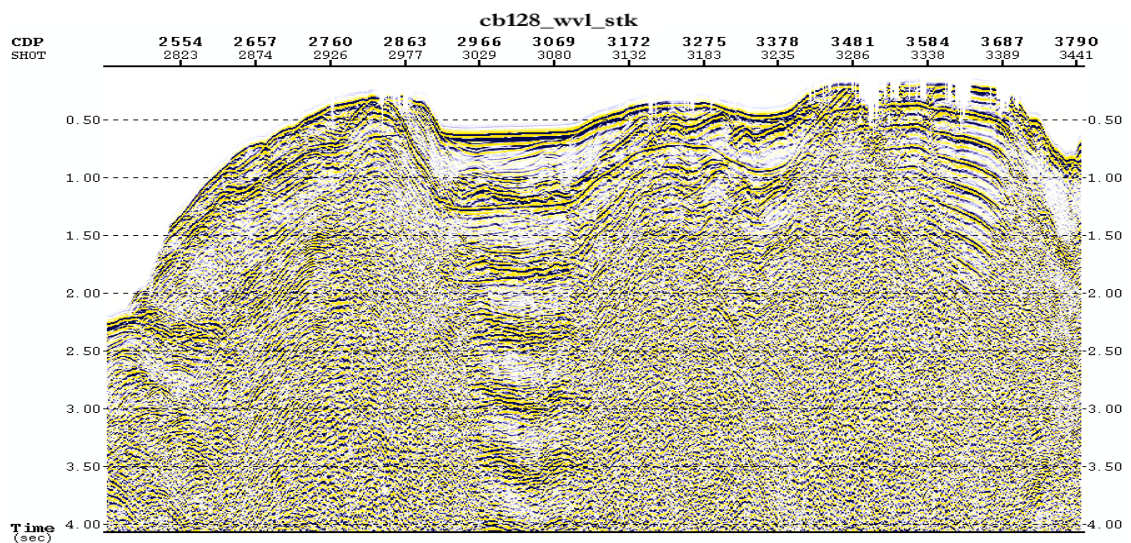


Figure 2.14 Constant water velocity stack of USGS line 128

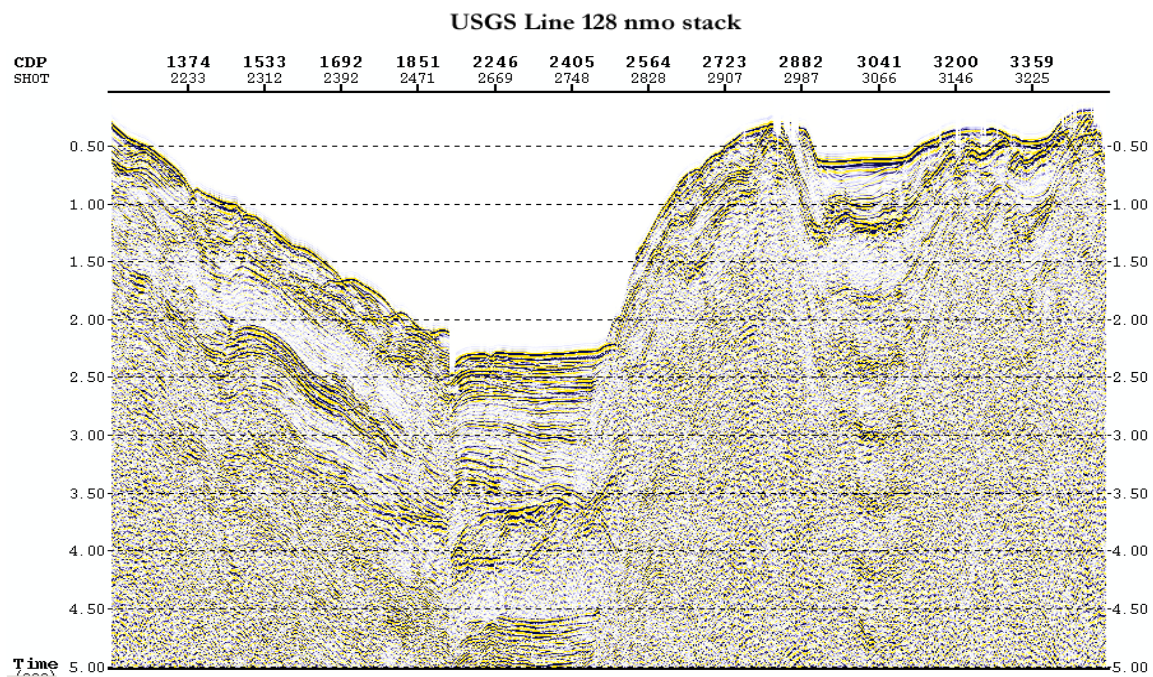


Figure 2.15 USGS line 128 Normal moveout stack, missing shots at SP 2646.

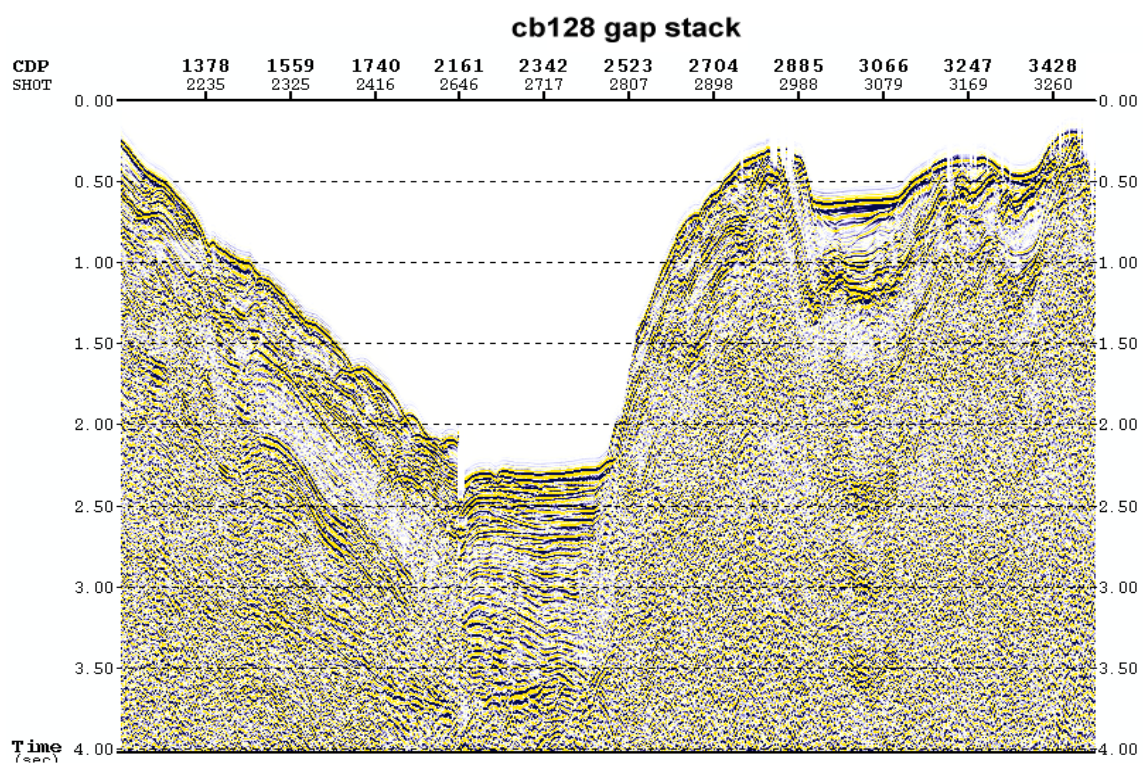


Figure 2.16 USGS line 128 Predictive deconvolution stack, missing shots at SP 2646

2.5.2 USGS Line 129: Figures 2.17 to 2.20 show results of basic reprocessing to enhance the USGS 1990 survey data. The normal moveout stack shows attenuation of multiples in the basin and ridge areas (Figure 2.18). Prestack predictive deconvolution attenuates sea bottom multiples and brings out primaries in the basin area from 3 s to 4 s (Figure 2.14). Figure 2.12 shows a comparison of constant water velocity stack and predictive deconvolution section that brings out interpretable results to about 4.5 s.

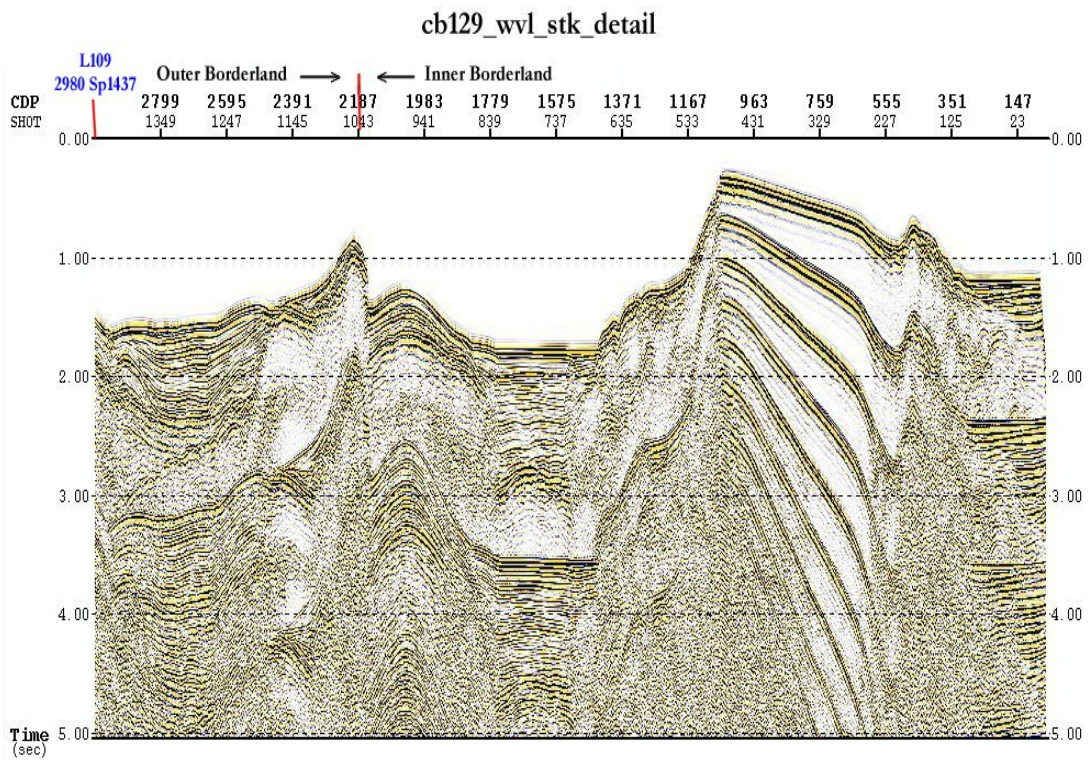


Figure 2.17 USGS Line 129 constant water velocity stack

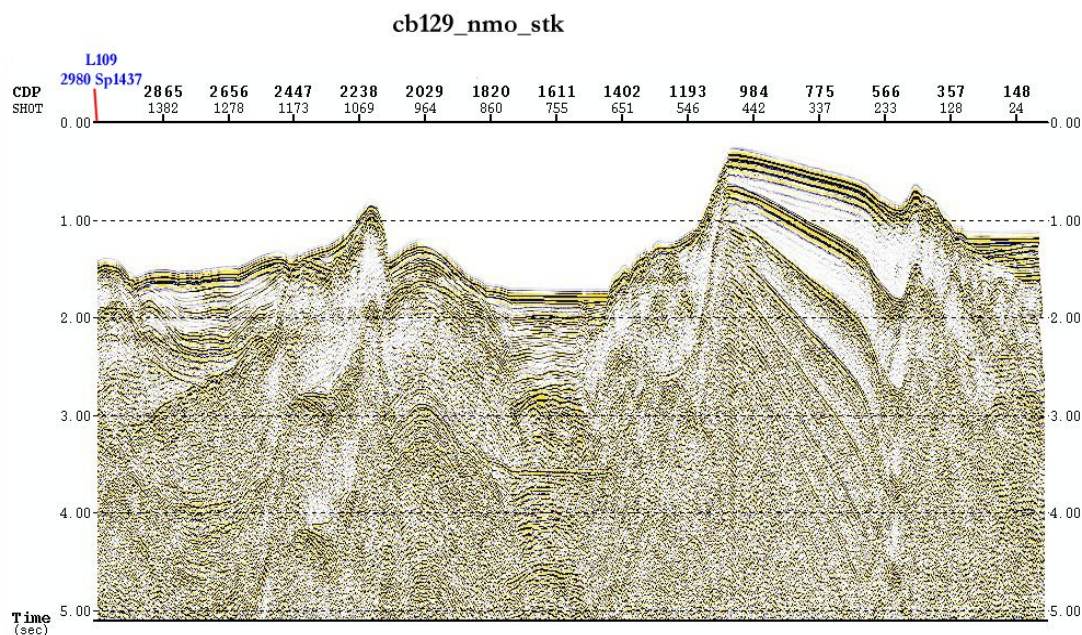


Figure 2.18 USGS Line 129 NMO stack showing attenuation of sea bottom multiples

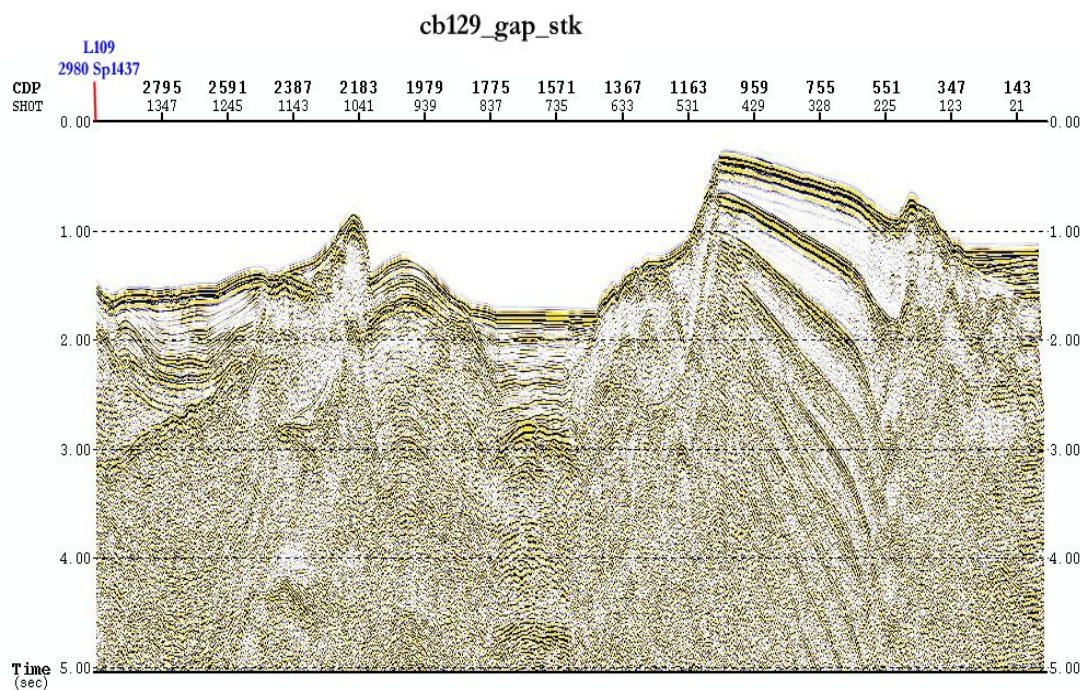


Figure 2.19 USGS Line 129 prestack predictive deconvolution attenuated sea bottom multiple revealing a primary reflector at time 4 s in the Catalina Basin.

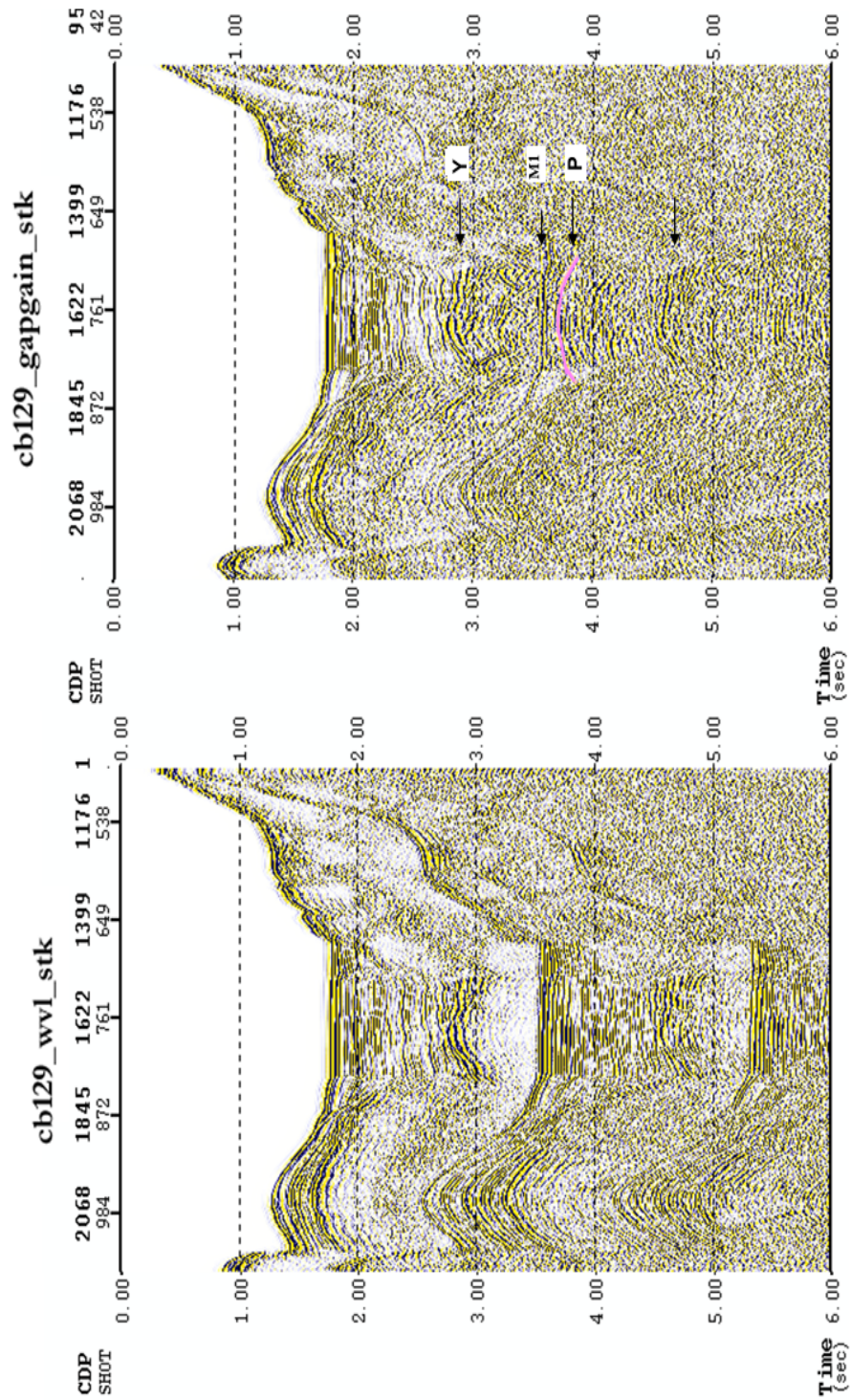


Figure 2.20 USGS Line 129 prestack predictive deconvolution attenuated sea bottom multiple revealing a primary reflector at time 4 s in the Catalina Basin.

2.6 Imaging with multiples

Processing of LARSE reflection data using basic methods of spiking and predictive deconvolution was not successful in attenuating sea bottom multiples. The SRME method was designed to remove all surface-related multiple energy by prestack inversion, and it also did not succeed in producing interpretable seismic sections.

Prestack reverse time migration (RTM) has been used successfully to remove multiples in other areas. RTM uses multiples as signal rather than noise to process real seismic data and to model data (Zhou, 2014. Youn and Zhou, 2001). Two-way wave equation migration methods consider the whole seismic wavefield as the input, without distinguishing the primaries from the multiples. RTM was used to improve images of the onshore segments of LARSE lines 1 and 2 (Thornton and Zhou, 2008.) The present study applies RTM to de-mask the multiple artifact in the offshore segments of LARSE lines 1 and 2, which cross Santa Catalina Basin in the ICB. Chapter 3 covers in detail the RTM process and results.

2.6.1 An example of RTM using synthetic data: This example from Youn and Zhou, 2001, demonstrates how prestack RTM with multiples program using synthetic shots acquired over a simple multiple-generating model (Figure 2.21) can attenuate sea bottom multiples to produce accurate migrated depth image. The model has four layers with a porous reservoir in layer 3. The parameters of model were so designed with high velocity contrasts that generate abundant water bottom multiples. Figure 2.22 is a shot gather with nine orders of sea bottom multiples.

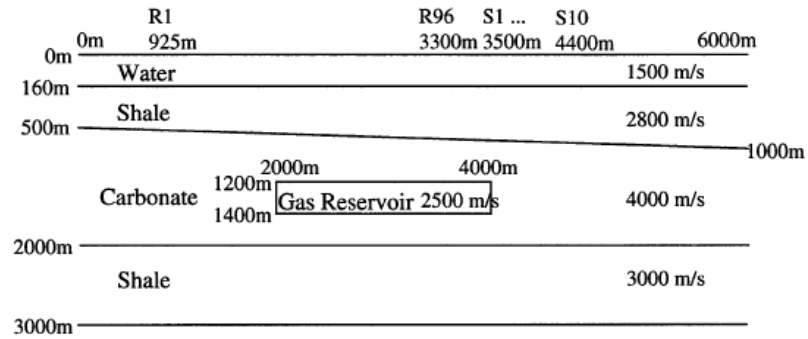


Figure 2.21 A simple multiple generating model showing velocity-depth and shooting geometry.
(From Youn and Zhou, 2001)

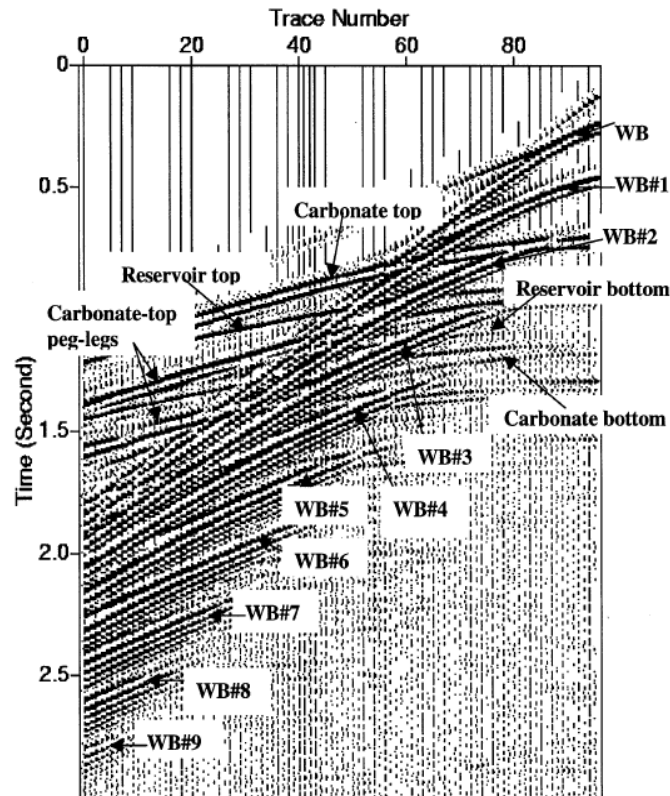


Figure 2.22 Shot gather of shot 10 showing water bottom multiples down to 9th order.
(From Youn and Zhou, 2001)

The RTM stack section (Figure 2.23) shows water bottom, top of carbonate, reservoir compartment, and base of carbonate with accurate locations with accurate dip. This is an application of the use of noise free synthetic data.

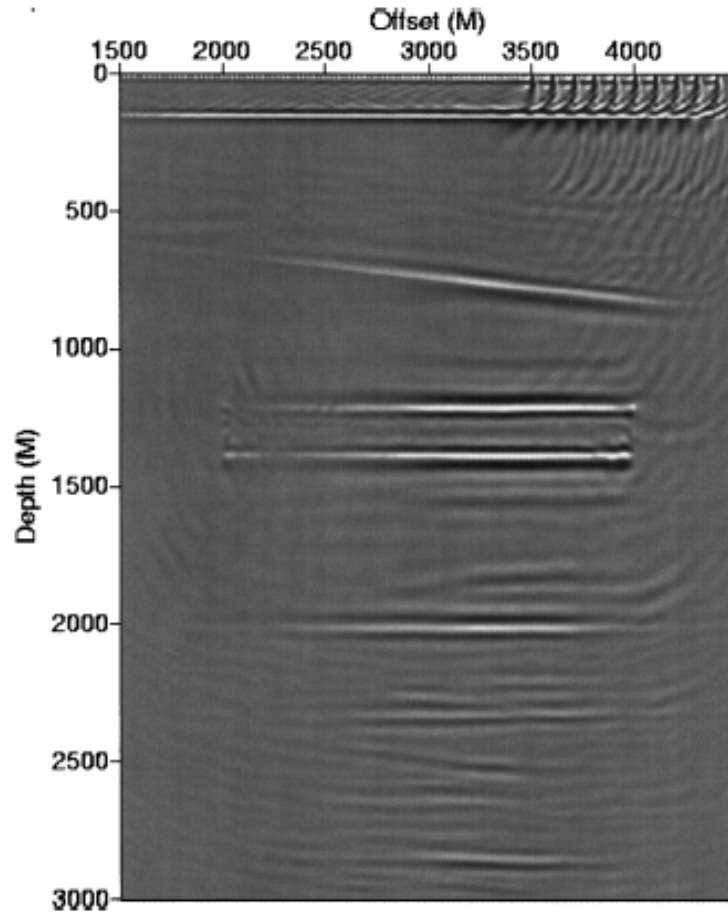


Figure 2.23 RTM with multiples stack section using correct velocities. (From Youn and Zhou, 2001)

Applying RTM to the LARSE data, which has high noise content and was recorded over a complex subsurface structure, presents a greater challenge. The results of RTM applied to two LARSE lines are shown below with a comparison of constant water velocity stack sections to show the magnitude of the sea bottom multiple noise. The following two pairs of displays show constant water multiple stack with comparison of RTM depth images.

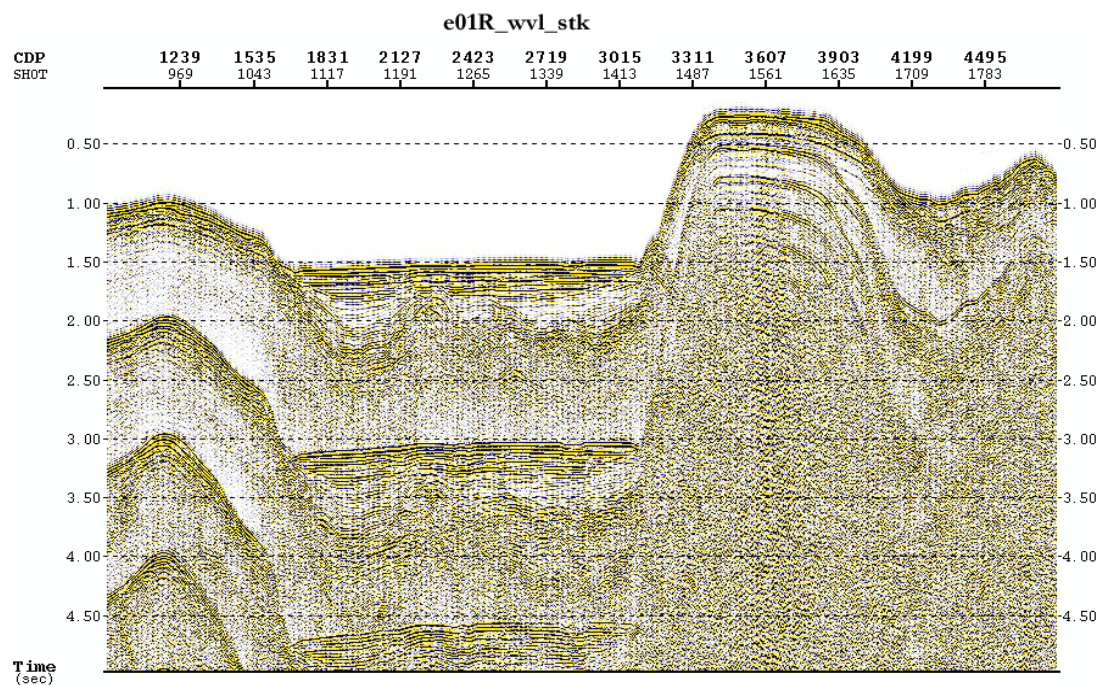


Figure 2.24 LARSE Line 1 constant water velocity stack. Input shot gathers that produced this stack were input to RTM program that produced the display below.

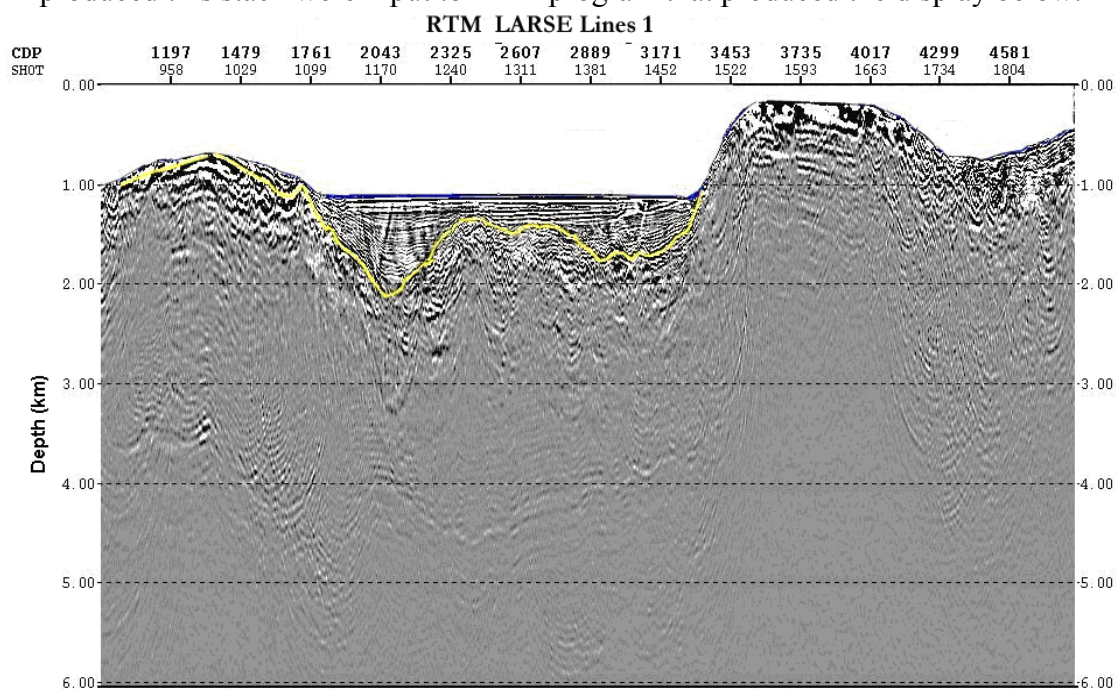


Figure 2.25 Reverse time migration of LARSE Line 1 in depth.

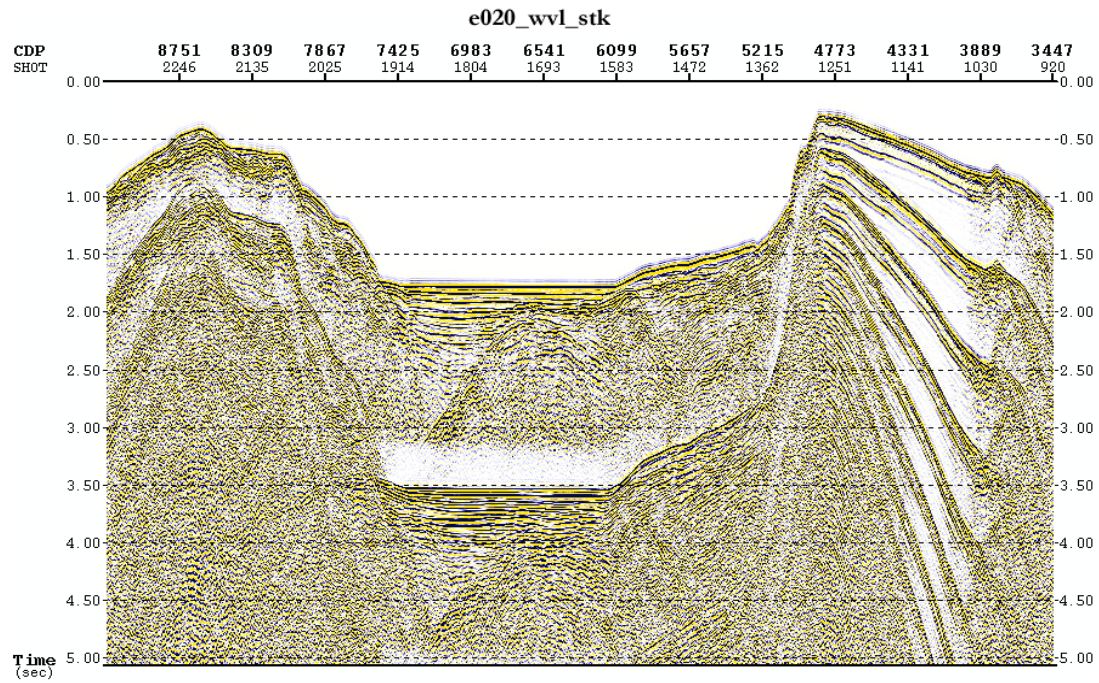


Figure 2.26 LARSE Line 2 constant water velocity stack. Input shot gathers that produced this stack were input to RTM program that produced the display below

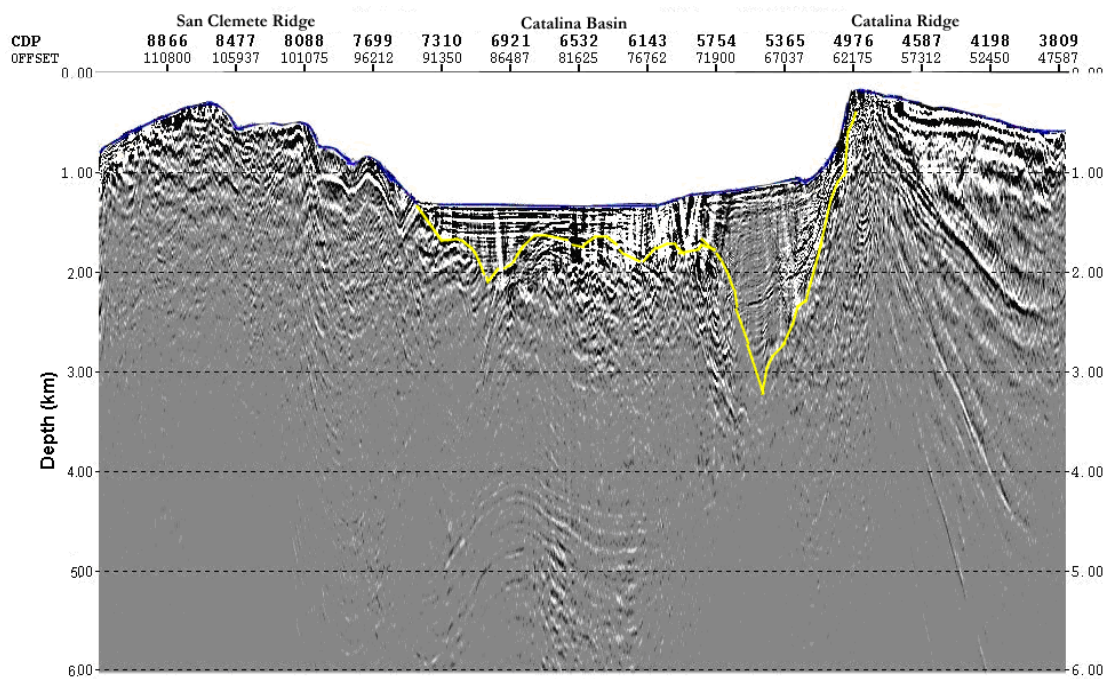


Figure 2.27 Reverse time migration of LARSE Line 2 in depth

The contrast of constant water velocity stacks and RTM depth images is remarkable in that the sea bottom multiples have been successfully attenuated showing high definition subsurface events. The shallow sedimentary section shows high resolution layering with truncations against unconformities. The yellow marker is an unconformity at the base of the Miocene strata. Concordant and continuous reflections on depth sections below the yellow marker to 6 km depth are similar to reflections from known forearc strata in the area. Strong reflection events between 3.5 to 4.5 km on line 1 and 4 to 5 km depths on line 2 were not evident in previous studies. The reprocessing of vintage seismic data by applying RTM to the data has successfully attenuated much of the sea bottom multiple artifact and dramatically improved the possibility to interpret the deeper structure and stratigraphy of the California borderland.

3. Depth imaging of LARSE data by reverse time migration

By the use of two major regional marine reflection surveys conducted in the California continental borderland, the California borderland MCRS survey (USGS 1990) and the Los Angeles Region Seismic Experiment (LARSE), and data from several offshore drill holes, the principal lithotectonic belts that comprise the California continental borderland a model of the tectonic framework of the area has emerged (Crouch and Suppe, 1993; Bohannon and Geist, 1998a; ten Brink et al., 2000). Strong sea bottom multiples present in LARSE and USGS 1990 data sets severely limit the interpretation of deep structures because primaries beyond the first occurrence of first-order multiples are masked by this noise.

Multiples pose one of the serious problems in seismic data processing. It has been shown that deconvolution in time domain applied to LARSE data did not succeed in suppressing multiples. The problem with multiples is that they are not separable from primaries by criteria such as periodicity, moveout, velocity and spectrum. It has been shown in chapter 2 that RTM including multiples has successfully attenuated multiples from two line segments of LARSE data. The rest of this chapter gives the particulars of the method, results and comparison of previous results using the data.

3.1 Reverse time migration (RTM)

Most ray-based or one-way wave-equation migration methods use only primaries and diffractions as signals to image subsurface reflectors. Multiple reflections are regarded as noise and are eliminated prior to the imaging process. Removal of multiples is very difficult in areas where the sea bottom is hard and the bathymetry is highly variable like in the California borderland. Since multiples contain information of the target zone along their travel paths, use of multiples as signal improves illumination coverage and thereby enhances the image. The source wavelet is estimated from direct arrival of marine seismic data. The migration velocity model is derived from an integrated model building workflow, and the sharp velocity interfaces near sea bottom needs to be preserved in order to generate multiples in the forward and backward propagation steps. RTM is a pre-stack depth imaging technique. When based on a two-way wave equation, RTM uses both primaries and multiples to map reflection boundaries without identifying them as primaries or multiples. Several factors, including source wavelet, velocity model, background noise, data acquisition geometry, and preprocessing workflow may influence the quality of image.

3.2 Velocity models for reverse time migration: One of the processing requirement of RTM is a migration velocity model. The velocity model for LARSE line 1 is based on inversion of the first arrival times of wide angle LARSE data recorded by ocean bottom seismometers and onshore data (Baher et al., 2005, ten Brink et al., 2000, and Wright 1991).

First arrival times and distance from source were input to MacRay (Luegert, 1992), a two-dimensional ray tracing and forward modeling program. Verification of the velocity structure was made by comparing computed arrival times with the observed times (Figure 3.1).

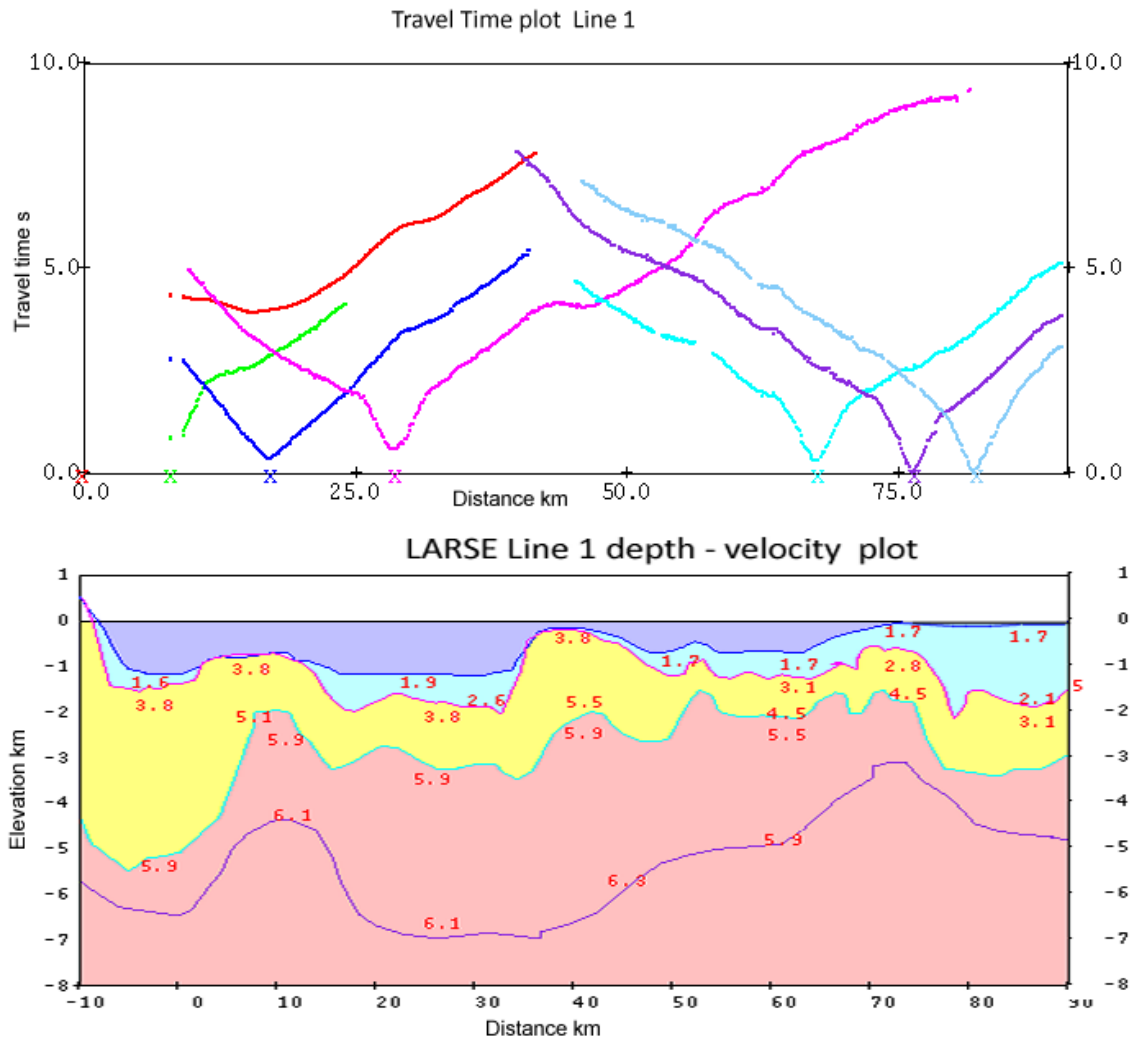


Figure 3.1 LARSE Line 1 top: OBS first arrival plot. Bottom: Five layers with variable velocity values cover the entire LARSE line 1.

Velocity functions for each CDP of LARSE line 1 were computed based by interpolation in both vertical and horizontal direction using a grid interval of 12.5 m, which is the CDP interval. These functions were input to FOCUS display program in SEG Y format (Figure

3.2). As this model is a seismic gather display and velocity bar could not be displayed but spot velocity values labeled on the displays.

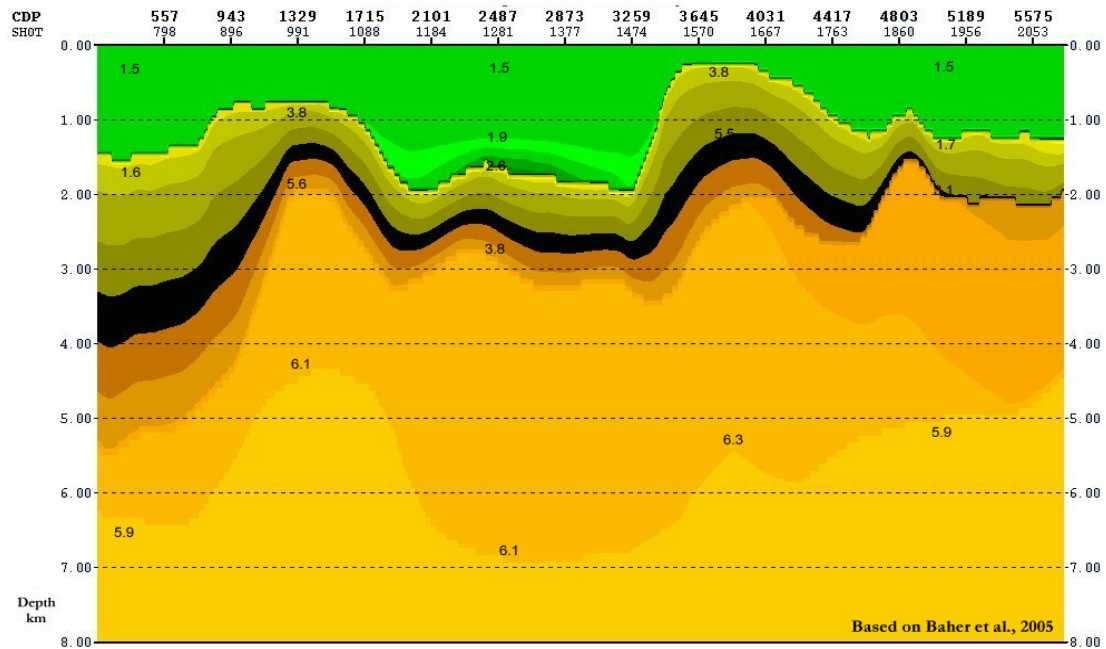


Figure 3.2 Migration velocity model for Line 1 with velocity values in km/s.

Velocity model for LARSE Line 2 was developed using results from deformable layer tomography DLT (Zhou, 2003). The input data are first arrival times of receiver gathers recorded by four ocean bottom seismometers. Constant layer velocities are obtained from other studies in the area (ten Brink et al., 2000). Figure 3.3 A shows input first arrival time plot. Figure 3.3 B shows smoothed velocity layers and Figure 3.3 C is program output of final 2D DLT depth-velocity model. Figure 3.4 is velocity model for LARSE line 2.

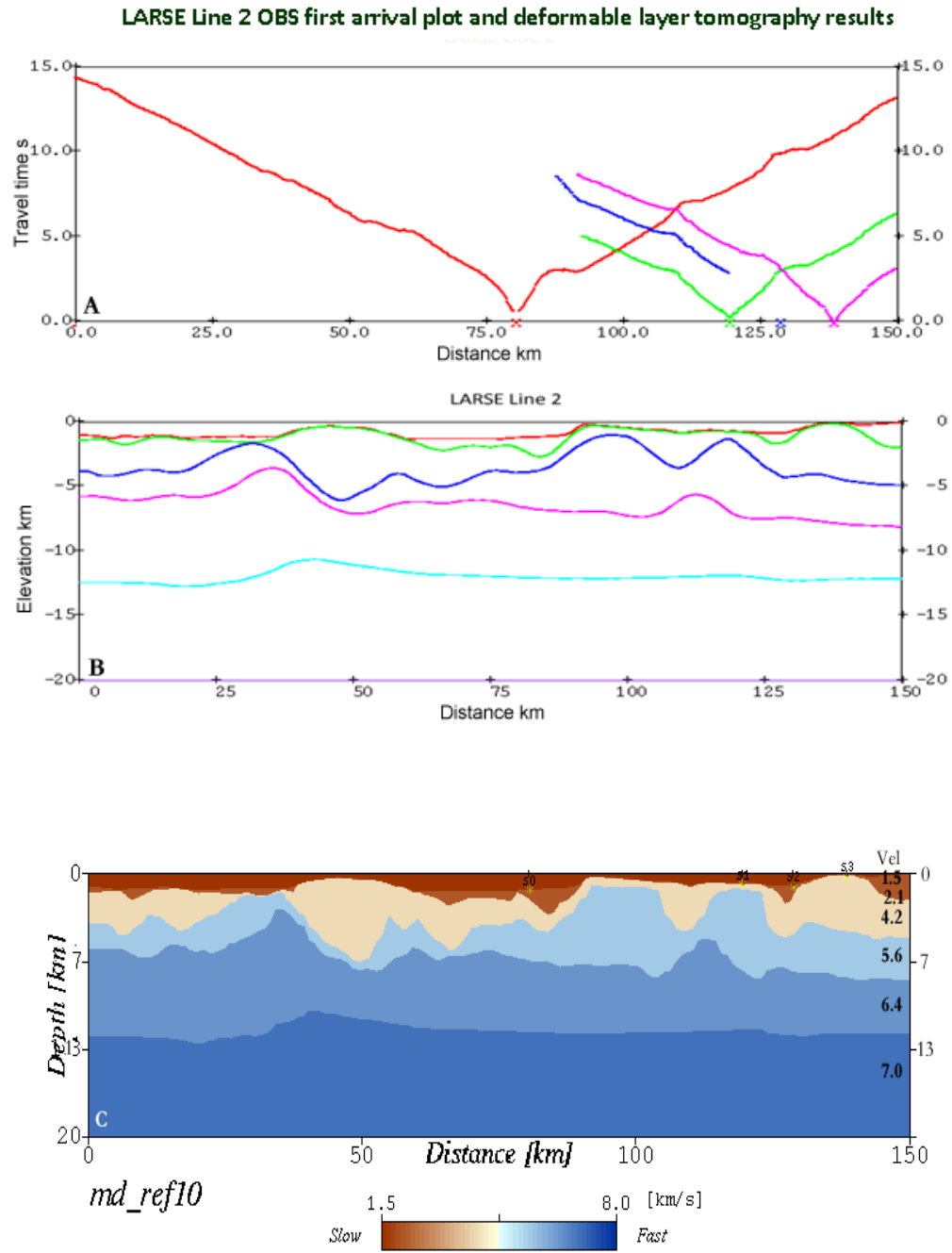


Figure 3.3 LARSE line 2 A: Travel time plots of first arrivals from OBS. B: Smoothed depths of velocity interfaces. C: Velocity depth structure from DLT program.

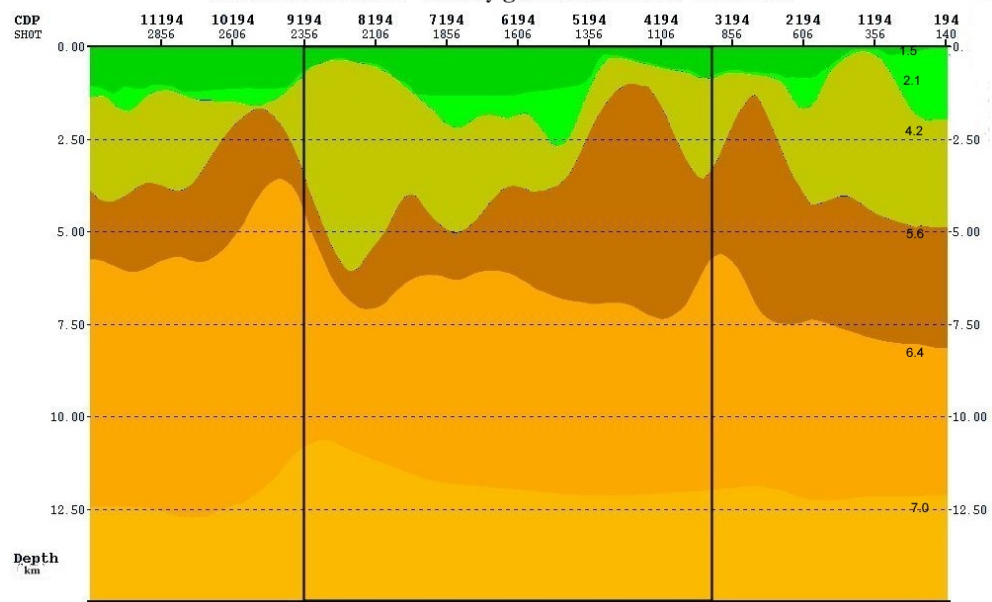


Figure 3.4 Migration velocity model for Line 2 with velocity values in km/s

3.3 Reverse time migration technique

The traditional multiple elimination methods that are based on data or model-driven have drawbacks. They involve prediction of multiple and then subtraction of multiple. Major issues include amplitude and phase that are not predicted perfectly and primaries that are affected and/or damaged in the process. The RTM method does not have these shortcomings. .

The basic steps of RTM are as follows:

1. The forward propagation wavefield is excited at source location from time zero to maximum recording time using a waveform modeling engine. The modeling engine may be based on one-way or two-way wave-equations.

2. The preconditioned data traces are time reversed as pseudo source wavelets and are excited at receiver locations to produce a reversely propagated wavefield using the modeling engine and the velocity model.
3. The forward and reversely propagated wavefields at each image grid and each time step are multiplied and summed over time to obtain a raw shot image.
4. The final stack is produced by stacking all raw shot images and then is enhanced by post processing, including amplitude balancing, filtering, and muting.

The basic steps of RTM below gives image condition:

Basic steps for RTM

- Forward propagation of wave field from source position
- Inverse propagation of wavefield from all receivers
- Apply image condition through stacking

$$I(r) = \int_0^T F(r,t)B(r,T-t)dt$$

$$I(r) = \frac{\int_0^T F(r,t)B(r,T-t)dt}{\int_0^T F(r,t)F(r,t)dt}$$

- Post stack processing to enhance image

Snapshots of down going wavefield from source and up going wavefield from receiver at 800 and 2000 ms time are shown in Figure 3.5.

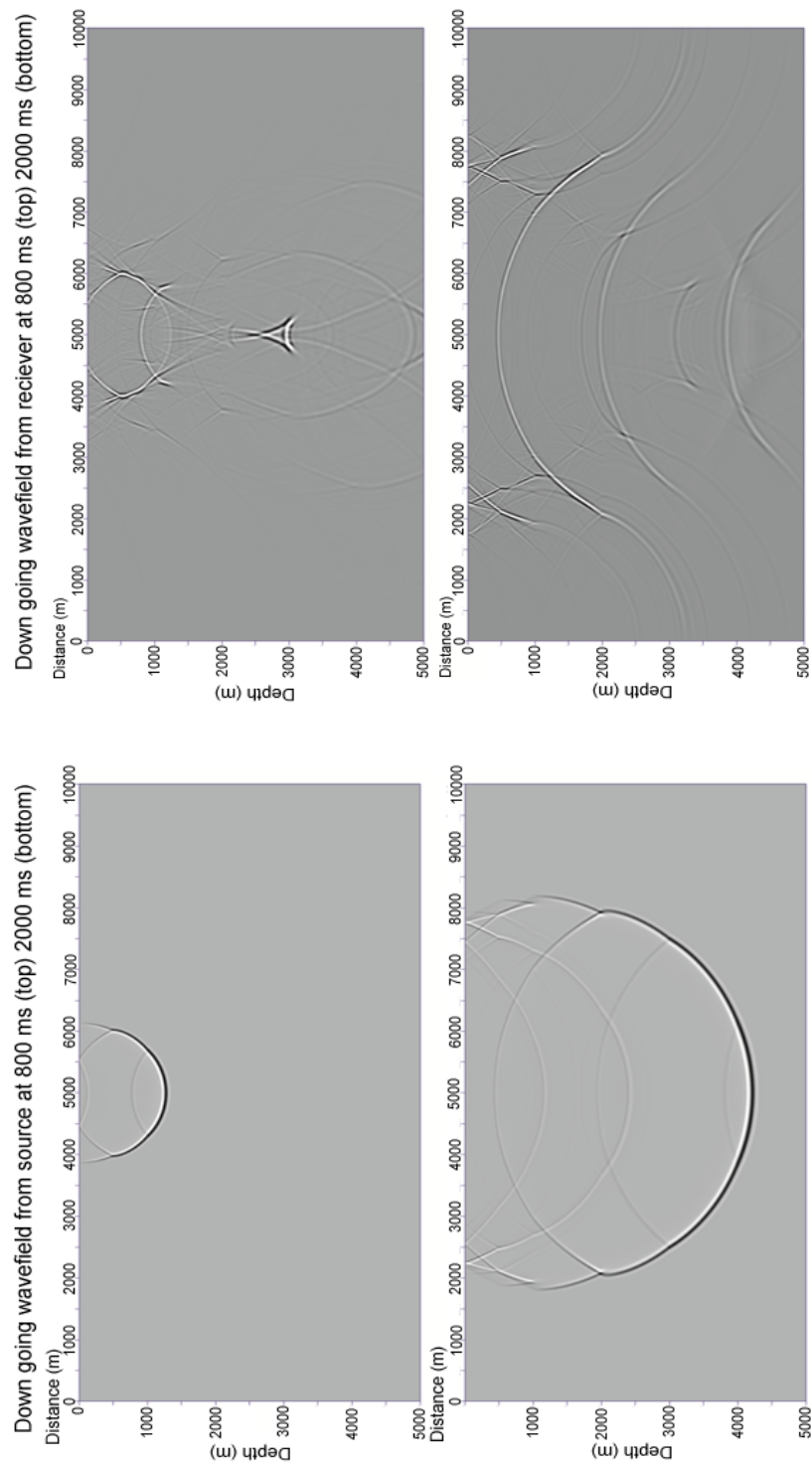


Figure 3.5 Down going and up going wavefields at 800 ms and 2000 ms of a flat layer velocity model.

In this study, a finite difference modeling approach with up to eighth-order accuracy in space and second-order accuracy in time was used as the modeling engine to produce primary and multiple reflections. A free surface boundary condition was used at the sea surface to generate multiples, and absorbing boundary conditions were used to eliminate reflections from three artificial boundaries of the migration velocity model.

Factors that influence the quality of RTM images are: the source wavelet, velocity model, background noise, data acquisition geometry and preprocessing workflow. The sharp velocity interface near sea bottom is preserved in order to generate multiples in the forward and backward propagation steps. Strong amplitude and low frequency marine background noise are removed before the migration process.

Artifacts observed on the shallow portion of the raw migration results are generated by the RTM process. They are produced where high velocity contrast exists at the sea bottom interface. They are also produced when diving waves, head waves, or backscattered waves cross-correlate (Guitton et al, 2007).

3.4 Results and discussion

Comparison of conventional seismic depth profile (Figure 3.6a, ten Brink et al., 2000) with RTM depth profiles produced in this study (Figure 3.6b) shows some of the most prominent events on the conventional profiles are probably artifacts produced by multiples. In the RTM depth profiles, due to the process of de-masking of multiples, the

primary reflections have been significantly enhanced, resulting in higher resolution of structural and stratigraphic features in both shallow and deeper parts of the profile.

Five stratigraphic units are recognized on the RTM depth images of the Catalina Basin and Ridge area (Figure 3.6b and 3.7b). Unit 1 includes the near-horizontal reflectors from the sea bottom to the green horizon. Unit 2 underlies Unit 1 and consists of discontinuous and deformed strata in places. The base of Unit 2 is the yellow horizon, which truncates some of the strata in Unit 1. Unit 3 is the interval between the yellow and pink horizons with discontinuous and deformed strata in the upper part. Unit 4 includes the pink reflector and underlying reflectors that range to depths of 3.5 to 5 km. These strata are near-horizontal when the vertical scale is not exaggerated and contrast sharply with the shape of the base of Unit 2. Since near-horizontal reflectors underlie and overlie Unit 2, the base of Unit 2 is probably an erosional surface and not cut by faults. The top part of Catalina Ridge with strong, northeast-dipping irregular reflectors is Unit 5.

Sparse data are available to definitively determine the identification and age of the five stratigraphic units defined above. Miocene volcanic rocks crop out on San Clemente Island. Miocene volcanic rocks, a Miocene quartz diorite pluton and the Mesozoic Catalina Schist facies crop out on Santa Catalina Island. Sea bottom samples are probably detritus from all of these outcrops, which are separated from the Catalina Basin section by major basin-bounding faults and not necessarily reliable indicators of the lithologies of the underlying subsurface strata.

Unit 1 and Unit 2 are generally equivalent to the Pliocene and younger strata and Miocene syntectonic fill strata respectively, mapped on USGS 1990 Line 120 (Bohannon and Geist, 1998a), about 30 km east of LARSE Line 1, but RTM profiles are of higher resolution. The age correlations are loosely based on reflectivity similarities to coastal seismic lines that are tied to well data. The interval below the yellow horizon is probably what most who work in the area would consider “basement,” that is, the Mesozoic Catalina Schist, but the depth of “basement” in the Catalina Basin has not been clearly defined in published papers (Vedder, 1987, Crouch and Suppe, 1993, Bohannon and Geist, 1998).

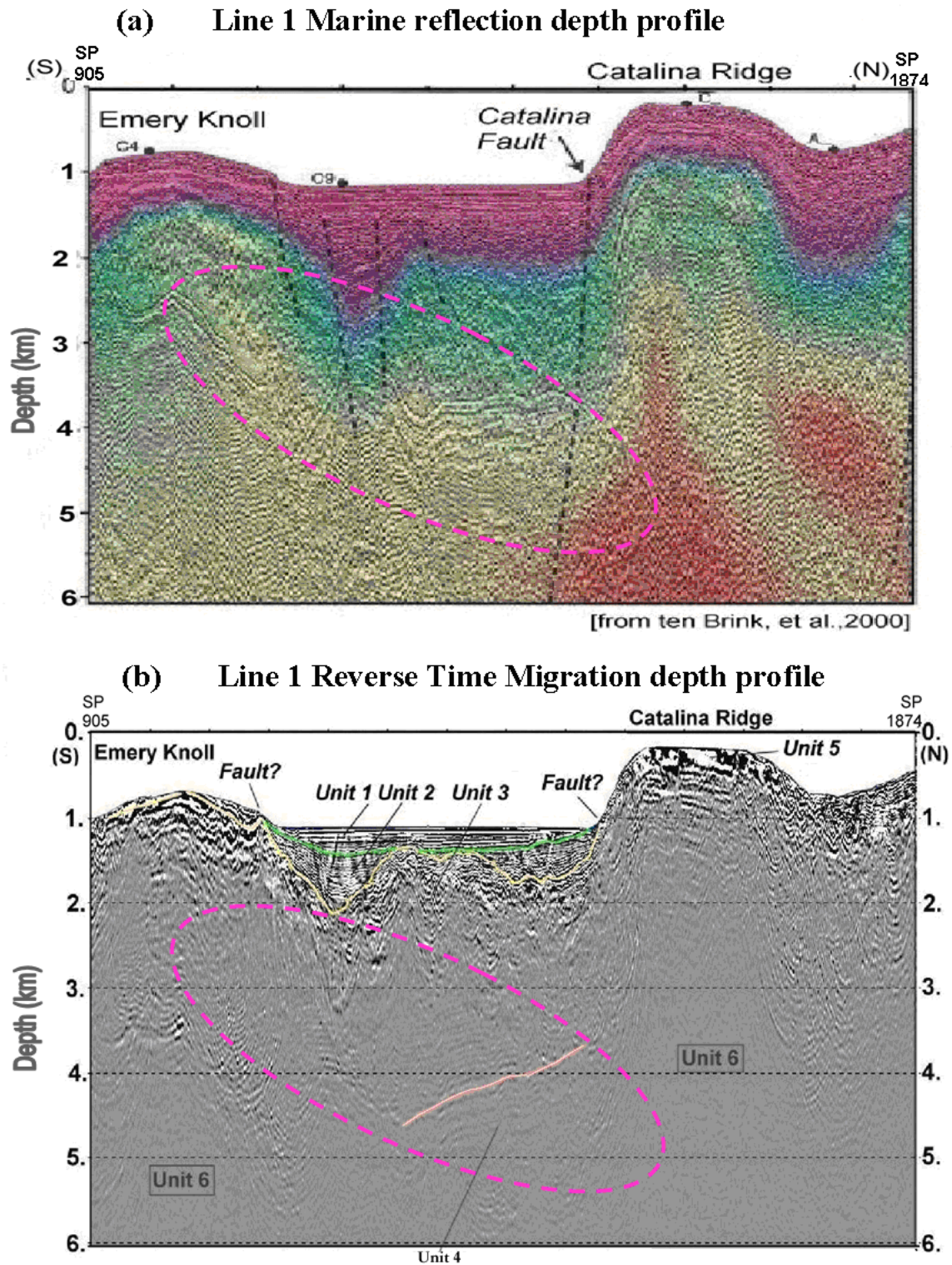


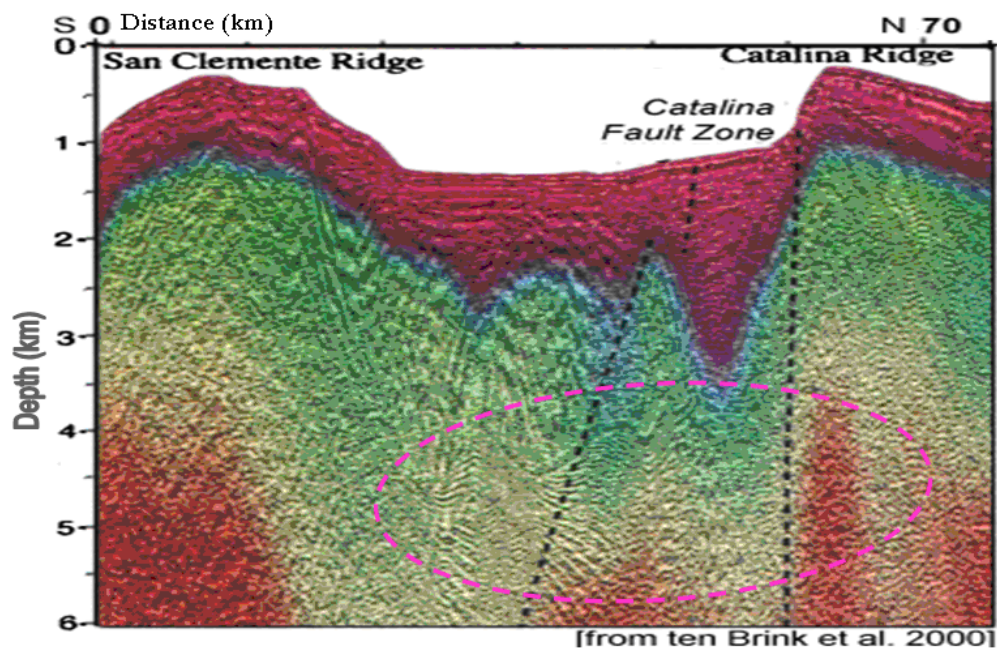
Figure 3.6 Comparison of Line 1 conventional processing with RTM depth profile

Definitive lithological and age data on Units 3, 4, and 5 are lacking in the Catalina Basin and Ridge area. Deep reflectors, such as the top of Unit 4, are masked by the reflection artifact on published seismic profiles (e.g. Bohannon and Geist, 1998; ten Brink et al., 2000). Several interpretations of these stratigraphic units are possible, including the following:

1. The seismic characteristics of Unit 3 and 4 are similar to those of the Paleogene to Cretaceous forearc section of the Outer Continental Belt (OCB), which Bohannon and Geist (1998) described as a section of “pronounced reflectivity”. Forearc strata would indicate the presence of a heretofore unknown, narrow, deep Miocene basin. Such a basin could have potential for hydrocarbon accumulations.
2. The continuous reflector at the top of Unit 4 may be upper Cretaceous unconformity.
3. The Unit 5 reflectors may be Miocene intrusive rocks such as diorite sills in a section of unknown lithology or age.

The shallow, strong, northeast-dipping reflectors of Unit 5 on Santa Catalina Ridge are possibly Miocene volcanic rocks similar to those that crop out on Santa Catalina Island and San Clemente Island. Volcanic rocks would tend to resist erosion and cap bathymetric and topographic high areas. Some of these reflectors are interbed multiples, possibly from volcanic flows, that were not de-masked by the limited RTM process.

(c) Line 2 Marine reflection depth profile



(d) Line 2 Reverse Time Migration depth profile

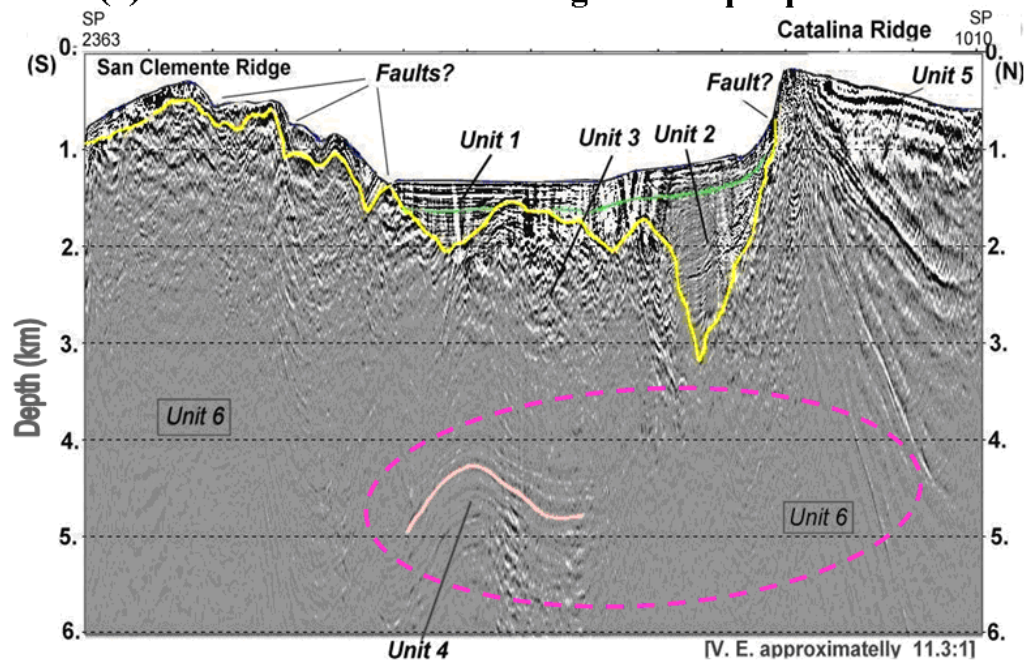
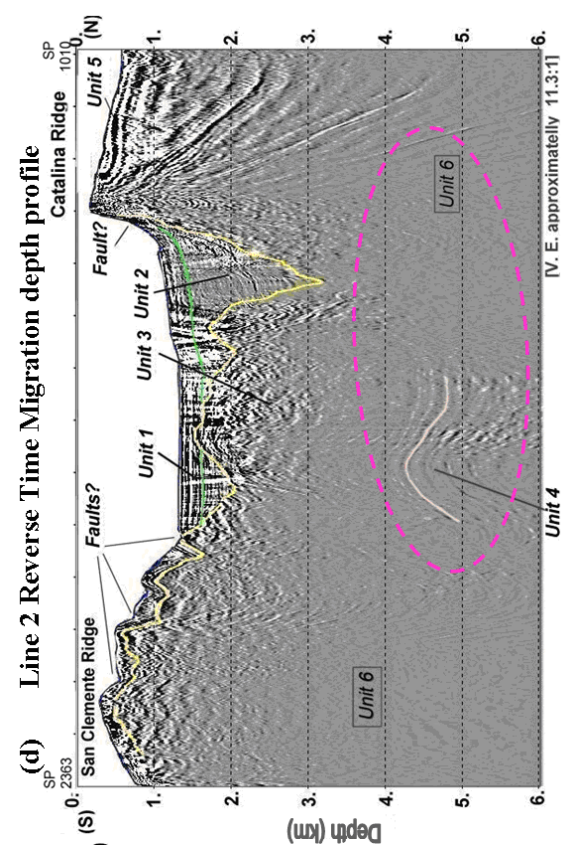
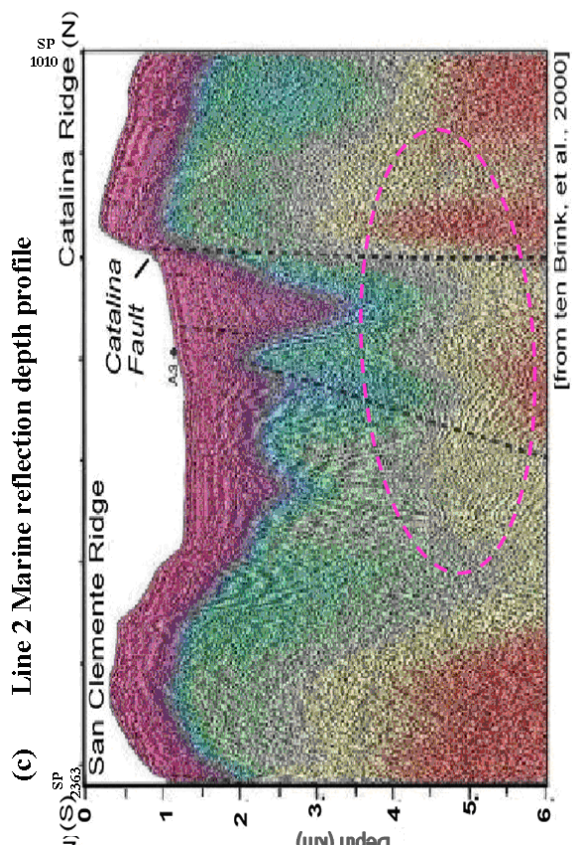
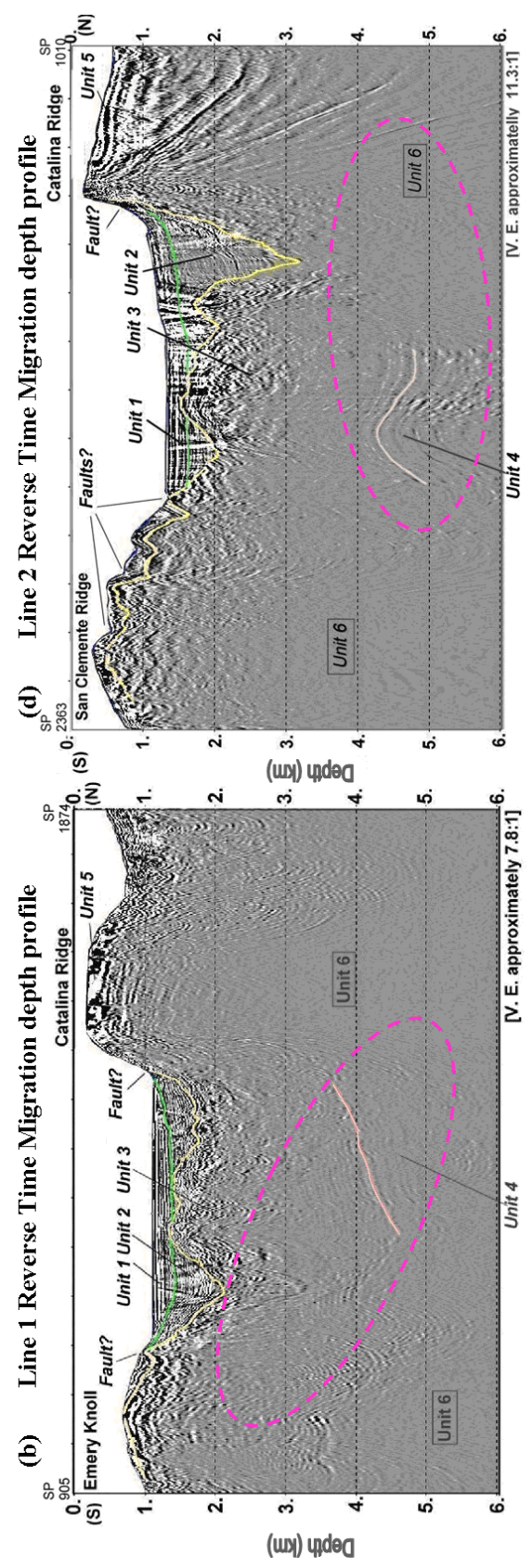
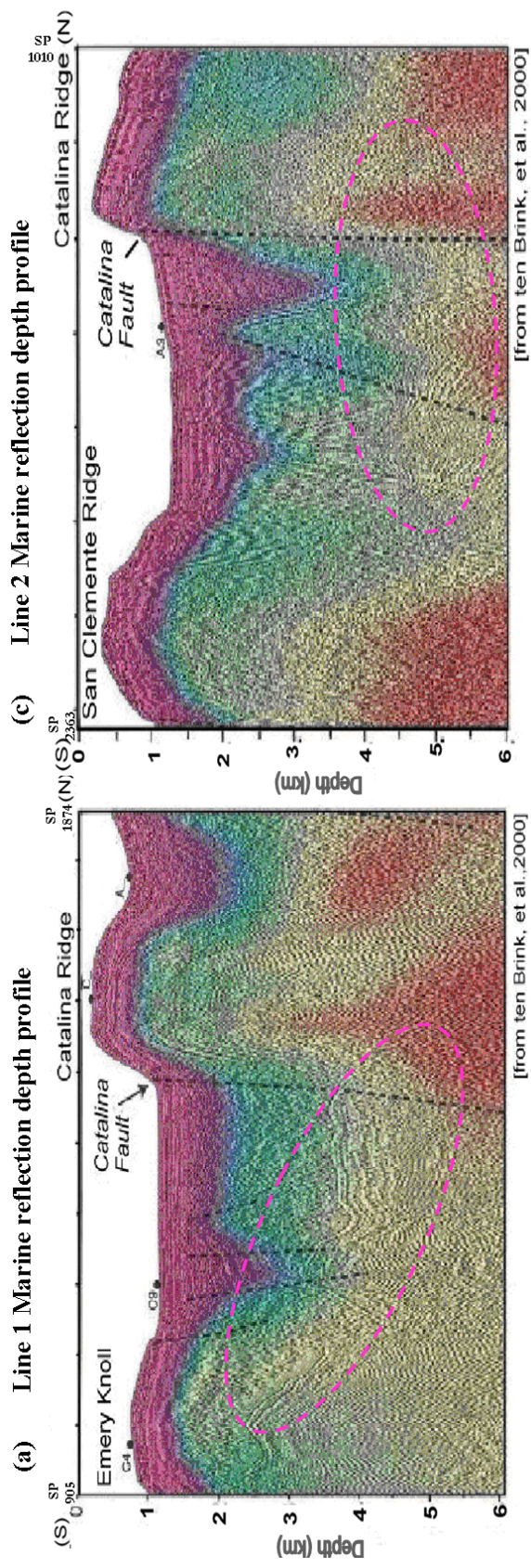


Figure 3.7 Comparison of Line 2 conventional processing with RTM depth profile

Unit 6 consists of possible plutons that may underlie San Clemente Island, Santa Catalina Island and Emery Knoll based on the absence of reflectors on RTM profiles (Figure 3.6b and 3.7d). The presence of Miocene plutons in the upper crust has been inferred from gravity and magnetic data and outcrops on Santa Catalina Island (Rowland, 1984; Ridgway and Zumberge, 2007). Tomographic results and the distribution of overlying volcanic rocks suggest the presence of a diorite pluton in the subsurface of the southeastern Los Angeles Basin (Bjorklund, et al., 2002). Volcanic rocks are interbedded with Miocene strata that are present throughout the ICB. The source of these igneous bodies could be an underplated fossil oceanic layer at the base of the continental crust in the transition zone of a stalled segment of the Pacific subducting plate (Crandall et al., 1983; Miller et al., 1992; Brocher et al., 1999).

Figure 3.8 (a) and (c) LARSE Lines 1 and 2 reflection depth profiles with color overlays of velocity model [plate 1 a and b, ten Brink et al., 2000]. (b) and (d) LARSE Lines 1 and 2 RTM depth sections. The dashed ellipses in color highlight places where many events in (a) and (c) are likely multiple artifacts. Labeled in (b) and (d): Unit 1 = Pliocene and younger strata and Unit 2 = probably Miocene syntectonic strata after Bohannon and Geist (1998). The base of Unit 1 is the green line. The base of Unit 2 is the yellow line. Unit 3 = Strata between the yellow and pink lines. Unit 4 = pronounced reflectors at 4-5 km. The top of Unit 4 is the pink line. The age and lithology of strata below probably the Miocene Unit 2 are unknown. Unit 5 = strong, near surface reflectors on Catalina Ridge. The strong events may represent Miocene volcanic strata. Unit 6 is an area characterized by the absence of reflectors that may indicate the general location of a shallow, Miocene, igneous intrusion (pluton) underlying a bathymetric high



Encouraged by RTM results that reveal stratigraphic units that were misinterpreted or not evident in the previous studies, re-processing and interpretation of the USGS 1990 marine reflection data led to the recognition of sedimentary strata in the Santa Catalina Basin underlying Neogene strata. The deeper strata recognized on the reprocessed seismic data and the RTM data generally correlate with Miocene volcanic rocks and the underlying Cretaceous-Paleogene forearc section penetrated by OCS drill hole P 289, which is located in the inner continental borderland.

4. Processing and interpretation of USGS 1990 data

The LARSE survey mainly covers the inner borderland and extends into the outer borderland. The USGS 1990 survey covers the entire California continental borderland (Figure 4.1). The study area is between longitudes 120 and 117 degrees W and latitudes 32.2 and 34 degrees N covering both inner and outer borderlands. The Santa Catalina Basin lies between the Santa Catalina Island and San Clemente Island and trends southeast to northwest direction. The purpose of reprocessing the USGS data is to establish stratigraphic correlations between well OCS-CAL P 289 and the LARSE lines along the axial area of the Santa Catalina Basin. The problem of sea bottom multiples in the USGS 1990 data is less severe compared to the LARSE data. The key wells that

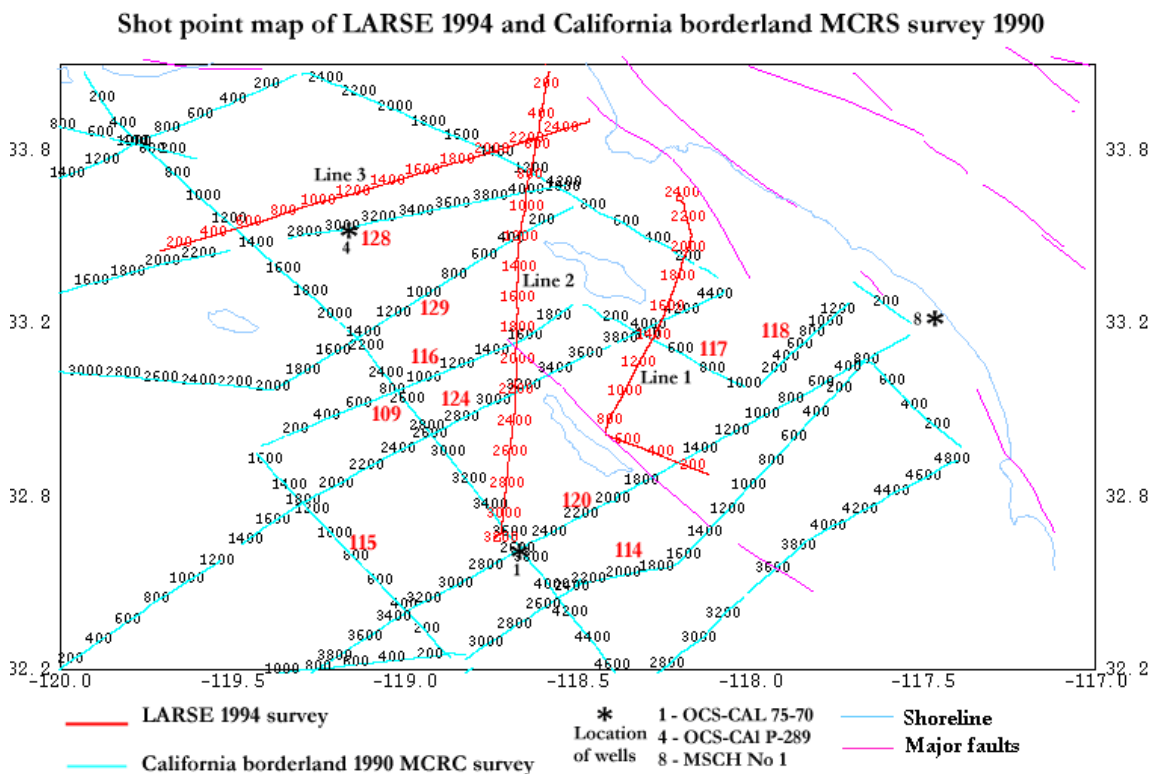


Figure 4.1 Shot point map of LARSE 1994 and USGS 1990 surveys.

penetrate Cretaceous-Paleogene strata and can be correlated with seismic data are 75-70 and P289. Well MSCH 1 penetrates Peninsular Ranges Miocene strata. The key lines for this study are LARSE lines 1 and 2 and USGS lines 109, 128 and 129.

4.1 Well Data: Deep stratigraphic wells in the area provide direct stratigraphic and velocity information of the shallow crust of the borderlands. Three important deep stratigraphic wells are: 1 OCS-CAL 75-70 in OCB, 4 MOBIL OCS P289 and 8 MSCH 1 (Figure 4.1). Well 75-70 penetrated Miocene and volcanic rocks overlaying Cretaceous-Paleogene forearc strata at a total depth of 3300 meters (Figure 4.2). The stratigraphic section encountered in this well is representative of the outer borderland lithotectonic belt. The well provides depths of formation tops, velocities and seismic two-way travel times for correlation with reflections on USGS line 120.

Well 1, Fig. 2, Bohannon et al. 1998
 Deep Stratigraphic Test OCS-CAL 75-70 NO. 1
 Cortes Bank, Total Depth = 3300 m

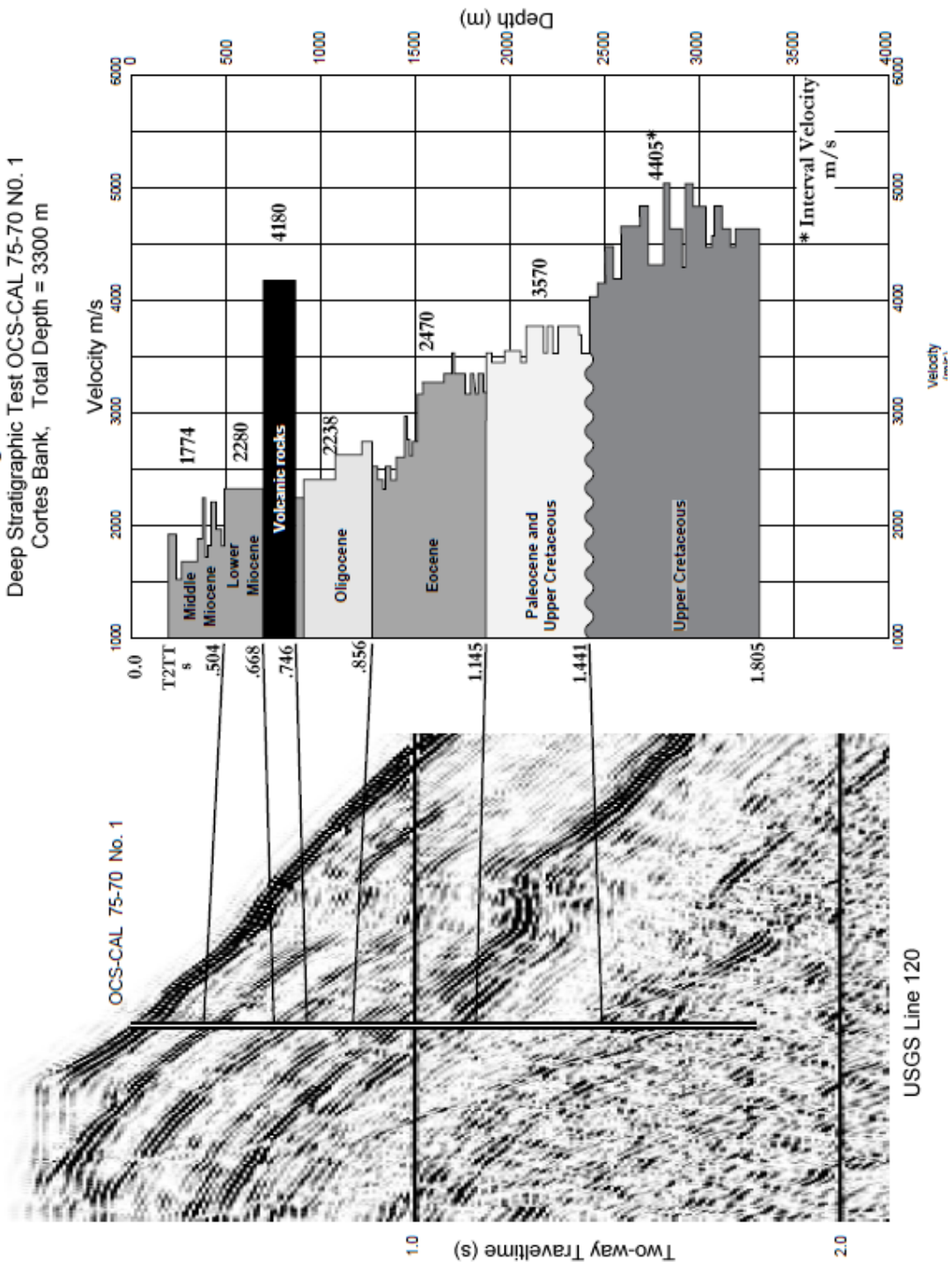


Figure 4.2 Lithology-velocity plot of well 1 located in the outer Continental borderland with two-way time correlated to USGS Line 120. All related values are given in the table below.
 (Modified from Bohannon et al., 1998)

Table 4.1 Cortes Bank OCS-CAL 75-70 N0. 1 well

Well	OCS-CAL 75-70 No. 1 Depth range of samples:410 – 3074 m
Age	Late Cretaceous to Miocene
Location	Cortes Bank Area, offshore southern California

Formation	Depth in meters below sea bottom	Velocity m/s
Middle Miocene and Lower (?)	225-696	1773, 2280
Volcanic rocks	695-867	4180
Oligocene sandstone and shale	869-1277	2238
Upper Eocene shale	1277-1393	2470
Eocene sandstone	1393-1628	
Eocene shale	1628 -1871	
Upper Cretaceous - Paleocene	1871–2428	3570
Upper Cretaceous	2428-3328	4405

Table 4.2 Santa Barbara Island OCS P289 well

Well	Mobil OCS P 289 No. 4 Depth range of samples: 140 – 2620 m
Age	Cretaceous to Miocene
Location	Near Santa Barbara Island

Formation	Depth in meters below sea bottom	Two-way time s
Miocene	138-914	1.859
Volcanic rocks	914-1345	1.014
Oligocene	1345-1827	1.220
Upper Eocene	1827-2155	1.652
Paleocene	2155-2500	1.917
Upper Cretaceous	2500-2620	2.110

Table 4.3 Mobil San Clemente core hole No. 1

Well	Mobil MSCH 1 No. 8 Depth range: 0 -1840 m
Age	Upper Miocene to Miocene San Onofre Breccia
Location	On the shelf a few km to NE end of USGS line 120

Formation	Thickness m
Upper Miocene sandstone and shale	930
Miocene Monterey Formation	480
Middle Miocene San Onofre Breccia	430

The well penetrated undifferentiated Miocene strata of Peninsular Ranges belt at total depth. Outcrop data indicate that Cretaceous-Paleogene forearc strata are present below the total depth of the well. The well location is east of Newport-Inglewood fault.

4.2 Seismic data processing of USGS 1990 data

Basic processing of USGS lines 128, 129, and 109 was performed by using spiking and predictive deconvolution by the use of long operators. Spiking deconvolution using 151 samples for operator length and predictive deconvolution with 151 sample operator plus zero crossing time gave sections with higher resolution and attenuation of multiples.

Lines 128 and 129 cross the northwest part of the Santa Catalina Basin and intersect with LARSE line 2 (Figure 4.1). Line 128 crosses the only well in the inner borderland that has penetrated Cretaceous-Paleogene forearc strata. USGS Line 109 is located along the axis of the San Nicolas Basin near several stratigraphic wells and crosses Lines 128 and 129. Correlations between these seismic lines, the nearby wells and the LARSE seismic

lines provide important new constraints on the areal distribution of pre-Neogene strata in the California borderland.

4.2.1 Line 128: MOBIL OCS P289 well, drilled to a depth of 2620 m, is located close to USGS Line 128 (Figure 4.3) that traverses Santa Rosa-Cortes Ridge, Santa Cruz Basin and Santa Cruz–Santa Catalina Ridge. There is uncertainty about the location of the well. The only information that is available are X and Y co-ordinates (1099205, 513563); and exploration report (<http://www.boem.gov/2014-667-2011-National-Assessment/>) of OCS Report BOEM 2014-667 2011 states: “Well (OCS-P 289 #1) was drilled across a fault immediately east of the Santa Cruz basin.”

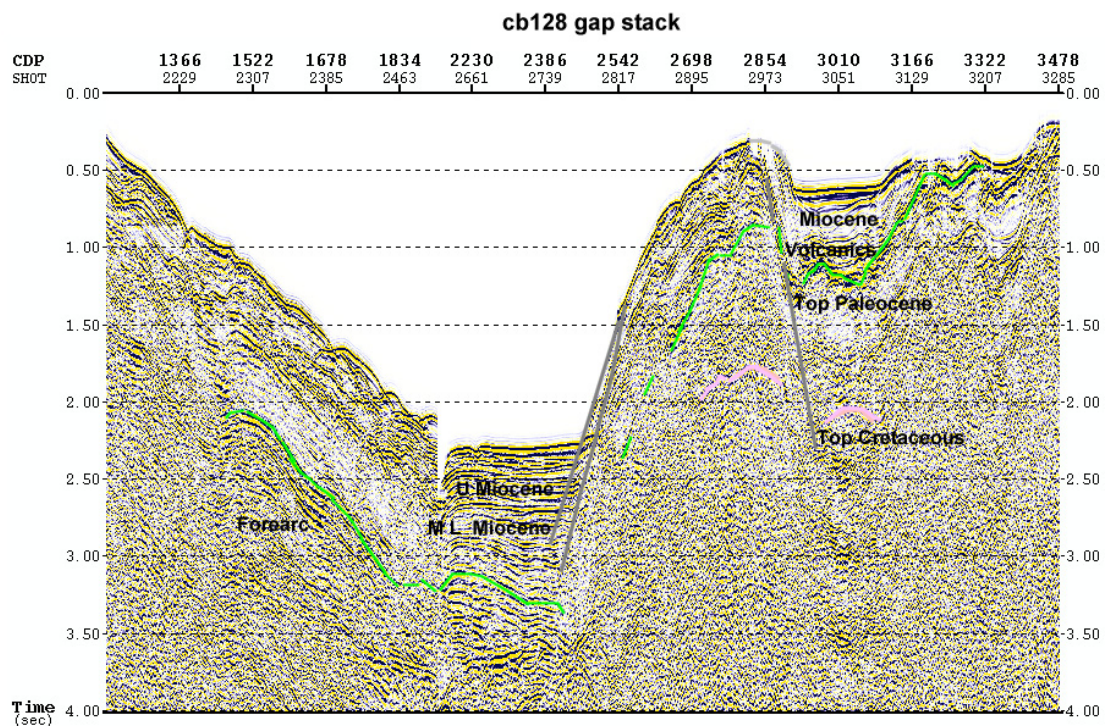


Figure 4.3 Shows interpretation of Miocene and top of forearc sedimentary section in the Santa Cruz Basin.

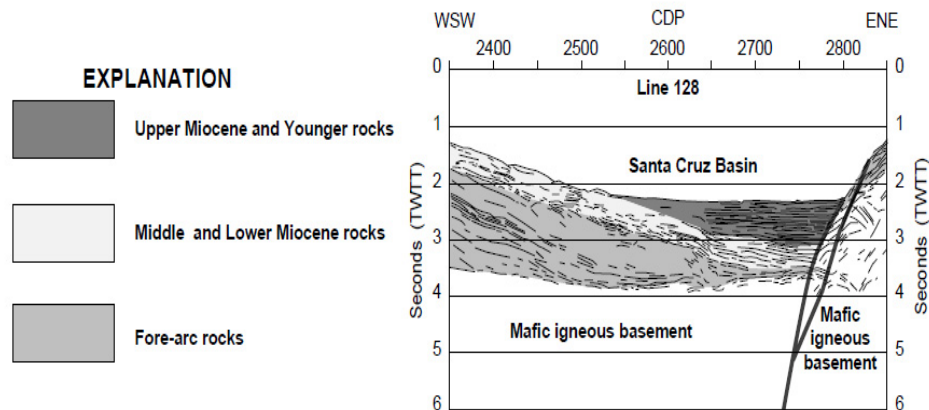


Figure 4.4 Line drawing of west end of Line 128 with interpretation of Cretaceous-Paleogene and Neogene sedimentary strata (Bohannon et al., 1998).

Upper Miocene, middle and lower Miocene and forearc sections are identified in San Nicolas Basin (Figure 4.3) using Bohannon et al., 1998 line drawing (Figure 4.4). This line drawing also shows location of East Santa Cruz Basin Fault. This feature establishes that the well is in the inner borderland with 765 m of Miocene, 330 m of volcanic rocks, and 345 m of Paleogene. The well is drilled into 120m of Cretaceous strata.

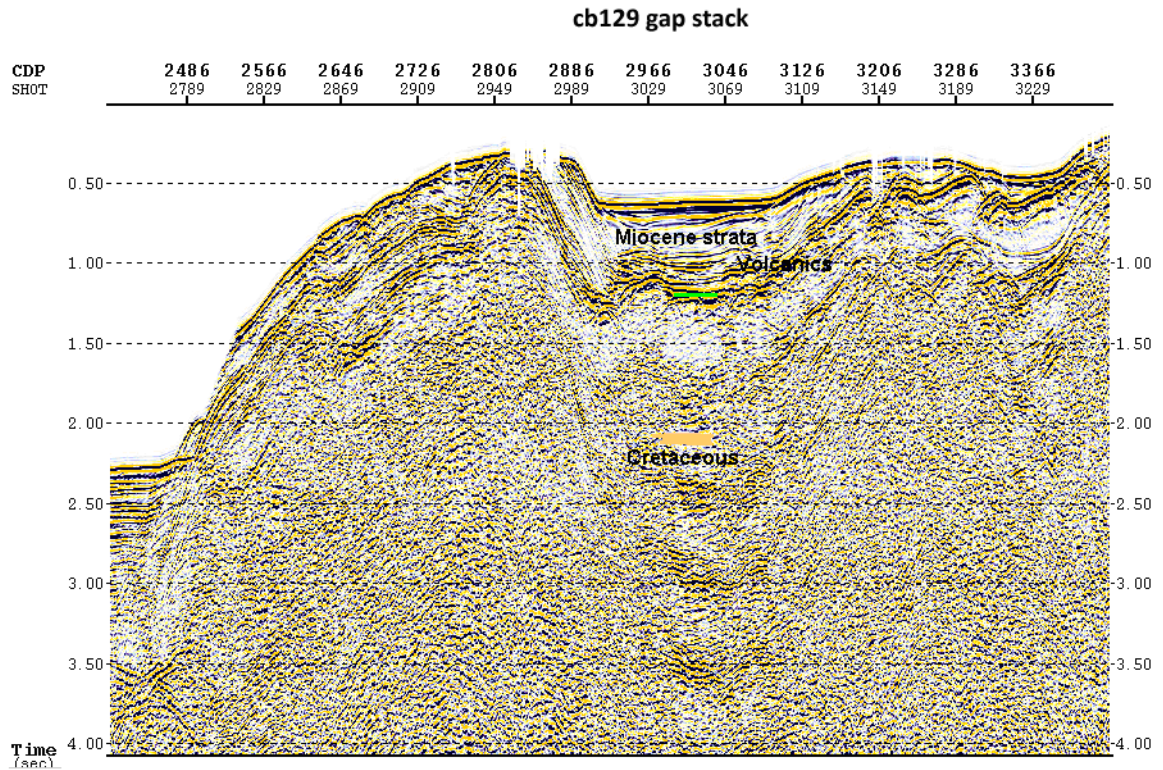


Figure 4.5 Predictive deconvolution section of Line 128 with labels of tops of Miocene and forearc stratigraphic section.

The top of Miocene column, under younger strata, is a strong reflection event. Volcanic rock column is distinct with strong events having somewhat irregular layering. This seismic character of volcanic rocks overlying the forearc section has been used in interpretation of other seismic lines. The top Oligocene of is a strong reflection event. The top of Cretaceous reflection is mapped at about 2.25 s.

4.2.2 Line 109: Seventy-five kilometers of axial Line 109 were processed for this study.

A constant water velocity stack section of line 109 over the San Nicolas Basin shows enhanced multiples and a window of primary reflectors from 2.2 s to 4.5 s in Paleogene and Neogene strata (Figure 4.6).

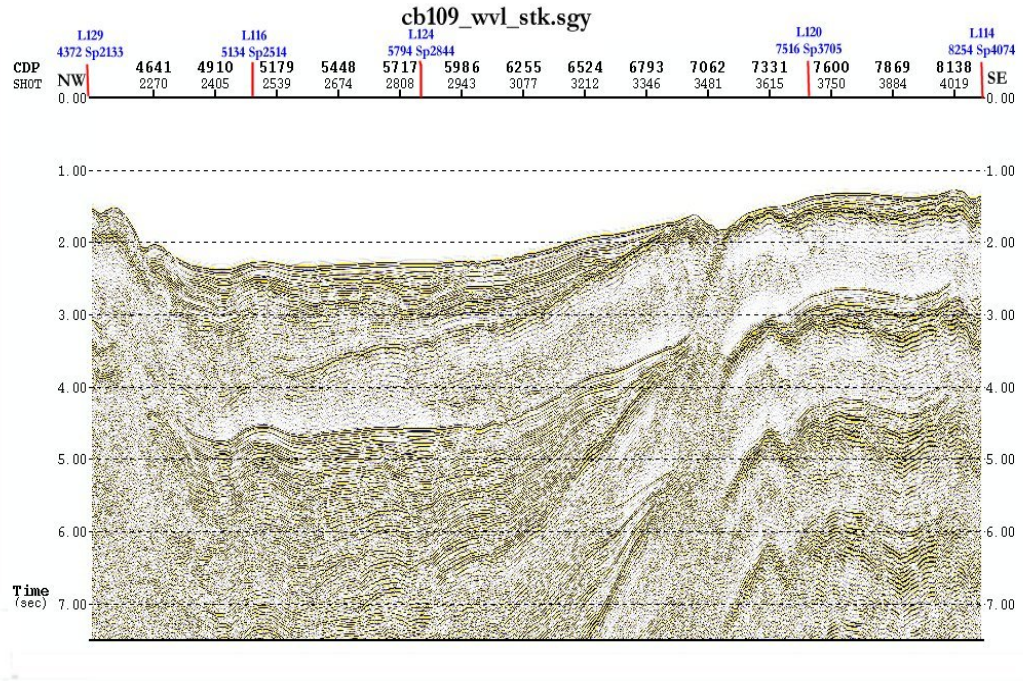


Figure 4.6 Constant water velocity stack section of line 109. Cross lines: 129, 116, 124, 120

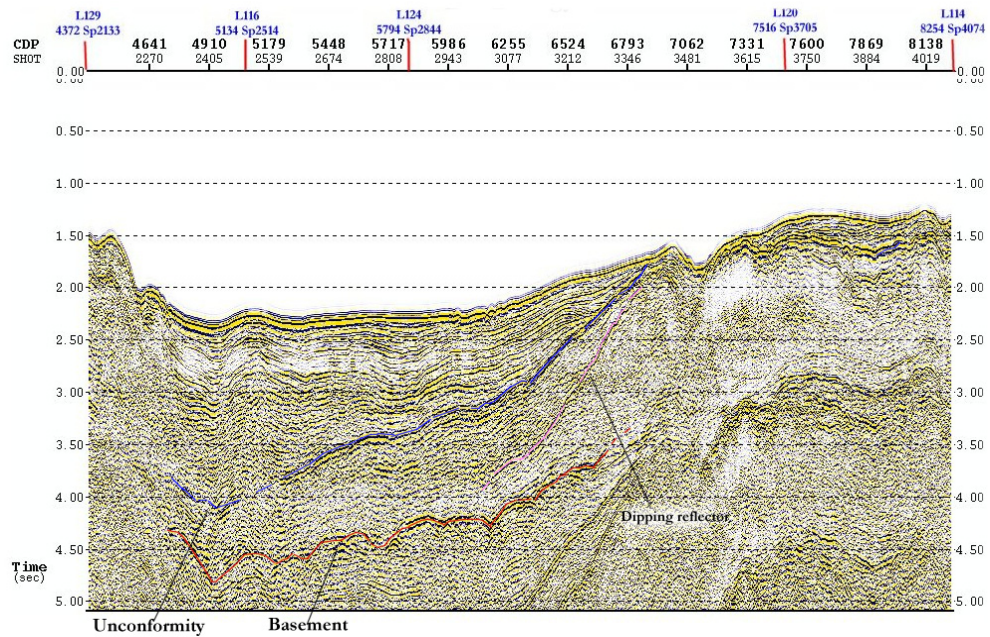


Figure 4.7 Spiking deconvolution stack section of Line 109. The blue marker is the top of forearc strata, Paleogene and Cretaceous, undifferentiated. The red marker is the top of acoustic basement, mafic igneous rocks (from Bohannon and Geist, 1998)

The seismic tops have been correlated with data from several deep stratigraphic wells on Cortes ridge adjacent to San Nicolas Basin, including well 75-70 (Figure 4.2). The discordant relationships between overlying and underlying beds at the pink marker may indicate an unconformity within the forearc sequence (Figure 4.7).

4.2.3 Line 129: Line 129 intersects Line 109, perpendicularly, and from west to east, crosses Tanner Basin, San Nicolas Basin and Catalina Basin of the continental borderland (Figure 4.8). The variation of sea bottom depth, on a constant water velocity stack, with ridges and basins create a complex waveform that is typical of a dip line. A sea bottom multiple arrival time of 4.3 s (SP 1700) in the San Nicolas Basin allows a window of 2.2 s of primary section. Application of a long operator with lengths of 151 samples attenuated sea bottom multiples to a large extent revealing primary events.

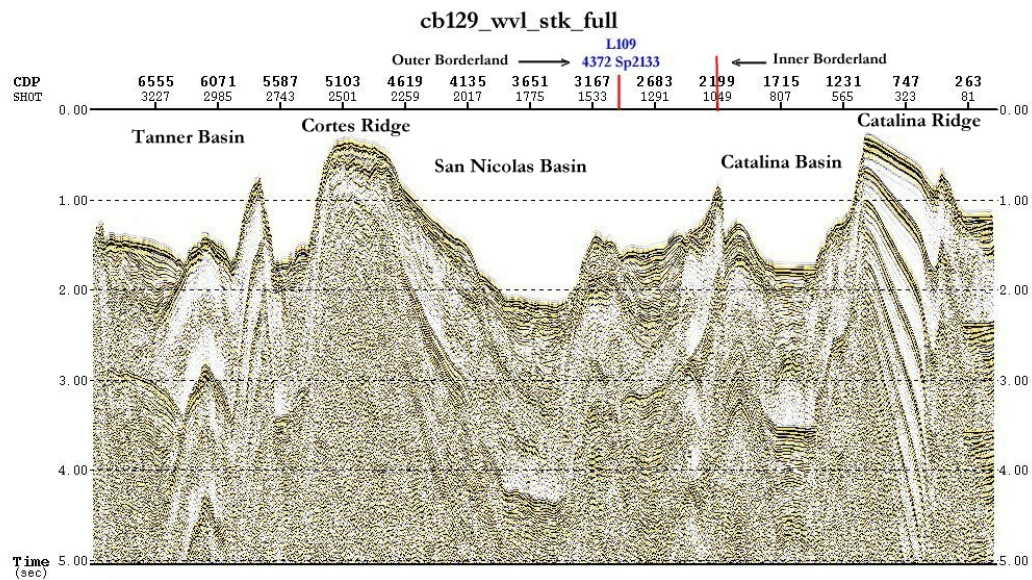


Figure 4.8 Water velocity stack of the entire Line 129 showing complex sea bottom relief and alternating basins and ridges.

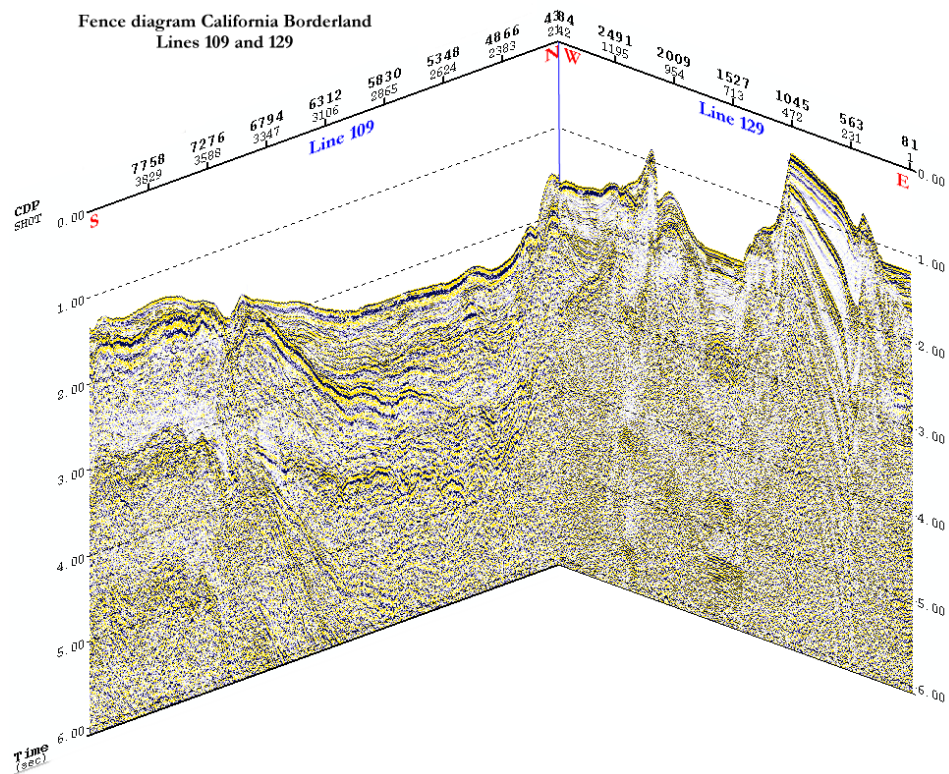


Figure 4.9 Fence diagram of Lines 109 and 129 gives 3D picture of the San Nicolas Basin.

Fence diagram (Figure 4.9) of merged lines 109 and 129 shows 3D structure of San Nicolas Basin. The difference in coherency and S/N is apparent between strike and dip line. The merge section of 109 to 129 (Figure 4.10) allows interpretation of blue marker. It has been picked by Bohannon for the top of the forearc sequence only. Several apparent near surface faults from SP 1165 to 1062 may be associated with the East Santa Cruz basin fault, which most workers consider to be the boundary between the inner and outer Continental borderland. The ridge at SP 1062 is San Clemente ridge with San Clemente fault to the east. Overlying a strong reflector at 2.8 s (volcanic rocks?), a thick Miocene section is identified in the Catalina Basin from sea bottom reflection to time

about 2.75 s. Below this strong reflector, primaries from sedimentary strata are evident below 2.8 s to about 3.5 s.

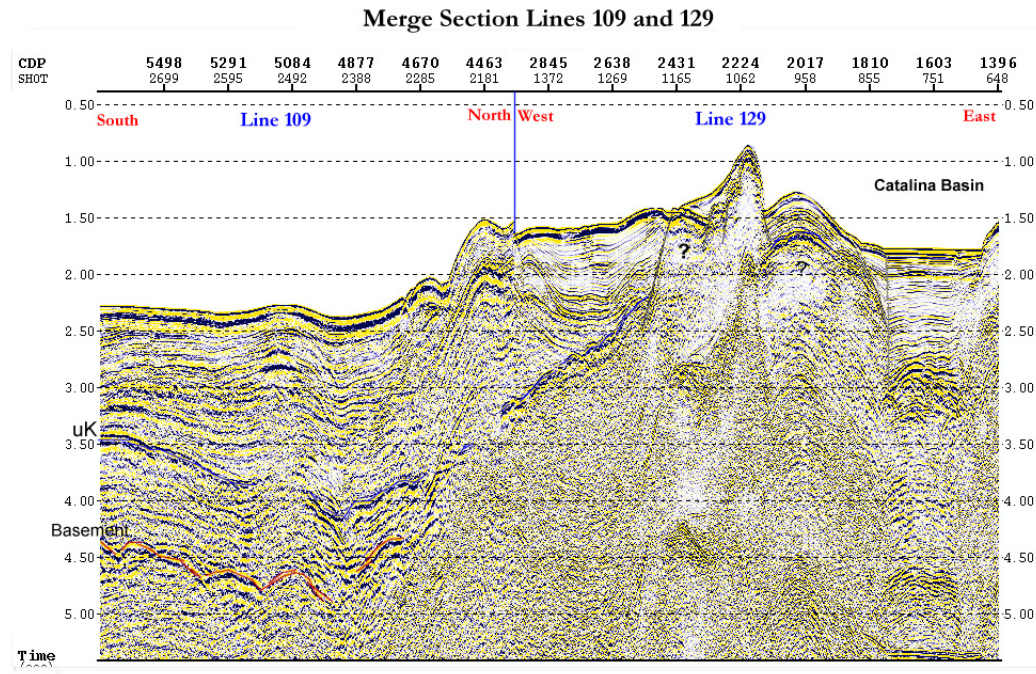


Figure 4.10 Merge line 109-129 showing continuation of interpretation of Cretaceous marker.

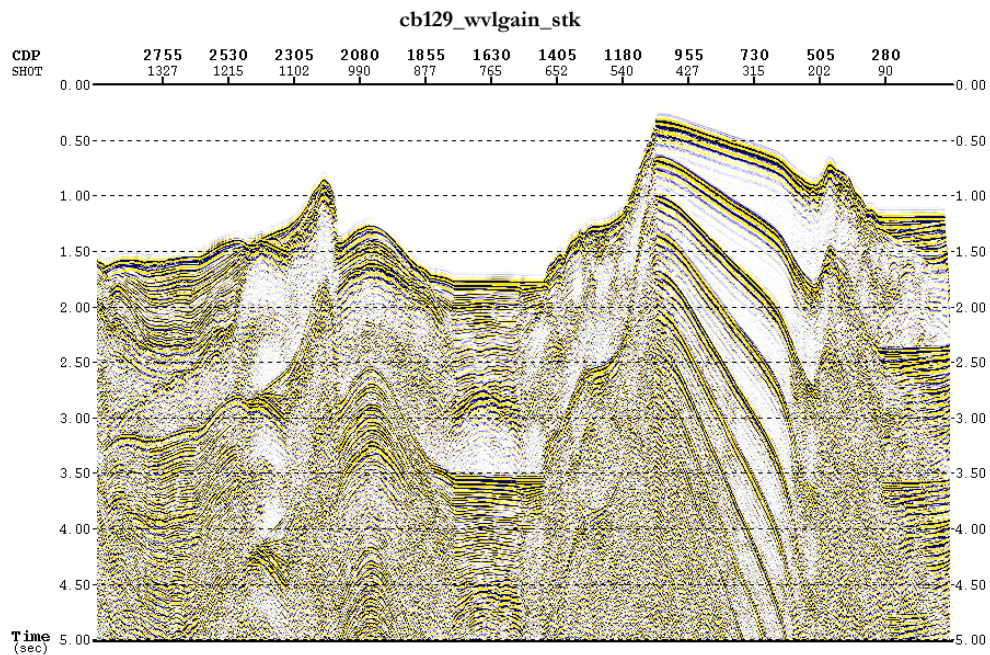


Figure 4.11 Line 129 constant water velocity stack showing enhanced sea bottom multiples.

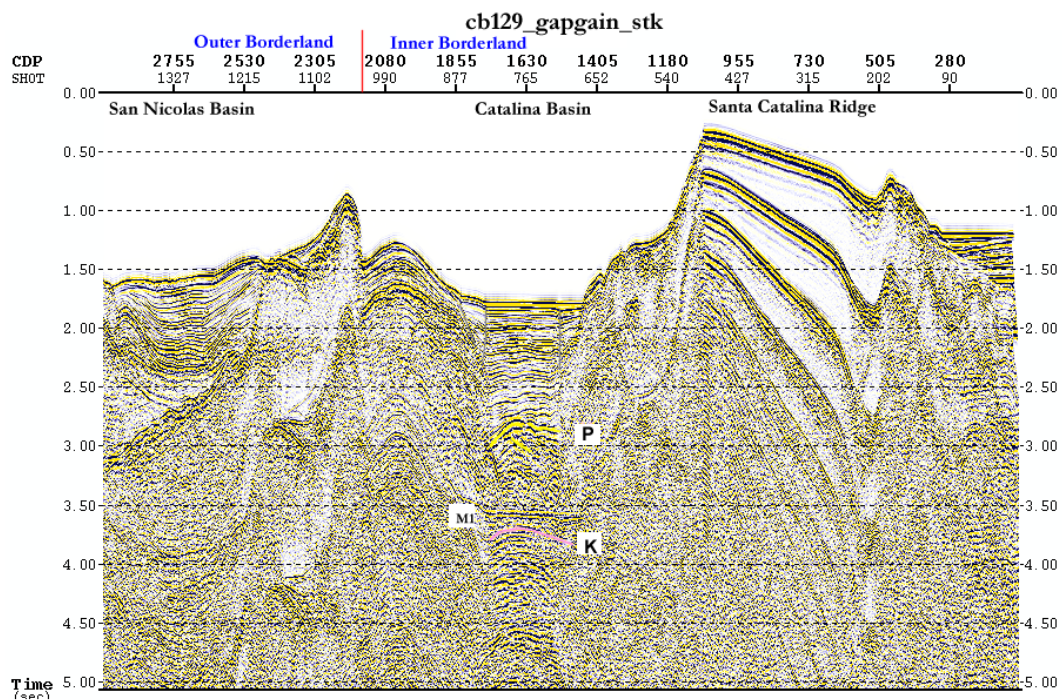


Figure 4.12 Line 129 with interpretation of top of Base of Miocene (P) and pink marker (K) is correlated to pink marker in RTM sections.

A comparison of Figures 4.11 and 4.12 shows that predictive deconvolution has attenuated sea bottom multiples particularly in the basin area. Line 129 and LARSE line 2 intersect on the Catalina Ridge. LARSE Line 2 depth section was converted to time to compare with line 129 both in time. The two-way time of the marker in pink is 3.3 s on LARSE line 2 compared to pink marker (K) on 129 at about 3.7 s. Figure 4.13 shows a comparison of assumed interpretation of forearc sedimentary strata. This interpretation of using seismic character to identify reflection events becomes clear when compared to reflection identifications on Line 128 with a tie to the well. From sea bottom to 2.8 s in Figure 4.13 the sedimentary section is interpreted to be Miocene with volcanics.

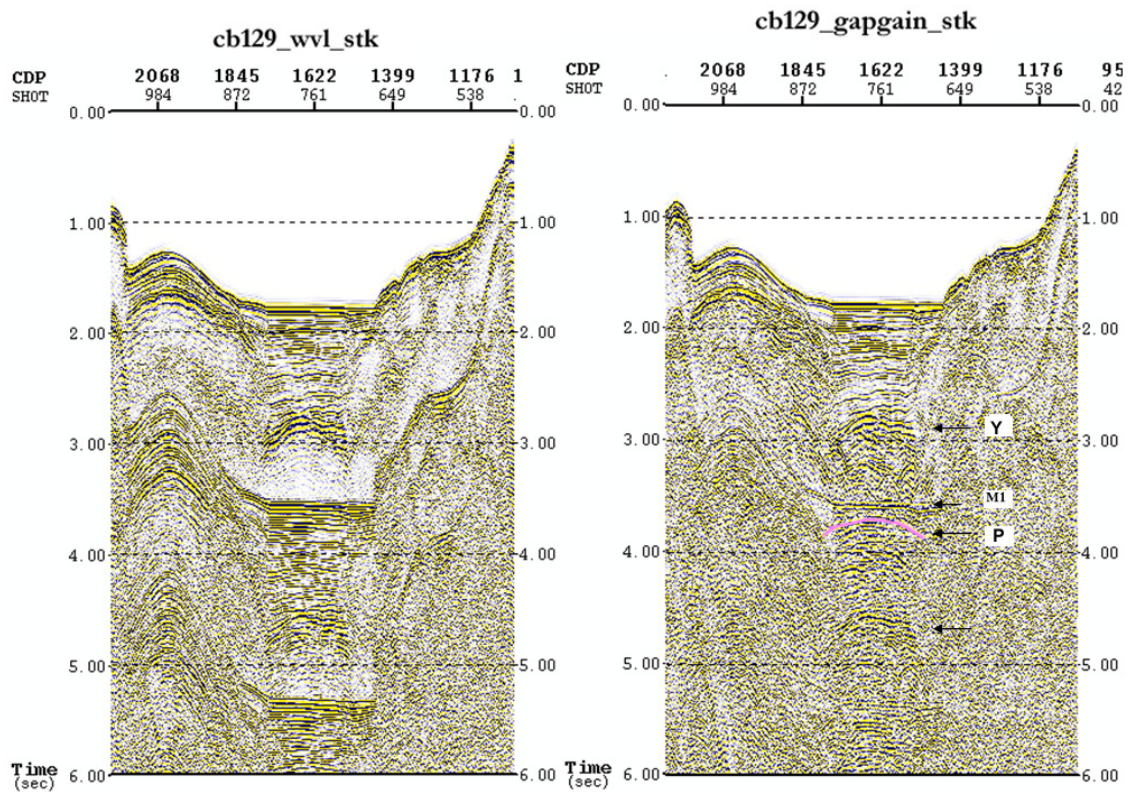


Figure 4.13 Line 129 constant water velocity stack (left) and predictive deconvolution stack (right) with interpretation of forearc section. Yellow marker (P) is an unconformity at the base of Miocene and (K) is the pink marker correlated to the one in RTM section.

The base of this section is an unconformity. At 2.8 s is a strong reflection event that could be interpreted to be top of Paleocene as identified event in Figure 4.5 of line 128. The pink reflector at 3.7 s is inferred to be base of Paleocene strata. Time conversion of LARSE RTM depth section gave 3.4 s for pink event identified to be top of Cretaceous. Paleocene strata compares with RTM unit 3 and Cretaceous with unit 4.

In processing USGS 1990 data, it was observed that sea bottom multiples are not that strong and severe as in LARSE data. Long operator deconvolution attenuated multiples in basin areas revealing primaries. Neogene and younger formations are not generally masked by sea bottom multiples. On both the lines 128 and 129, Paleogene and upper Cretaceous stratigraphic column could be identified and mapped in the Santa Catalina Basin.

The most direct evidence of the presence of forearc Cretaceous-Paleogene sedimentary strata in the ICB is the 1275 meters of forearc section penetrated at total depth by well OCS-CAL P289 near Santa Barbara Island. Vedder et al. (1993) reported that, “A tiny remnant of the forearc section is exposed in the easternmost part of the Santa Catalina Island. Crouch and Suppe (1993) consider this evidence of forearc strata in the inner borderland to be uncertain and infer that the Catalina Island fragment and similar fragments elsewhere in the inner borderland are simply isolated remnants of forearc strata stranded on a regional detachment fault that juxtaposes Catalina schist and forearc rocks. The vintage reprocessed seismic data in this study provide new evidence that suggests the extensive presence of Cretaceous-Paleogene strata in the inner borderland.

Depth images of LARSE lines 1 and 2 (Figures 5.2 and 5.3) revealed stratigraphic units 3 and 4 that appear to correlate with Paleogene and Cretaceous forearc strata penetrated by well P289 near Santa Barbara Island. We have inferred that from reasonable projections of the age-dated units in the well, but until samples are recovered from wells in the area of the seismic lines, other interpretations are possible and likely will be pointed out by workers in the area. The strong reflections from the upper part of unit 3 on LARSE lines 1 and 2 correlate with a 1400 meter interval of probable Middle Miocene volcanic rocks in Well P289. Underlying Oligocene strata is the top of the forearc sequence in this area. The top of unit 4 on LARSE Lines 1 and 2 is a high amplitude reflection event K on USGS line 128. Unit 4 consists of over 1200 meters of concordant, strong reflectors that are similar to a sequence of reflectors on a seismic line near San Clemente Island that Bohannon et al. (1998) described as having “pronounced

reflectivity” and interpreted to be forearc strata. This event is can be traced from 3.5 to 4.5 km depths from northeast to southwest on LARSE Line 1. On LARSE Line 2, the top of Unit 4 is a low relief anticline between depths of 4.2 to 5 km. On USGS Line 129, the top of the volcanic layer is 2.8 s and the K marker is 3.8 s. On Line 128, the top of Paleogene (Oligocene) is at 1.22 s and K marker is 2.11 s. No age data are available to definitively locate the top Cretaceous within the forearc strata. Based on the tops in well P289, the likely location is about 1100 meters below the base of volcanics.

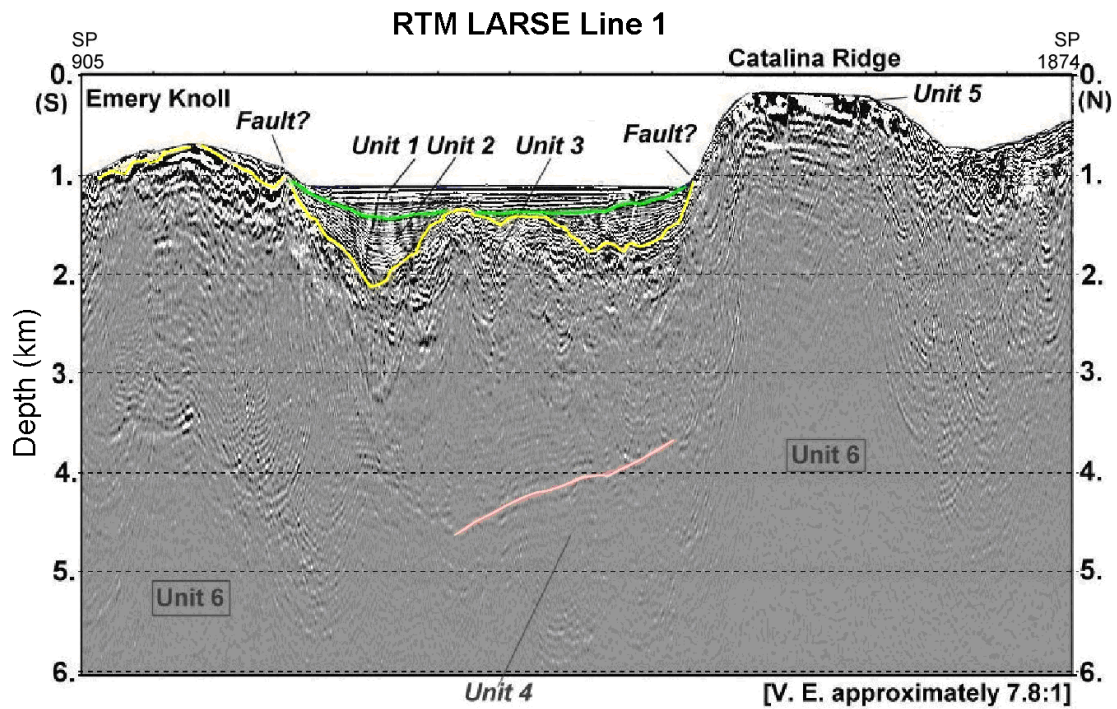


Figure 5.2 RTM section LARSE Line 1 with interpretation of forearc section underlying Miocene formation.

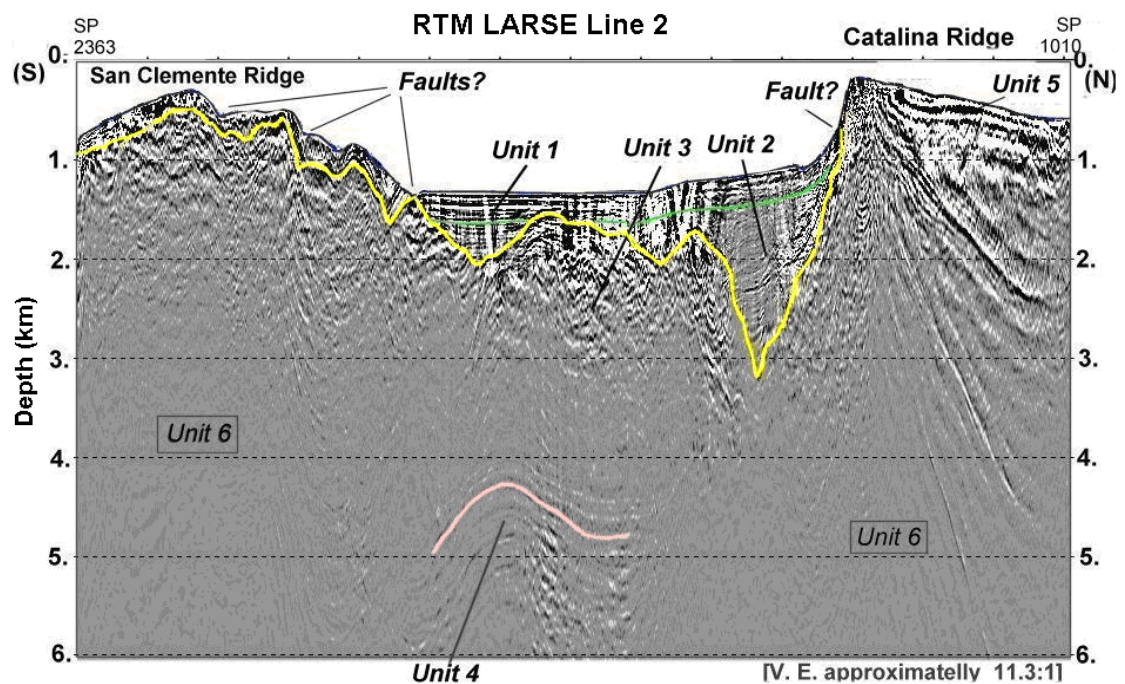


Figure 5.3 RTM section LARSE Line 2 with interpretation of forearc section underlying Miocene formation. Need units for the vertical and horizontal axes and indication of section orientation with respect to N, S, E and W.

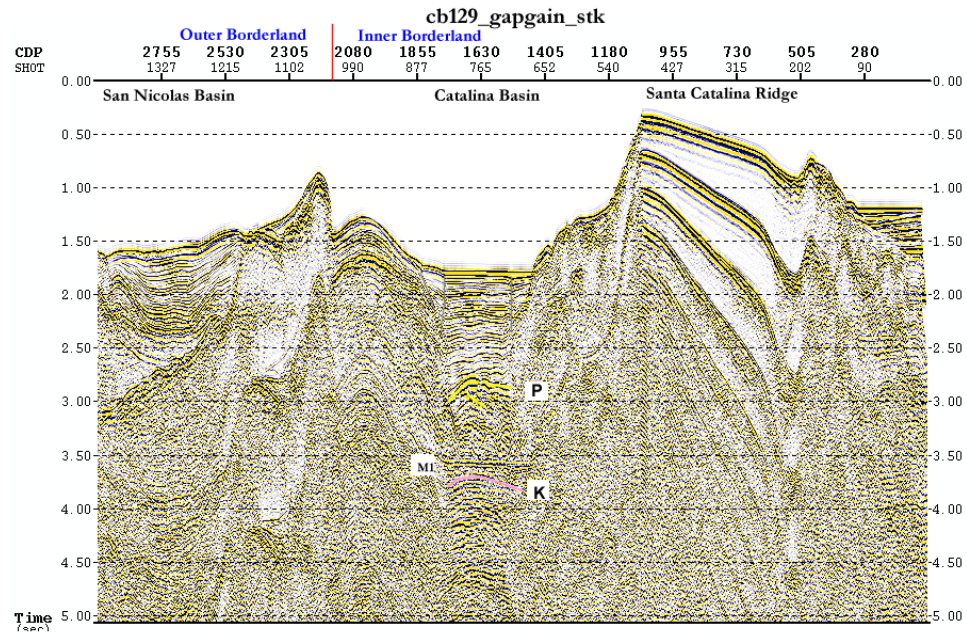


Figure 5.4 Predictive deconvolution stack of line 129 with interpreted tops Paleogene P and Marker K

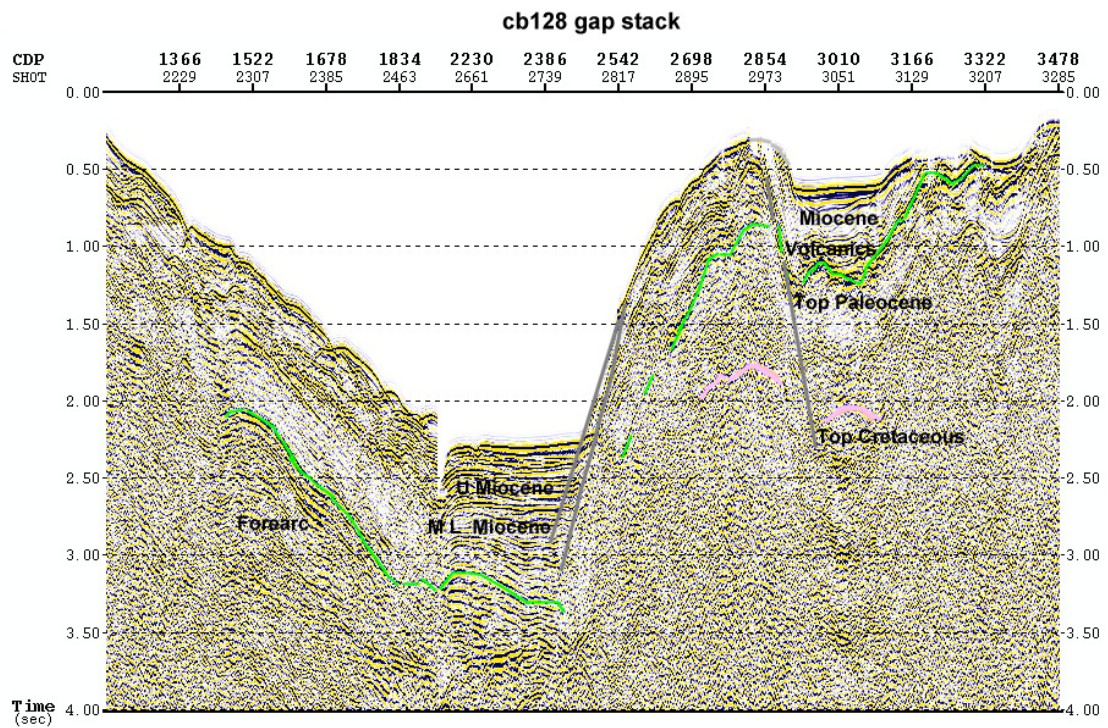


Figure 5.5 Predictive deconvolution stack section of Line 128 showing formation tops from the well

The horizontal extent of possible forearc strata reflections on the four seismic lines across the Santa Catalina Basin is given below:

Table 5.1 Width of forearc strata in the Santa Catalina Basin from NW to SE

Survey	Line No.	from SP	to SP	Width of Basin km.
USGS	128	2977	3255	5.00
	129	540	877	14.25
LARSE	1	745	1434	34.50
	2	1315	1964	22.00

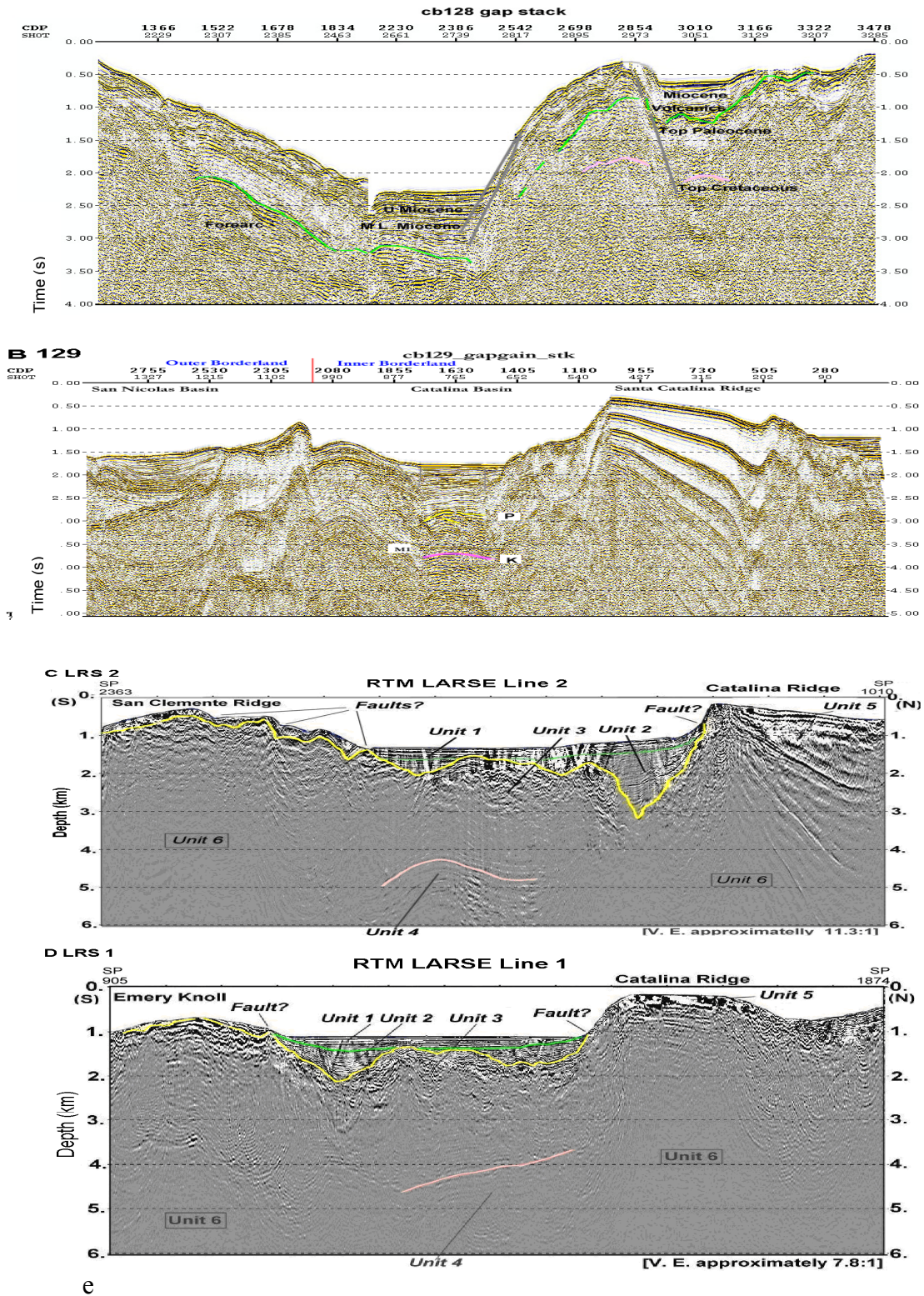


Figure 5.6 Display of 4 seismic sections showing forearc sedimentary sections in the Santa Catalina Basin, California inner borderland.

6. Summary

In the California continental borderland, severe sea bottom multiples mask reflections from the section below the first multiple. All previous studies that have led to the current models of the tectonic framework and geologic history of the borderland have been hampered by significant residual noise on seismic profiles, limited deep well data and ambiguous sea bottom sample data. The focus of this study has been to remove noise from the seismic data by using innovative reprocessing methods and to use the results to better understand the distribution of lithostratigraphic units in the Santa Catalina Basin. In this study we have applied a reverse time migration (RTM) method to process LARSE seismic data and a predictive convolution method to process other vintage USGS seismic data. RTM processing attenuated and removed multiples, improved the resolution of the shallow section and extended the depth of interpretable seismic data to as much as 6 km in basin areas.

Five stratigraphic units have been recognized on RTM depth profiles of the segments of LARSE Lines 1 and 2. They are Pliocene and younger strata; Miocene syntectonic strata; two units that together comprise a largely Cretaceous-Paleogene forearc sequence; and Middle Miocene volcanic rocks on Santa Catalina Ridge. A sixth unit consists of igneous intrusions inferred to underlie bathymetric high areas in the ICB.

Except for a few near shore wells, the only deep well in the ICB is Well 4 (Mobil OCS-CAL P-289), located near Santa Barbara Island. The well penetrated Miocene

sandstones, shale and volcanic rocks and 1265 meters of Paleogene-Cretaceous forearc strata at a total depth of 2620 meters. This well definitively establishes the presence of forearc rocks underlying Miocene and younger strata within the ICB at the northwest end of the Santa Catalina Basin. The stratigraphic section penetrated in Well 4 can be recognized on reprocessed seismic lines along the axial part of the Santa Catalina Basin from Well 4 to the southeast end of the basin near Emory Knoll, a distance of 110 km.

Vedder (1975) reported a “tiny remnant of the forearc section” on Santa Catalina Island. Crouch and Suppe (1993) consider the Santa Catalina forearc fragment and similar fragments interpreted on seismic lines to be remnants of forearc strata stranded on a regional detachment fault that juxtaposes Catalina schist and forearc rocks. The only offshore outcrop of Catalina Schist in the ICB is on Santa Catalina Island. Numerous near-shore and onshore wells west of the Newport-Inglewood fault penetrate the Catalina Schist. Isolated samples of the Catalina Schist in offshore bottom samples are ambiguous. The samples could be interpreted to be autochthonous or allochthonous. From these observations and a regional interpretation that the upper surface of the Catalina Schist was originally a detachment fault, the west boundary of the inner Continental borderland, which has been defined by previous workers to coincide with the East Santa Cruz Basin Fault, has been inferred to mark the seaward limit of Catalina Schist basement of the ICB (Crouch and Suppe, (1993).

Based on well and seismic data, we infer that forearc strata underlie Miocene and younger strata throughout the Santa Catalina Basin. Catalina Schist basement might not

extend further offshore than the Santa Catalina ridge and fault system, although new data are not available everywhere seaward of the San Clemente fault. A reduced extent of the Catalina Schist offshore California suggests that current models of the structural history of the Southern California area should be revisited. The presence of a previously unknown, deep marine sedimentary basin offshore California may warrant an increase in the undiscovered hydrocarbon resource potential of the region.

7. REFERENCES

- Atwater, T., 1998, Plate tectonic history of Southern California with emphasis on the Western Transverse Ranges and Santa Rosa Island, in Weigand, P. W. ed., *Contributions to the geology of the Northern Channel Islands, Southern California*: American Association of Petroleum Geologists, Pacific Section, MP 45, p. 1-8.
- Baher, S., G. Fuis, R. Sliter, and W. R. Normark, 2005, Upper-crustal structure of the Inner Continental Borderland near Long Beach, California, *Bulletin of the Seismological Society of America*, 95(5), 1957–1969.
- Bjorklund, T., K. Burke, R. S. Yeats, and H. Zhou, 2002, Miocene rifting in the Los Angeles basin: Evidence from the Puente Hills half-graben, volcanic rocks and P-wave tomography, *Geology*, 30, 447-450.
- Bohannon, R.G., S. L. Eittreim, and J. R. Childs, 1990, Cruise Report of R/V S.P. Lee, Leg 4, 1990, California continental borderland: *U.S. Geological Survey Open-File Report 90-0502*.
- Bohannon, R. G. and E. Geist, 1998, Upper crustal structure and Neogene tectonic development of the California continental borderland, *GSA Bulletin*; 110(6), 779–800.
- Boundy-Sanders S. Q., J. G. Vedder, C. O. Sanders and D. G. Howell, 1987, Miocene Geologic history of eastern Santa Catalina Island, California, in Third California Islands Symposium, Recent advances in research on the California Islands: Santa Barbara Museum of Natural History, p. 5-14.

- Brocher T. M., R. W. Clayton, K. D. Klitgord, R. G. Bohannon, R. Sliter, J. K. McRaney, J. V. Gardner, and J. B. Keene, 1995, Multichannel seismic reflection profiling on the R/V Maurice Ewing during the Los Angeles Seismic Experiment (LARSE) California 1995. U.S. Dept of the interior, *U.S. Geological Survey*, Open-File Report 95-228.
- Brocher, T. M., U. S. ten Brink, and T. Abramovitz, 1999, Synthesis of crustal seismic structure and implications for the concept of a slab gap beneath coastal California, *International Geological Review*, 41, 263-274.
- Crandall, G. J., B. P. Luyendyk, M. S. Reichle, and W. A. Prothero, 1983, A marine seismic refraction study of the Santa Barbara Channel, California, *Marine Geophysical Research*, 6(1), 15-37.
- Crouch, J. K., and J. Suppe, 1993, Late Cenozoic tectonic evolution of the Los Angeles basin and inner California borderland: A model for core complex, *GSA Bulletin*, 105, 1415-1434,
- Forman, J. A., 1970, Age of the Catalina Island pluton, California, in Bandy, O. L., ed. Radiometric dating and paleontologic zonation: *GSA Special Paper*, 124, 37-45.
- Gantela C., A. Bian, H. Zhou and T. Bjorklund, 2015, “De-masking multiple artifact in crustal seismic images from marine reflection data in the southern California borderland, *Journal of Earth Science* (accepted for publication).
- Guittou, A., B. Kaelin, and B. Biondi, 2007, Least-squares attenuation of reverse-time-migration artifacts, *Geophysics*, 72, 19–23.

- Howell, D. G., C. J. Stuart, J. P. Piatt, and D. J. Hill, 1974, Possible strike-slip faulting in the southern California borderland: *Geology*, v. 2, p. 93-98.
- Howell, D. G., and J. G. Vedder, 1981, Structural implications of stratigraphic discontinuities across the southern California borderland, in Ernst, W. G., ed., *The geotectonic development of California (Rubey Volume 1)*: Englewood Cliffs, New Jersey, Prentice-Hall, p. 535-558.
- Legg, M. R., B. P. Luyendyk, J. Mammerickx, C. de Moustier, and R. C. Tyce, 1989, Sea Beam survey of an active strikeslip fault—The San Clemente fault in the California Continental Borderland: *Journal of Geophysical Research*, 94, p. 1727-1744.
- Luetgert, J. H., 1992, MacRay: interactive two-dimensional seismic raytracing for the Macintosh, U.S. Geol. Surv. Open File Rept. 92-356.
- Miller, K. C., J. M. Howie, and S. D. Ruppert, 1992, Shortening within underplated oceanic crust beneath the central California margin, *Journal of Geophysical Research*, 97, 19,961-19,980.
- Nicholson, C., C. C. Sorlien, T. Atwater, J. C. Crowell, and B. P. Luyendyk, 1994, Microplate capture, rotation of the western Transverse Ranges and initiation of the San Andreas transform as a low-angle fault system, *Geology* 22, 491–495.

- Paul, R. G., J. P. Arnal, G. E. Baysinger, G. E. Claypool, J. L. Holte, C. M. Lubeck, J. M. Patterson, R. E. Foote, R. L. Slettene, W. V. Sliter, J. C. Taylor, R. B. Tudor, and F. L. Webster, 1976, Geological and operation summary, southern California, deep stratigraphic test OCS-CAL 75–70 No. 1, Cortes Bank area offshore southern California: U.S. Geological Survey Open-File Report 76–232, p. 65.
- Ridgway J. R. and M. A. Zumberge, 2007, Deep-towed gravity surveys in the southern California Continental Borderland, *Geophysics*, 67, 777–787.
- Rogers, T. H., compiler, 1965, Geologic map of California, Santa Ana sheet: California Division of Mines and Geology, scale 1:250 000.
- Rowland, S. M., 1984, Geology of Santa Catalina Island, *California Geology*, 37(11), 239-251.
- Thornton, M. P., and H. Zhou, 2008, Crustal-scale prestack depth imaging for 1994 and 1999 LARSE surveys, *Geophysical Prospecting*, 56, 577-585.
- Youn, O. K. and H. Zhou, 2001, Depth imaging with multiples, *Geophysics*, 66, 246–255.
- ten Brink, U. S., J. Zhang, T. M. Brocher, D. A. Okaya, K. D. Klitgord, and G. S. Fuis, 2000), Geophysical evidence for the evolution of the California Inner Continental Borderland as a metamorphic core complex, *Journal of Geophysical Research*, 105(B3), 5835–5857.

- Vedder, J. G., 1987, Regional geology and petroleum potential of the southern California borderland, in Scholl, D. W., Grantz, A., and Vedder, J. G., eds., *Geology and resource potential of the continental margin of western North America and adjacent ocean basins-Beaufort Sea to Baja California*: Circum-Pacific Council for Energy and Mineral Resources, Earth Science Series, 6, 403-447.
- Wright, T. L., 1991, Structural geology and tectonic evolution of the Los Angeles basin, California, in Biddle, K. T., ed., *Active margin basins*: American Association of Petroleum Geologists Memoir 52, p. 35–134.
- Zhou, H., 2003, Multiscale traveltime tomography, *Geophysics*, 68, 1639–1649.
- Zhou, H., 2014, *Practical Seismic Data Analysis*, Cambridge University Press.

